THE THERMAL CONDUCTIVITY OF INTERMETALLICS

by

STEPHEN ASHCRAFT ANDERSON

A dissertation submitted to the Faculty of Engineering, University of Cape Town in fulfilment of the requirements for the Degree of Master of Science (Applied Science).

Department of Materials Engineering
University of Cape Town
April 1996

ABSTRACT

The thermal conductivity of titanium aluminide and several ruthenium-aluminium alloys has been studied from room temperature up to 500°C. Ruthenium aluminide is a B2-type intermetallic which is unusual and of special interest because of its toughness, specific strength and stiffness, oxidation resistance and low cost. The possible use of ruthenium aluminide in high temperature industrial applications required an investigation of the thermal properties of this compound. Apparatus, capable of measuring thermal conductivity at elevated temperatures has been designed and constructed. This study represents the first experimental results for the thermal conductivity of ruthenium aluminide alloys.

The electrical resistivity of the intermetallic compounds has been measured using apparatus based on the Van der Pauw method. The Weidemann-Franz ratio of the ruthenium aluminide alloys has been calculated and this indicates that the primary source of heat conduction in these alloys is by electronic movement and that the lattice contribution is minor. The electrical and thermal properties of ruthenium aluminide are shown to be similar to that of platinum and nickel aluminide. This has important implications for the use of these alloys in high temperature applications.

ACKNOWLEDGEMENTS

I would like to express my sincere appreciation to all who assisted me in this work, and in particular:

Dr. Candace Lang, my supervisor, for her patience, support and advice throughout this project.

Dr. Herman Steyn, Dr. Michael Cortie and Dr. Ira Wolff of the Council for Mineral Technology (MINTEK), for their interest and practical assistance.

Mr. Nick Dreze and Mr. Glen Newins for the quality components and assistance in the workshop.

Mr. Bernard Greeves and Mr. James Petersen for all the photographic development work.

Mr. David Dean and Mrs Mira Topic for their technical assistance.

Mrs. Anne Ball for her administrative support.

The departmental staff and fellow students for their encouragement and support and for creating a pleasant working environment.

The financial support of MINTEK and the Foundation for Research Development is gratefully acknowledged.

Table of Contents

1. INTRODUCTION

A knowledge of the thermophysical properties of materials is important in the development of new technology and in the implementation of new materials in industrial applications. However, because of the experimental difficulties in measuring these properties, sufficient data is seldom available. The thermal conductivity and thermal diffusivity of new materials are especially important since these quantities can influence the ability of a material to withstand service conditions which may include thermal shock and localised heating.

Ordered intermetallics are a class of compounds that present special opportunities for unusual combinations of lightness with high temperature stiffness and strength. Since the limits set on the performance of modern jet engines is determined by the thermal properties of the materials used, intermetallic compounds have been studied intensively as part of an effort to meet aircraft and aerospace demands for materials that are strong at increasingly elevated temperatures.

The past two decades have seen extensive research and advances in the field of mechanical properties and processing of intermetallics. Despite this however there are large gaps in our understanding. The mechanisms of creep and fracture in ordered systems are not well understood and because of this there has been resistance to the use of intermetallics in air and aerospace applications. There is also suprisingly little thermal property data available for most intermetallics. Terrestrial applications are assured for multiphase intermetallics but before they can gain wide acceptance in industry it is necessary to expand our understanding of some high temperature processes.

The thermal conductivity and thermal diffusivity of intermetallics are of particular interest owing to the proposed use of these materials in high temperature applications.

The thermal properties of intermetallics are sensitive to microstructural variations and consequently values quoted in the scientific literature serve only as a guide. Facilities for the measurement of these properties, particularly at elevated temperature, are not always readily available; this is certainly the case in South Africa.

Intermetallic compounds containing aluminium offer new opportunities for developing low density, high strength structural alloys that might be used at higher temperatures than currently possible with conventional titanium and nickel based alloys. More specifically, ruthenium aluminide is a promising material in terms of strength, stiffness, oxidation resistance and cost. It also shows attractive room temperature toughness, which is unusual for intermetallic compounds.

Since South Africa is the world's leading producer of ruthenium, and there presently exist only a limited number of uses for this element, it is in the country's interest to encourage the development of ruthenium alloys. Knowledge of the thermal properties of ruthenium-aluminium alloys is therefore important for the proposed use of these materials in certain industrial applications.

The aim of this project is to design and construct apparatus for the measurement of thermal conductivity at elevated temperatures, to measure the thermal conductivity of intermetallic specimens and to investigate the relationship between thermal properties and microstructure with particular emphasis on ruthenium aluminide. Sample dimensions were limited by the processing route and machining constraints applicable to brittle specimens and this had an influence on the test method and apparatus used to measure thermal conductivity. Three ruthenium aluminide samples and a titanium aluminide sample were tested. A comparative method was used to measure the thermal conductivity of the specimens and a section of the thesis has been devoted to detailing the construction of the test apparatus.

It is useful, when measuring thermal conductivity, also to conduct measurements of electrical conductivity. The electrical resistivity of the intermetallic specimens was therefore measured, using equipment based on the Van der Pauw method. These additional measurements provide us with a measure of the metallic or non-metallic character of these compounds.

Since the microstructure of alloys can have a profound effect on the thermal conductivity of a sample, microstructural studies were conducted on the intermetallic specimens. By relating the thermal conductivities of intermetallics to their structure, we hope to gain an insight into the heat transport mechanisms that operate in these materials and distinguish them from other alloy systems. This dissertation represents the first report of the thermal properties of ruthenium aluminide alloys.

2. LITERATURE SURVEY

This review covers the two main subjects of this research, namely intermetallic compounds and thermal conductivity. Intermetallics are discussed in general and with specific reference to ruthenium aluminide, which has several unique properties. The theoretical aspects of thermal conductivity are presented and this is applied to pure metals and alloys. Finally some methods of measuring thermal conductivity are discussed in detail.

2.1 Intermetallic compounds.

Many terms have been used to describe intermetallic compounds, either from a physical or chemical viewpoint, but few adequately describe what exactly an intermetallic compound is.

The term intermediate phase is commonly given to any new phase formed in a multi-component system and includes those phases resulting from the atomic ordering of primary random solid solutions resulting in the formation of superlattices (a compound is ordered if two or more sub-lattices are needed to describe its atomic structure)[1]. This gives rise to what is known as long range order (LRO) and is described by a long range order parameter. Usually phases do not exhibit LRO at elevated temperatures but can order at lower temperatures (e.g. β- brasses). Some phases do however exhibit stability over a wide temperature range and these phases are termed intermetallics.

The existence of ordered intermetallics arises from the presence of stronger bonding between unlike nearest neighbour atoms than between like nearest neighbour atoms and this gives rise to a structure that differs from that of either of the constituent metals. Intermetallics usually occur at a definite atomic ratio and most often exhibit a narrow homogeneity range[2] .

The chemical combination among metals has been studied since the last century. In the nineteenth century, chemists had difficulty in understanding how metals combine, often in several different proportions, since this often contradicted the elementary laws of valency. At the beginning of this century intermetallics were detected by chemists using the method of thermal analysis. This method depends on the fact that a change from one phase to another, such as the solidification of a liquid or the polymorphic transformation of a solid is always accompanied by the development or absorption of heat. The method is applied by determining, for a sufficient number of alloys in the series, the temperature at which such thermal changes take place during heating and cooling. In this way a number of curves are obtained at which each change takes place as a function of the composition of the alloys[3] . These curves then form the basis of the equilibrium diagram and led to the definition that, when small composition deviations cause a rapid rise in the free energy (G) of the system, the phase is referred to as an intermetallic compound which is usually stoichiometric and has the formula A_mB_n [4].

In 1914 the British metallurgist C. H. Desch published a classic monograph on intermetallic compounds[3] in which he admitted that 'attempts to form a theory of the constitution of intermetallic compounds has been comparatively unsuccessful', and that 'the subject offers a promising field of research'. Twenty years later, the range of intermetallic compounds investigated and their interpretation had advanced enormously and this was due, in part, to two major advances:

1. The application of X-ray diffraction in 1925 by Johansson and Linde[5] established the existence of long range order and the term superlattice was coined.

2. In 1936, Sykes[6] discovered anti-phase boundaries and correctly interpreted them as the consequence of the independent nucleation of LRO in many different locations within a disordered crystal.

Hume-Rothery[7] also contributed greatly to the early recognition that different intermetallics have crystal structures determined primarily by either size factor, electron/atom ratio or traditional valency considerations. In general, superlattices can be expected in cases where the atomic diameters of the solvent and solute are neither too similar or too unequal in size. Intermediate phases formed at definite electron concentrations are called electron compounds because electron concentration determines their stability. The quantum mechanical explanation of the formation of these phases followed the work of Hume-Rothery. He was the first to point out the importance of the valence electron/atom ratio in the description of isostructural intermediate phases in a large number of binary systems. With increasing electron concentration the β, γ, ε phases form having electron to atom ratios of $\frac{3}{2}$, $\frac{21}{13}$, $\frac{7}{4}$.

β is usually BCC, γ is complex cubic and ε is HCP. The above ratios are called the Hume-Rothery ratios[1].

Research on intermetallics in the early 1950's and 1960's was devoted to the investigation of the physical properties of intermetallics[8]. In the early 1960's the U.S. Airforce began to examine the possibility of creating useful alloys on the basis of the ordered phase Ti_3Al[9]. Because of high creep rates and poor thermal stability, continued development of these alloys was considered inadvisable (although independent research on these alloys continues today).

At the beginning of the 1970's Liu[10] at Oak Ridge began a programme of research on Ni-based ordered alloys. Following from the discovery in 1979 by Aoki and Izumi[11], that small additions of boron increased the ductility of Ni_3Al, several commercial intermetallic alloys based on the Ni_3Al system have been launched by the Oak Ridge National Laboratory[12].

Ductility has also been imparted to Ti_3Al by other methods and several companies in the U.S.A. offer the material in sheet or powder form. Jet engine components based on Ti_3Al have been flight tested in U.S.A.[12].

The past decade has seen extensive research carried out on the phase equilibria, mechanical and physical properties of ordered alloys, especially those that have potential in high temperature applications. In developing hypersonic aircraft, intermetallics may be crucial materials, due to the poor strength of Ni-based superalloys at elevated temperatures. However, before these intermetallics are used in aerospace applications it is necessary to understand the thermal properties as well as the creep and fracture mechanisms in intermetallics. The manufacturing and processing methods of multi-phase intermetallics also need to be refined. So despite the enormous amount of work which has been carried out in the last century on conventional and exotic intermetallics it is still too soon to say whether they will be used in high-technology applications, especially in the air.

Although development work has focused on advanced aerospace structural and propulsion systems, intermetallics have huge potential in terrestrial applications. The four principal categories of alloys which have gained the most attention this past decade are the nickel aluminides, titanium aluminides, iron aluminides and more recently the so called 'exotic' intermetallics[9]. Aluminides are good candidates for many applications because of their low density and good oxidation resistance.

A battery of sophisticated physical concepts is now used to make sense of the large number of both binary and multi-element intermetallic compounds and they are no longer regarded as chemical anomalies. Despite this, little attention has been paid to some important physical properties of intermetallics, such as heat capacity, electrical conductivity and thermal conductivity. In his review on the thermal behaviour of intermetallics, White[13] remarks as to the 'suprisingly meagre thermal property data available on most intermetallics'.

Intermetallic compounds with the B2 - type crystal structure form a major grouping in the intermetallic family. Among these compounds are several aluminides, such as NiAl, CoAl, FeAl and several titanides, such as FeTi, CoTi, and NiTi. The exotic aluminide, ruthenium aluminide also exhibits this crystal structure and is discussed in greater detail below.

2.1.1 Ruthenium Aluminide

Ruthenium aluminide (RuAl) can be considered as an exotic, high temperature intermetallic. An equilibrium phase diagram for the ruthenium aluminium system, from a recent study by Boniface and Cornish[14], is shown in figure 2.1. Ruthenium-rich compositions are expected to form a grain boundary phase consisting of the HCP ruthenium-rich α phase with a eutectic phase of approximately 30% aluminium. For aluminium-rich, off stoichiometry compositions, a succession of intermetallics can form, most notably Ru_2Al_3 or $RuAl_3$. This has a deleterious effect on properties, especially strength and ductility. Annealed, stoichiometric and ruthenium-rich samples both show a bulk B2 phase with ruthenium-α precipitates in the bulk phase[15].

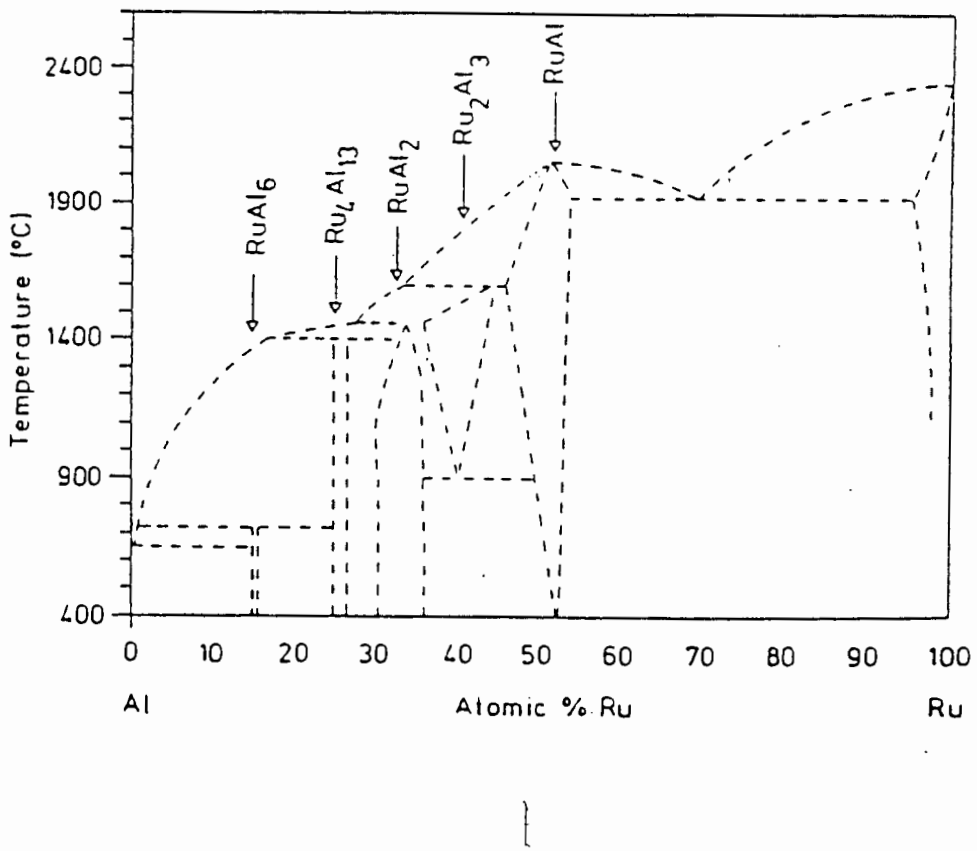

Figure 2.1: Equilibrium phase diagram for the ruthenium-aluminium system (after Boniface and Cornish[14]).

Ruthenium aluminide (RuAl) has a specific gravity near 8 and melts at 2060°C. It is unusual and of special interest because of its toughness, specific strength and stiffness, oxidation resistance and low cost[16]. It is able to undergo approximately 16% true strain at room temperature, since the observed slip vectors of <111>, <100> and <110> ensure that ample slip systems are available for polycrystalline deformation[15]. Alloying with 0.5% boron has been successful in enhancing ductility and suppressing intergranular fracture[16]. An excess of ruthenium increases strength and ductility, as shown in figure 2.2. The electronic structure of RuAl has been studied by Lin *et al*[17] in an attempt to explain its ductility compared to that of NiAl.

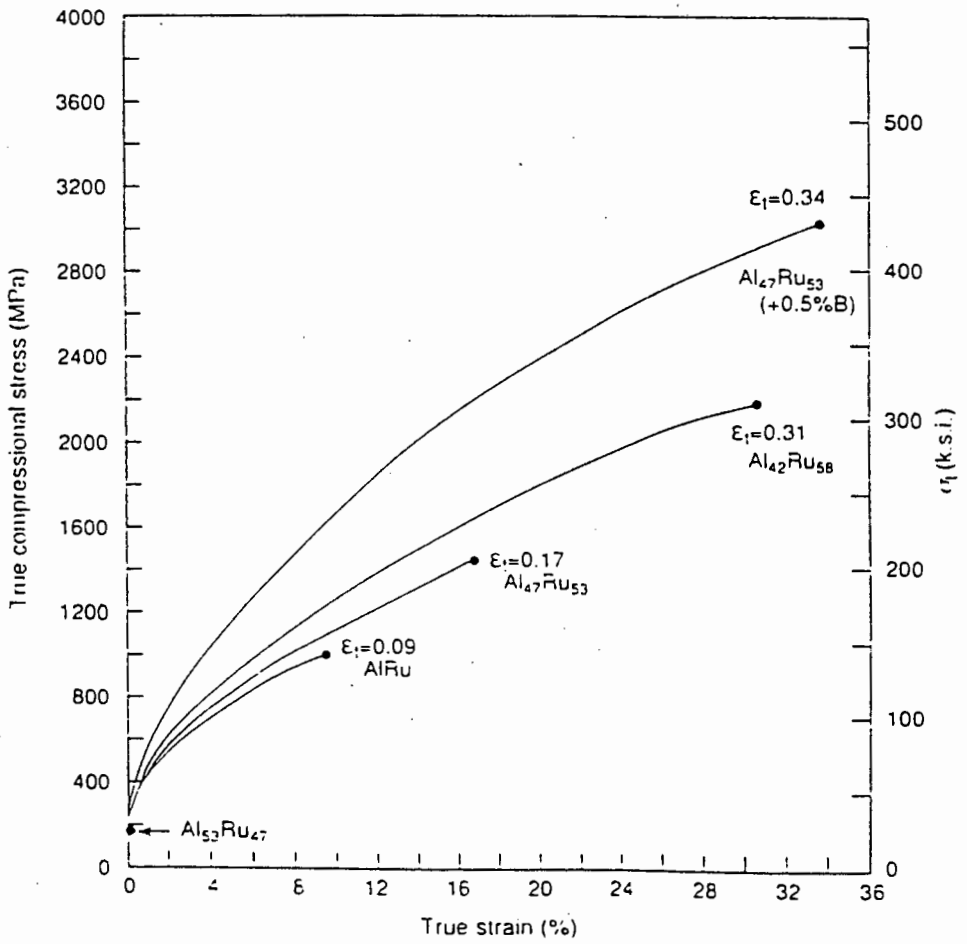

Figure 2.2: Compressional stress-strain curves for five Ru-Al alloys (after Fleischer[16]).

As RuAl and its alloys have shown mechanical promise, their oxidation resistance has been investigated[18]. RuAl alloys have an approximately parabolic oxidation kinetic up to 1200°C and above this temperature linear behaviour dominates.

RuAl has the B2 (CsCl) structure, as shown in figure 2.3 and 2.4, which consists of two interpenetrating simple cubic lattices with each Ru atom at the centre of the Al atoms or vice-versa[17]. The lattice parameter of RuAl is 0.22916nm as determined by Fleischer[18] or 0.303nm given by Lin[17]. It is generally accepted that the B2-type structure is stabilised with three conduction electrons per unit cell containing two atoms. RuAl and NiAl can therefore be considered as electron compounds with a Hume-Rothery ratio of 3/2[7].

Although some physical properties of RuAl have been investigated, such as microhardness, chisel toughness and compressional stress[15], many important properties remain unknown. Thermal properties have been ignored so far in the literature (even though high temperature applications will require such knowledge) and only recently have the electrical properties been investigated[19].

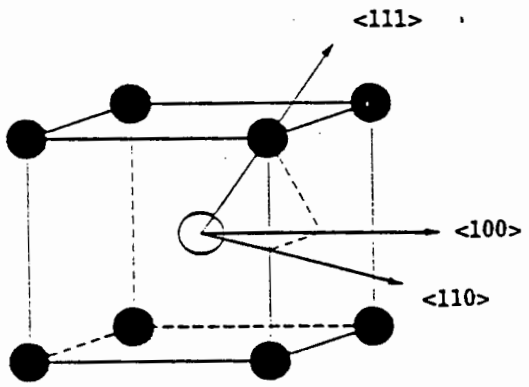

Figure 2.3: B2 structure of ruthenium aluminide (• - Ru, o - Al) (after Lin *et al*[17]).

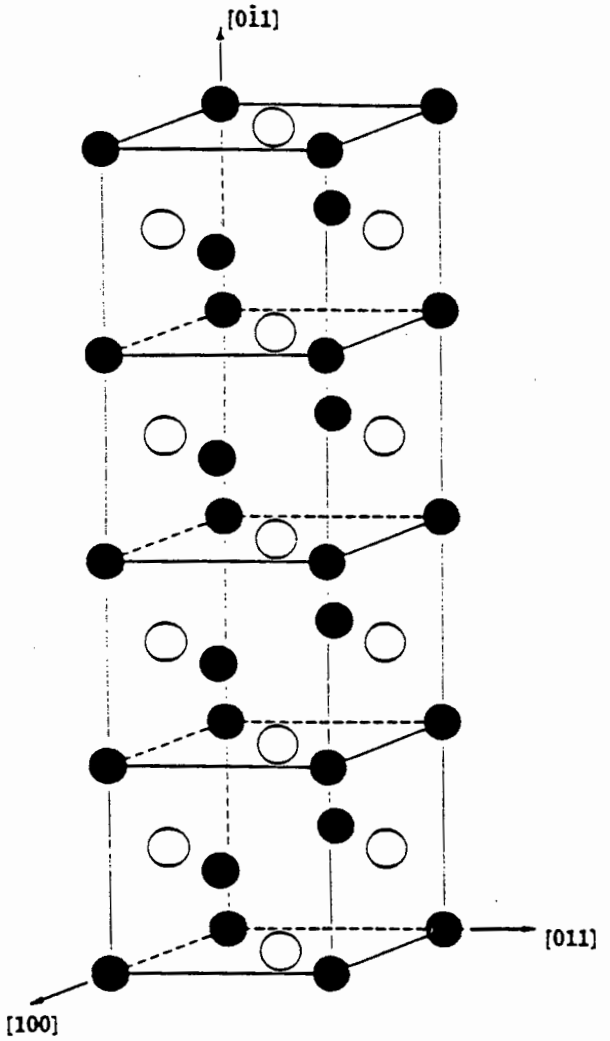

Figure 2.4: Eight layered B2 supercell of ruthenium aluminide (• - Ru, o - Al) (after Lin *et al*[17]).

2.2 Thermal conductivity.

The thermal conductivity of metals and alloys is of interest for two main reasons. Firstly, in conjunction with other properties such as the electrical conductivity, it throws light on the fundamental transport mechanisms occurring within metallic systems. The study of thermal conductivity has therefore played a crucial role in our understanding of the physics of metals. Secondly, knowledge of thermal conductivity and the factors which can influence it, are important in the application of materials in industry.

2.2.1 Theory

There are two processes by which heat conduction can take place in solids. Heat can be transferred by coupling between lattice vibrations (k_g), or by the electronic movement (k_e). The total thermal conductivity is therefore the sum of these components[20]:

$$k = k_g + k_e \qquad \text{Equation 2.1}$$

It can be shown by simple kinetic theory that the conductivity is given by[20]:

$$k = \frac{1}{3}cvl \qquad \text{Equation 2.2}$$

where c is the specific heat per unit volume, v is the mean particle velocity and l is the mean free path between collisions.

For dielectric materials, electrons are not free to move through the structure and so heat is transferred by lattice vibrations. The normal modes of vibration are quantized and, by analogy with photons of radiation theory, are called phonons.

For a discrete lattice, coupling between normal modes of vibration leads to phonon collisions equivalent to random scattering. Theoretical analysis of the thermal conductivity of dielectrics is concerned with determining the mean free path of phonon collisions[21].

For electronic conduction, in which electrons are scattered by collisions with the lattice owing to thermal vibrations of the lattice, conductivity can be written as:

$$k_e = \frac{1}{3} c_e v l_e \qquad \text{Equation 2.3}$$

where c_e is the electronic heat capacity. In pure metals the electronic conductivity is much larger than the lattice conductivity, but in alloys, the electronic and lattice conductivity play a part and therefore both should be considered[20].

In the case of lattice waves or phonons the mean free path is governed by various interaction processes: anharmonic interactions between lattice waves, scattering of lattice waves by crystal imperfections and solute atoms, and the interaction of the lattice with free electrons[22]. The mean free path of the valence electrons is also limited by various processes: interaction with lattice waves, scattering by imperfections and solute atoms and electron-electron interactions. With two thermal conductivity components, each of which is limited by a number of interaction processes, it is not surprising that the thermal conductivity of solids displays a wide variation, both in magnitude and temperature dependence[22].

Models developed to understand the above processes have to be modified to accommodate even the simplest of materials and so no present theories allow for the accurate prediction of thermal conductivity from first principles[20]. The theory for phonon conductivity has only been formulated in some detail for insulators while electronic conductivity has only been examined for monovalent metals with spherical Fermi surfaces over limited temperature ranges[23].

There is however a close relationship between the electronic thermal conductivity (k_e) and the electrical conductivity (σ). In metals, the comparison between theory and experiment is usually performed through analyses of the Weideman-Franz ratio, $\frac{k\rho}{T}$, where k is the total (measured) thermal conductivity, ρ is the electrical resistivity and T is the absolute temperature. Such comparisons involve separation of the observed thermal conductivity into its electronic and lattice components. To accomplish this one must use the theory either for the lattice or electronic part and this is complicated by the limitations of the current theoretical expressions. There seems to be confusion in the literature regarding the Weidemann-Franz ratio and the Lorenz function. Often the ratio $\frac{k\rho}{T}$, where k is the measured (total) thermal conductivity , is referred to as the Lorenz function or even the Lorenz number. In this work I have used the definitions explained by Laubitz[23] where the measured ratio of $\frac{k\rho}{T}$ is called the Weidemann-Franz ratio and the theoretical ratio $\frac{k_e\rho}{T}$ is called the Lorenz function (L). The Sommerfeld value (or Lorenz number) is given as,

$$L_0 = (\frac{\pi^2}{3})\frac{K^2}{e^2} \qquad \text{Equation 2.4}$$

where K is the Boltzmann constant and e is the electronic charge.

L_0 is related to the electronic thermal conductivity by the equation,

$$k_e = \frac{L_0 T}{\rho}. \qquad \text{Equation 2.5}$$

For most metals at room or elevated temperatures the ratio $\frac{k\rho}{T}$ is roughly constant. Experimental values[20] of the Weidemann-Franz ratio fall between 2.13×10^{-8} $J.\Omega.s^{-1}.K^{-2}$ and 2.6×10^{-8} $J.\Omega.s^{-1}.K^{-2}$. These values correspond with the relationship between electrical and thermal conductivities theoretically expected for a completely degenerate electron gas, namely 2.445×10^{-8} $J.\Omega.s^{-1}.K^{-2}$ (or $2.445 \times 10^{-8} V^2K^{-2}$) as calculated by Sommerfeld. This relationship is therefore useful for estimating transport mechanisms in solids as well as deriving thermal conductivity values, since electrical conductivity is simpler to measure than thermal conductivity.

Experiments at very low temperatures on metals shows that the Weidemann-Franz ratio approaches the Sommerfeld value very closely because impurities are the dominant cause of electron scattering. At intermediate temperatures, the scattering is inelastic and the Weidemann-Franz ratio may be much smaller than L_0 in pure metals[22].

Although the Weidemann-Franz ratio is useful we should not accept it blindly. If the electronic relaxation time varies sufficiently rapidly with electronic energy we can have deviations in either direction. This is most likely to be important in the transition metals, where electrons can be scattered into *d* bands[24]. High temperature experimental studies[25] have shown that the correlation between electrical and electronic thermal conductivities expected for a completely degenerate electron gas is not valid for several transition metals.

2.2.2 Thermal conductivity of the metallic elements

In metals the thermal conductivity is mainly electronic while the lattice component is usually minor. In a few cases, first principle calculations have successfully predicted the electronic part of the thermal conductivity although these calculations are extremely complex. For metallic elements at high temperature the goal is to test the applicability of the Sommerfeld value (Lorenz number, L_0). Very roughly, the electronic component obeys the Lorenz relation (equation 2.5) at room temperatures and above. There are however three deviations. 'Vertical' movement on the Fermi surface becomes important at low temperatures and tends to decrease L. Incomplete degeneracy, sometimes called Fermi smearing, tends to increase with increasing T and can lead to departures from L_0 of either sign. Finally electron-electron scattering will decrease L at high temperatures[22].

The thermal conductivity of pure metals is highest for metals having a closed electron shell plus one valence electron (copper, silver, gold, and the alkali metals) as is true of their electrical conductivity.

Since Ru is a member of the VIIIA group elements a summary of the group's thermal conductivities is discussed. For the elements in group VIIIA data for Fe, Co, Ni, Pd, and Pt are reliable. In the iron subgroup, none of the results definitely establish that L differs from L_0 and this is also true for Rh and Ir. Cobalt shows behaviour similar to that of Ti. In this element, L exceeds L_0 at high temperatures while at lower temperatures L is constant at about $0.8\,L_0$. These results have been interpreted on the Fermi smearing model[26]. For the Ni, Pd, and Pt subgroup calculations show that k_g is not very important and for Pd and Pt this has been confirmed at lower temperatures. All three elements produce L values which exceed L_0 at high temperatures and, except for Ni, the deviations increase with increasing temperature. Laubitz and Matsumara[27] have successfully fitted their data for Pd to the Fermi smearing model. A summary of L deviations from L_0, in the group VIIIA elements, is given in table 2.1.

Positive deviations $L>L_0$	$L=L_0$	Negative deviations $L<L_0$
Cr	Nb	Na
Ni	Ta	K
Pd	Mo	Rb
Pt	Fe	Cs
Co	Ti	Ca
Ru	Zr	Sr
	V	Ba
	Re	Li

Table 2.1: Summary of L variation for VIIIA group elements at high temperature (after Klemens and Williams[22]).

Most B group elements have relatively insignificant phonon conductivities and high temperature L values agree with the Sommerfeld value. In the A group the situation is more complicated and phonon conduction can be an important factor[22]. Deviations from L_0 can be as much as 25%. The interpretation of these L deviations in terms of inelastic electron-electron scattering seems to be more successful than the Fermi smearing model[22].

2.2.3 Thermal conductivity of alloys

In the case of dilute alloys, where electrons are strongly scattered by solute atoms, the electronic thermal conductivity is reduced and the lattice conductivity becomes relatively important. There are many alloy systems, and only for a small fraction do thermal conductivity measurements exist.

In disordered alloys, impurity or disorder scattering is important at all temperatures, so that the measured Weidemann-Franz ratio may lie within a few percent of L_0[22]. In these alloys scattering reduces the electronic component k_e more effectively than it reduces the lattice term k_g. The lattice component becomes more significant and can dominate in a high resistance alloy.

Changes in chemical composition of a single phase can have a profound effect on the thermal conductivity of an alloy. The effect of different alloying elements varies markedly. Additions of elements of the same atomic size lead to small differences whereas additions of quite different atomic size lead to large variations. New additions of an element are additive and the thermal resistance is increased approximately linearly for small additions. The conductivity for a continuous series of solid solutions shows a minimum at intermediate compositions while compound formation or ordering gives a maximum [20]. This is obviously of importance in intermetallics.

The effect of impurities in the lattice is to act as additional disturbances analogous with thermal motion. As the temperature increases the effect of impurities decreases since the impurity mean free path is fixed while the conductivity of the pure metal decreases[20] due to thermal scattering by the lattice.

Aluminium alloys are dominated by the simple band structure of aluminium and are representative of the alloys of highly conducting metals such as Cu, Ag, Au. The phonon conductivity is limited by anharmonic processes and point defect scattering, and the electronic thermal conductivity is usually large[22].

The physical structure of a solid may have a greater effect on the thermal conductivity of a material than the chemical composition. To summarise, the factors that affect the thermal conductivity of alloys are temperature, chemical and phase composition, the arrangement of phases, electronic structure, crystal structure and alloy atomic size[20]. Other important microstructural features are grain size, impurity levels, porosity and phase distributions[20].

Because of the effect that these features have on thermal conductivity, the microstructural analysis and characterisation of an alloyed sample is a critical part of any thermal conductivity investigation.

2.2.4 Thermal conductivity of intermetallics.

As has been discussed above, thermal conductivity is influenced by the amount of order in a solid. Disorder, in what ever form, will impede the flow of the heat carriers (electrons and phonons). A well ordered intermetallic compound should therefore have a higher conductivity than its disordered neighbour, presuming that the charge carriers are the same.

Thermal conductivity data as well as electrical data in intermetallic compounds are quite limited. The reason for this is that the measurement, especially the preparation of specimens, is problematic because of the low ductility of the compounds. Collings *et al*[28] have discussed the influence of order-disorder on the electron states for various categories of compound-forming binary alloy systems. The alloys were divided into categories. The first category, category A, comprises of compounds such as Cu_3Au ($L1_2$ structure) for which the component elements have rather similar atomic potentials, and which order without much change in their density of states. Category B compounds (such as Ti_3Al of $D0_{19}$ structure) have elements of very different atomic potential and exhibit major changes in electronic properties on ordering. Category C compounds (such as NiAl and RuAl with a B2 structure) are a large class that often have a definite composition range about stoichiometry and which do not disorder prior to melting. The other large class, class D, comprises of those intermetallics which are semiconducting in the crystalline state and include InSb. Since the present research is particularly interested in RuAl and other similar intermetallics, category C will be discussed in more detail.

Category C compounds do not disorder prior to melting and their electron energy states are different in the stoichiometric compound compared with neighbouring phases. The thermal conductivities may be higher by a factor of five or more in the ordered intermetallic compounds compared to similar alloys[28]. This increase in conductivity depends on stoichiometry and heat treatment.

Darolia[29], in a recent overview of nickel aluminide alloys for use in high-temperature structural applications shows thermal conductivity values for NiAl of 70-80 $W.m^{-1}.K^{-1}$ in the temperature range 300-1400K. These values are approximately eight times larger than the disordered nickel-based superalloys and convey an important practical benefit.

Terada *et al*[30] measured the thermal conductivity of B2-type aluminides and titanides at room temperature. A laser flash technique was used because samples were brittle and difficult to prepare. In the study, eight intermetallic compounds with the B2-type crystal structure were selected. The materials examined were NiAl, CoAl, FeAl, FeTi, CoTi, NiTi, CoGa and NiGa. A summary of the measured thermal conductivities for these compounds is given in table 2.2.

Compound	Thermal conductivity ($W.m^{-1}.K^{-1}$)
FeAl	12
FeTi	73
CoAl	37
CoGa	10
CoTi	25
NiAl	92
NiGa	23
NiTi	15

Table 2.2: Thermal conductivities at stoichiometry of several intermetallic compounds (after Terada *et al*[30]).

Terada[30] found that the thermal conductivity reaches a maximum at stoichiometry except for FeAl. These results are shown in figure 2.5. The measured value for NiAl showed the largest conductivity with a room temperature value of 92 $W.m^{-1}.K^{-1}$ and Terada[30] concludes that his results are "in rather good agreement' with Darolia's[29] results. Fairly large variations in the measured thermal conductivities of many materials seem to be the norm rather than the exception. Using published values for the electrical resistivity Terada[30] concludes that the Weidemann-Franz law is applicable and that the heat carriers are electrons rather than phonons in these intermetallic compounds.

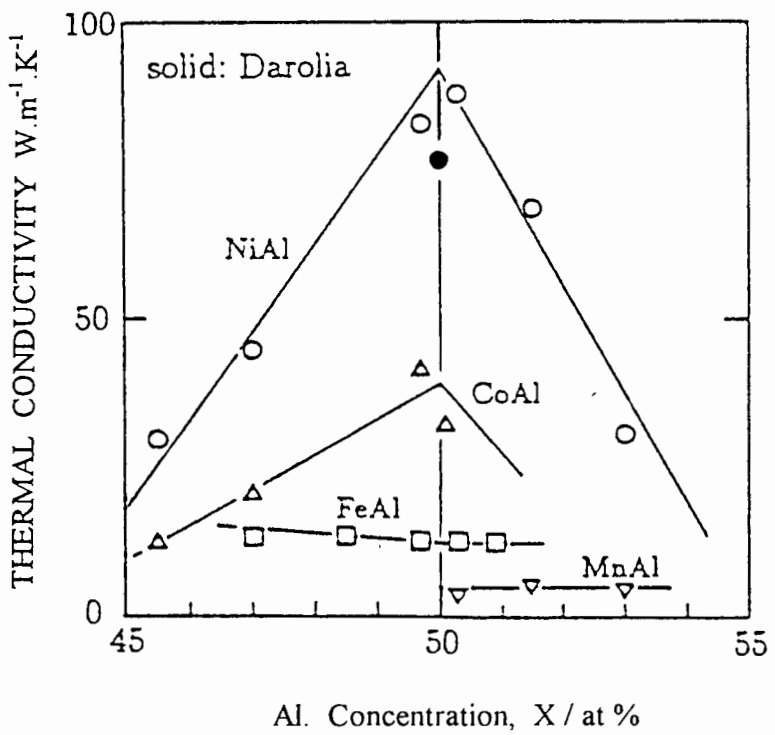

Figure 2.5: Thermal conductivity of MnAl, FeAl, CoAl, and NiAl as a function of Al concentration at room temperature (after Terada *et al*[30]).

2.3 The measurement of thermal conductivity

In the absence of convection or radiation the transport of heat at any point in a homogenous isotropic body depends on the thermal conductivity (k) of the material and the temperature gradient.

The basic relation for heat transfer by conduction was proposed by Fourier (1822) where[31]:

$$\text{The rate of heat flow (q)} = -kA\frac{dT}{dx} \qquad \text{Equation 2.6.}$$

The rate of heat flow is proportional to the product of the cross sectional area, A, and the temperature difference per unit length $\frac{dT}{dx}$.

The thermal conductivity (k) has the dimensions (energy.length)/(area.time.degree) so the mks unit is (joule.meter)/(meter^2.sec.°C) or W.m^{-1}.K^{-1}. Other hybrid units encountered in the literature include the watt unit: watt/cm.°C, the calorie unit: calorie/(cm.°C.sec), and the engineering unit: Btu.in / ft^2.hr.°F.

Thermal conductivity is a quantity of interest in its own right, since it characterises one of the most fundamental energy transport processes in solids. However, while the literature on thermal conductivity is fairly extensive, comparatively little attention has been paid to the design of apparatus for accelerated, precision tests[32]. It is widely recognised that the measurement of thermal conductivity, particularly at high temperatures, is susceptible to large experimental errors. Results obtained in different laboratories on similar samples sometimes differ by amounts exceeding the combined experimental errors of the measurements. A good example of this is the results reported for the high temperature thermal conductivity of pure platinum, a problem addressed by Laubitz and van der Meer[33] and shown in figure 2.6.

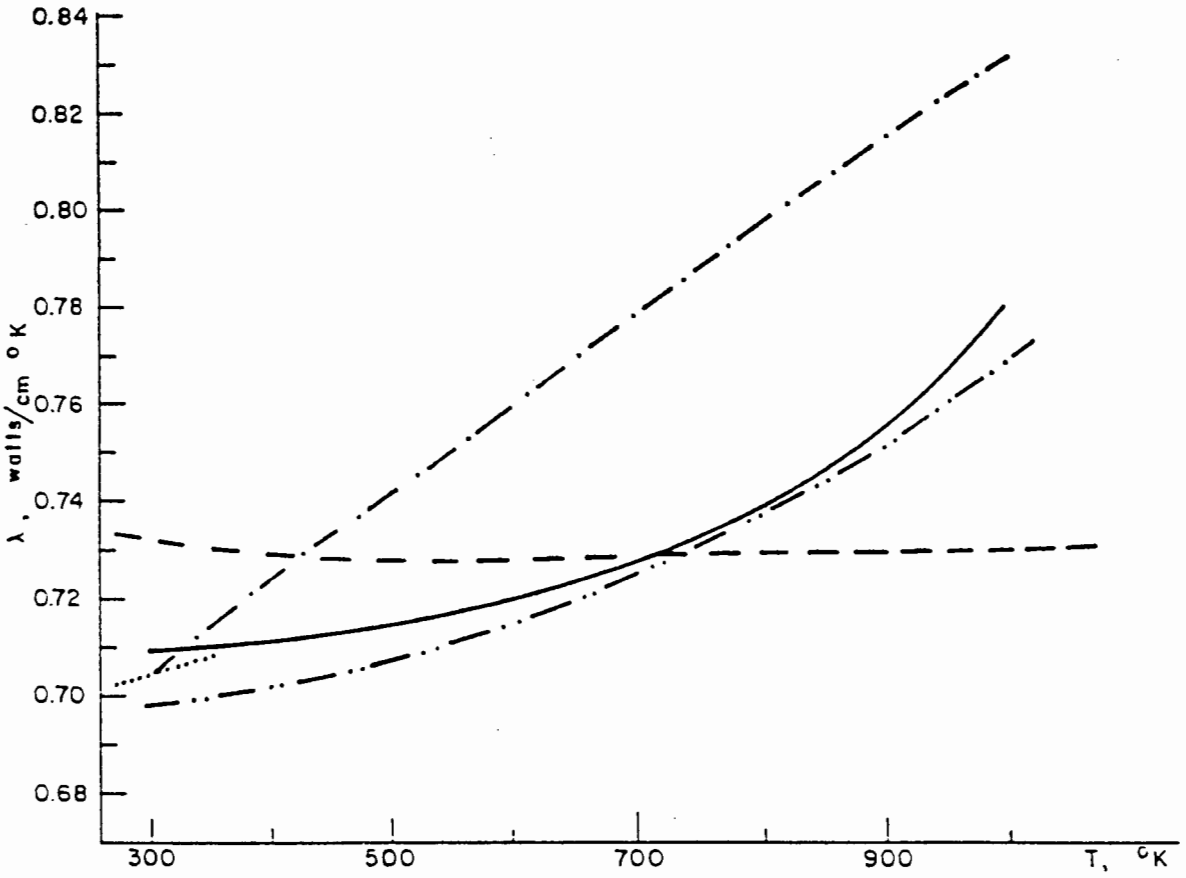

Figure 2.6: Thermal conductivity of pure platinum. Each line represents the experimental data obtained by different researchers[33].

In an attempt to eliminate these experimental discrepancies new measurement techniques have been proposed and developed, both theoretically and experimentally, by a number of researchers in recent years[34].

It should be emphasised from the outset that no single method of conductivity determination is suitable for all conditions of measurement. Different sample materials and different temperature ranges require quite different techniques[20]. Generally, poor conductors are tested using the guarded hot plate method[35], while moderate to good conductors are tested using a longitudinal heat flow technique.

Of the 800 references pertaining to the measurement of the thermal conductivity of solids this century, 600 employ linear heat flow methods[36]. Each publication however, differs significantly in experimental details resulting in differing levels of accuracy and reliability in recorded values.

The measurement of the thermal conductivity of metals, using longitudinal heat flow techniques, can be characterised into 2 main groups, namely:

1) Dynamic methods (transient)
2) Static methods (steady state)

2.3.1 Dynamic methods

In dynamic tests the specimen temperature varies with time during the measurement. Since the magnitude of the heat flow does not have to be measured but only the temperature variation with time, at two or more points, there is more latitude in arranging the heat source than in static methods[31]. Methods that have been applied at high temperature are ones that abruptly change the surface temperature or sinusoidally vary the temperature of the surface of a long rod.

One such method is to heat a long thin rod specimen with a sinusoidally varying heat pulse. Further along the rod are two thermocouples spaced at some convenient separation and a moving chart records the oscillating temperature versus time between the two[31]. If one measures the velocity with which the individual heat oscillations pass from the one thermocouple to the other and the amplitude of these temperature oscillations, which decrease with distance from the heat source, we have the thermal diffusivity (α):

$$\alpha = \frac{lv}{2\ln q} \qquad \text{Equation 2.7}$$

where l is the distance between the thermocouples, v is the velocity of the pulses and q is the ratio of the temperature amplitudes.

The thermal conductivity (k) is given by:

$$k = \alpha\eta c \qquad \text{Equation 2.8}$$

where α is the thermal diffusivity, η is the density and c the specific heat.

It can be seen from the above that dynamic methods yield values of diffusivity rather than thermal conductivity directly. The advantage of this technique is that radiation losses do not adversely affect measurements and the disadvantage is that heat capacity values must be available in order to determine the thermal conductivity.

In general, obtaining a closely controlled temperature variation at high temperatures is as difficult as the measurement of heat input and so transient methods have not been particularly successful at elevated temperatures. More recently, commercial instruments have become available that use a laser pulse to heat the specimen. This so called laser-flash method can be used to measure the thermal conductivity of disc shaped specimens up to temperatures of 1200°C. Terada[30] used this method to measure the room temperature thermal conductivity of some B2-type intermetallics since the equipment could accommodate the brittle specimen geometry. Disadvantages of the laser-flash technique are that thermal diffusivity is measured (as opposed to thermal conductivity) and that instrumentation is extremely expensive.

2.3.2 Static methods.

Static techniques can be divided into 4 categories

(i) Electrical methods

(ii) Direct methods

(iii) Lateral heat flow methods

(iv) Comparative methods

(i) Electrical methods.

These methods have been used successfully in the temperature range 100°K-2500°K. An early measurement of this type was that of Worthing[37] on the thermal conductivity of tungsten lamp filaments up to 2400°K. Generally, filaments are clamped between massive copper blocks which are cooled to maintain them at constant temperature. Because the filament resistance is very low, a small voltage difference between the blocks causes a large current to flow, and the temperature at the centre of the filament rises to high values. The method gives the Weidemann-Franz ratio directly and if the resistivity of the filament is known the thermal conductivity can be found[31]. Generally, samples used with this technique are so thin (filaments) that the surface temperature is uniform in a section perpendicular to the axis. Since the sample geometry of brittle intermetallics specimens does not conform to these requirements, this method has not been considered.

(ii) Direct methods.

Measurement of thermal conductivity in the steady state requires determination of the rate of heat flow, q, the temperature gradient between at least two points, $\frac{dT}{dx}$ and the area normal to the heat flow. A schematic diagram of this method is seen in figure 2.7. Heat is introduced at one end of a long rod of uniform cross-sectional area, A, at a rate $\frac{dQ}{dt}$ (power) and the steady state temperature difference of the two thermocouples at a distance *l* apart, is measured. The other end of the rod is attached to a heat sink, a good massive conductor, whose temperature rise is negligible with the introduction of the power. The thermal conductivity is[31]:

$$k = \frac{l}{A}\left(\frac{dQ}{dt}\right) / \Delta T \qquad \text{Equation 2.9}$$

Numerous researchers[38,39,40,41,42] have used variations of this technique to measure the thermal conductivity of metals. The major error is due to heat loss to the surroundings, but this can be minimised by using a vacuum furnace, keeping ΔT as small as possible and employing auxiliary heating coils to match the thermal gradient in the sample so as to eliminate radiation losses.

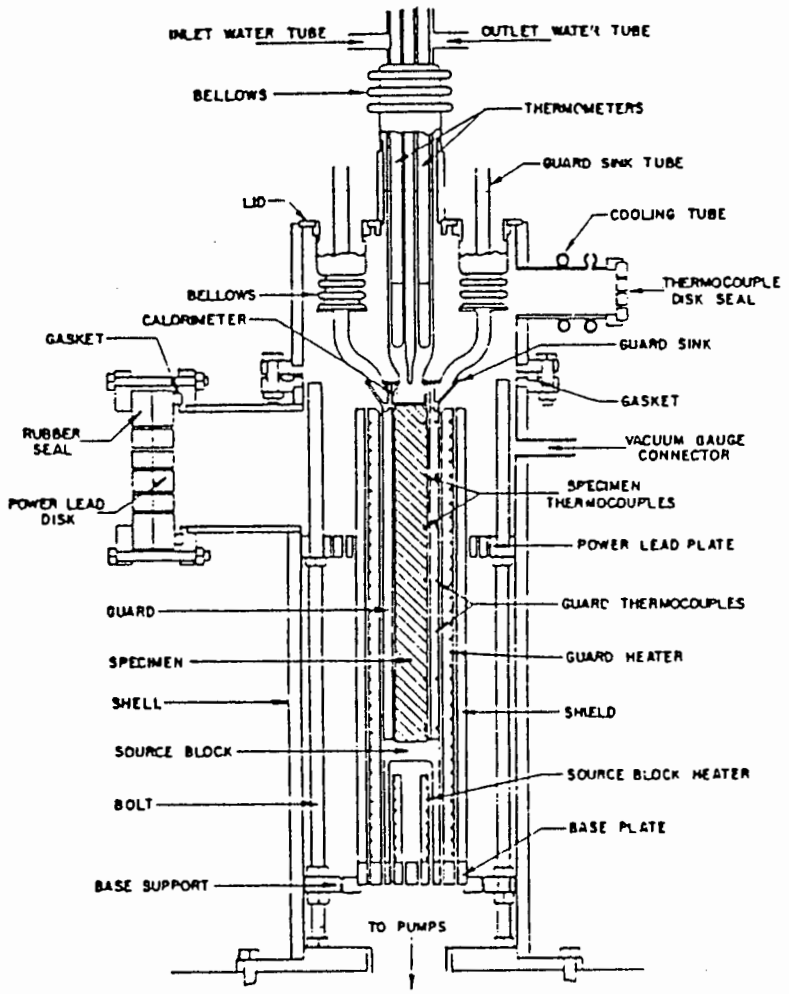

Figure 2.7. A schematic diagram of a static method for determining the thermal conductivity of a rod like sample (after M. Moss[41]).

(iii) Lateral heat flow methods

The lateral heat flow from the surface of rod shaped specimens, which the direct methods are designed to avoid, can in fact be used to determine the thermal conductivity if the lateral heat flow itself is measured.

Methods based on this principle involve two separate measurements:

(a) determination of the temperature distribution along the rod with lateral heat flow present and

(b) a separate measurement of the lateral heat flow.

These methods have the disadvantage that they require the assumption that the lateral flow is the same in both steps, although the specimen is isothermal in (b) but not in (a). By using small temperature differences in the apparatus, it is possible to approach equivalence of the two steps[31].

All methods that, rather than attempt to eliminate radial heat exchanges, evaluate and incorporate them into an analysis are categorised as "generalised Forbes Bar methods". The more modern methods in the Forbes Bar category can be divided into three parts:

1. Methods that employ essentially guarded linear heat flow, but in which the temperature of the guard is varied by small amounts to determine the correction for the radial exchanges between the slightly mismatched guard and specimen. An example of this group is the method of Watson and Robinson[43] . This method has been used extensively by the National Bureau of Standards (USA) for measuring the thermal conductivity of various metals. The specimen is usually a cylindrical rod, nominally 2.5cm in diameter and 37cm long.

2. Methods that in effect employ the 'thin rod' analysis, such as Hogan and Sawyer[44] and Laubitz[23] .

3. Methods that depend on a full two-dimensional analysis, such as Laubitz[45,46]. For historical reasons these are called the 'Unmatched Guard' methods.

Since methods 1 and 3 involve large specimens and complicated methods of analysis the original tests in the present work were based on the design of Hogan and Sawyer[44].

The Forbes method, described by Hogan and Sawyer[44], is based on axial heat conduction in a cylindrical bar of infinite length and radius r, for which the formula

$$\ln(\frac{\Delta t_0}{\Delta t_x}) = (\frac{2\gamma}{rk})^{\frac{1}{2}} x \qquad \text{Equation 2.10}$$

is valid[31], where $\Delta t_0 = t_0 - t_1$ and $\Delta t_x = t_x - t_1$; t_1 being the temperature of the cooling environment, t_0 the temperature of the heated end of the bar and t_x the temperature at a distance x along the bar. The heat transfer coefficient γ represents heat losses from the surface of the bar.

This is determined by a separate experiment in which the sample is heated by an axial electrical current (I) going through the sample and the formula[31]

$$I\frac{dV}{dx} = 2\pi r\gamma(t_2 - t_1) \qquad \text{Equation 2.11}$$

is used, where $\frac{dV}{dx}$ is the axial potential gradient and t_2 is the temperature of the sample due to I. Once γ has been determined the current is switched off and the sample is heated at x=0 to temperature t_0, and Δt_x is measured at a sufficient number of different values of x.

By conducting the two experiments and manipulating the equations we get a value for the thermal conductivity (k) where;

$$k = (\frac{x^2}{[\ln(\frac{\Delta t_0}{\Delta t_x})]^2})(\frac{I}{A}\frac{dV}{dx}\frac{1}{(t_2 - t_1)}) \qquad \text{Equation 2.12}$$

Laubitz[36] uses a theoretical method to analyse different experimental systems. The errors in the measurement values of thermal conductivity were divided into two categories: those that can be called practical errors and those that stem from faulty design. In the analysis Laubitz[36] was concerned exclusively with errors of the second type, attempting to determine design criteria by the application of which these errors could be reduced to below 1%. Laubitz[36] compared two experimental systems used to measure the thermal conductivity of metals, namely the guarded linear heat flow method and the generalised Forbes bar method.

The guarded linear heat flow systems analysed included those of Ditmars and Ginnings[47], Armstrong and Dauphinee[38] and Powell and Tye[42]. The more modern methods in the Forbes bar category analysed were those of Watson and Robinson[43], Hogan and Sawyer[44] and Laubitz[45,46]. These systems were chosen for analysis because of their intrinsic merit and good design.

Laubitz[36] concluded that, although each of the above methods have merit in terms of simplicity, accuracy and design, the Forbes bar method is a much more satisfactory method of measuring thermal conductivity than the guarded linear heat flow system.
The differences between the two methods appear if one considers realistic operating conditions. In the guarded method for instance the guard must be matched to the specimen at corresponding positions, and this is impossible at high temperatures. There is no corresponding source of error in the Forbes method, where, with suitable experimental techniques, one is essentially concerned with the temperature determination of the furnace at a point which need not be precisely defined. The second advantage of the Forbes bar method lies in the greater simplicity of operation, in as much as the temperature of the furnace need not be set at some predetermined value, as is the case with the guard, which has to be matched to the specimen temperature.

The analysis and conclusions reached by Laubitz[36] justify the use of the modified Forbes bar method in the measurement of the thermal conductivity of intermetallics at both room and elevated temperatures.

Generally, the degree of accuracy which can be obtained from these techniques, even with great care, is considerably less than that possible with the measurement of electrical properties. A typical problem is that of contact resistance between the thermocouples and the specimen. By attaching a thermocouple to the specimen one is effectively changing the heat flow through the material as heat is lost through the thermocouple leads. Also it is impossible to achieve thermal isolation to a degree comparable with that of electrical insulation. Furthermore, we have the competing processes of convection and radiation. The result of these and other effects mean that an accuracy better than 1% cannot be readily achieved when measuring the thermal conductivities of specimens. However, this accuracy is usually sufficient for engineering applications.

(iv) Comparative methods

Comparative measurements compare the conductivity of an unknown material with that of a known standard. The most common method is to place the unknown and standard samples in series, with the same rate of heat flow through both[48]. From equation 2.6 it follows that:

$$k_{sample} = k_{ref} \frac{A_r \left(\frac{\Delta T}{\Delta x}\right)_r}{A_s \left(\frac{\Delta T}{\Delta x}\right)_s} \qquad \text{Equation 2.13}$$

A comparative method, in effect, employs a known thermal conductivity as the basis for measuring the heat flow; that is as a calorimeter. Comparative methods have the advantage that the heat flow through the sample does not have to be determined calorimetrically, and that the guarding heat flow in all directions from a calibrated heater becomes unnecessary. This is a substantial advantage at high temperatures when heat input measurements become progressively more difficult. Another advantage is that a direct comparison between the two samples is obtained, using a relatively simple piece of apparatus with easily fabricated specimens. One of the disadvantages of the comparative method is that measurements depend on the use of a standard material.

Any error in the data for the standard will affect the results obtained. It is usually not satisfactory to accept values from the scientific literature for use as a standard. In equipment using comparative techniques, errors can occur mainly by lateral heat flow and interfacial resistance between samples. Lateral heat flow results in unequal heat flow through the standard and sample since some of the heat entering the standard does not reach the unknown sample. Lateral heat flow can be reduced by using large samples, suitable insulation and guard methods. Interfacial resistance may cause a nonuniform temperature distribution and adds thermal resistance to the sample. Interfacial energy can be reduced by forming smooth surfaces, applying mechanical pressure and introducing a metallic film of good thermal conductivity.

The use of comparative methods can be justified in circumstances where it is difficult to form specimens of a specific geometry. This is especially applicable to brittle specimens such as ceramics, and in the present case, intermetallics. If experimental errors of the order of 5% are acceptable, comparative tests are a quick, cheap way of measuring thermal conductivity.

Typical equipment for applying the comparative method to metals is described by Van Dusen and Shelton[49]. Powell[42] used a comparative method to measure the thermal conductivity of Nimonic alloys while Francl and Kingery[48] and Vasilos and Kingery[50] used similar equipment to measure the thermal conductivity of some ceramic materials. This equipment is shown in figure 2.8.

Mirkovich[51] describes an improved version of the apparatus in which a heat stabiliser is used to eliminate heat channelling. Commercial equipment is also available for measuring the thermal conductivity of samples using the comparative method.

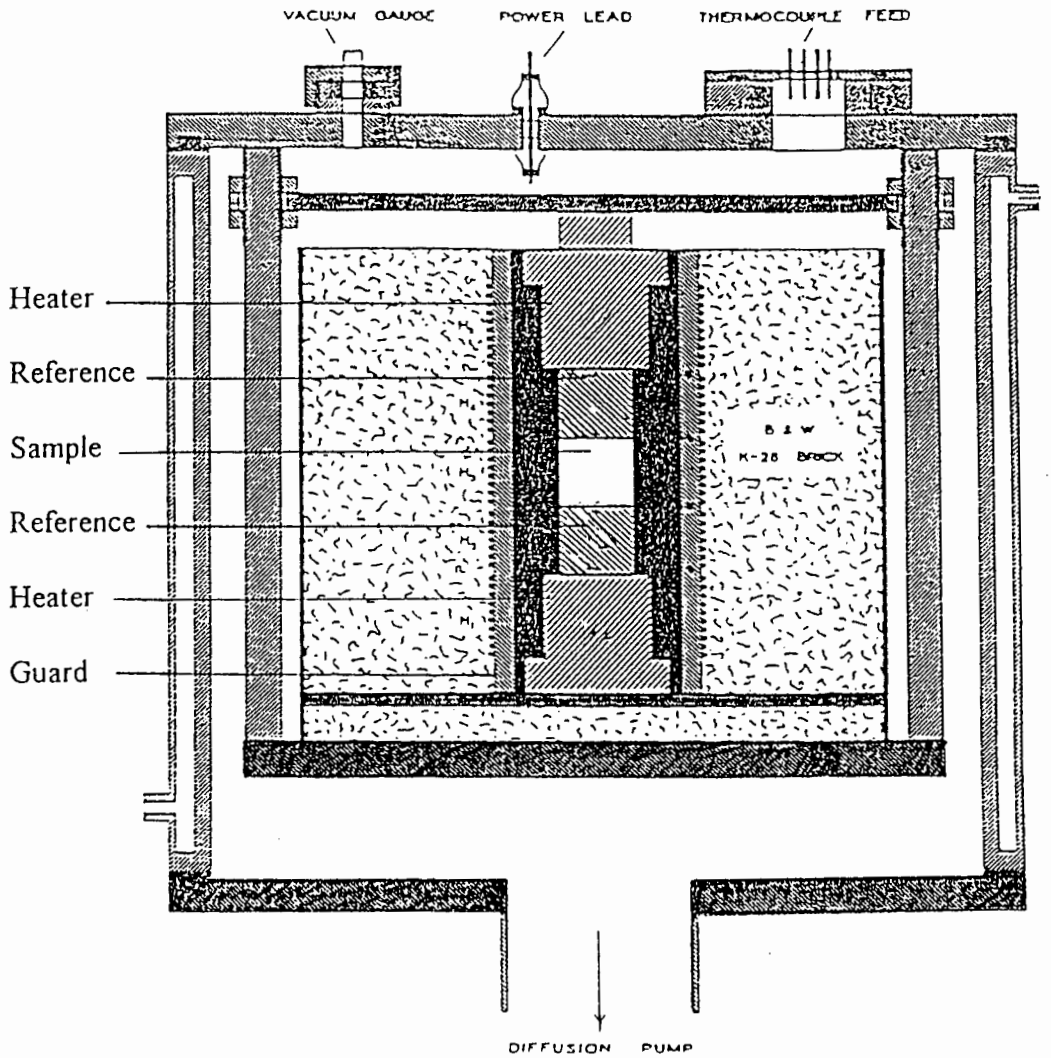

Figure 2.8: Sample assembly and vacuum enclosure for comparative method of testing (after Vasilos and Kingery[50]).

Corsan[52] designed a compact apparatus for accurate thermal conductivity measurements in the range 10 $W.m^{-1}.K^{-1}$ to 380 $W.m^{-1}.K^{-1}$, from 50 °C to 500 °C. It operates on the linear heat flow principle using bar shaped specimens clamped between a guarded heater unit and a water cooled heat sink. This apparatus provides an absolute method for thermal conductivity measurements and includes the additional feature of a built in comparator (standard) to check the validity of each measurement.

2.4 Overview

Binary and multi-element intermetallic compounds are no longer regarded as chemical anomalies; but important properties of intermetallics, such as heat capacity, electrical conductivity and thermal conductivity are still relatively unknown. Little or no thermal property data is available for most intermetallic compounds and ruthenium aluminide is no exception. While ruthenium aluminide is unusual because of its toughness, stiffness, oxidation resistance and low cost, the thermal properties of this compound have been ignored in the scientific literature.

Thermal conductivity is a quantity of interest in its own right, since it characterises one of the most fundamental energy transport processes in solids. Models developed to understand the thermal conductivity in solids have to be modified to accommodate even the simplest materials and so no present theory allows for the accurate prediction of thermal conductivity from first principles. In metals the thermal conductivity is mainly electronic while the lattice component is usually minor. The comparison between theory and experiment is usually performed through the analysis of the Weideman-Franz ratio and this will be used to analyse the thermal conductivity of the intermetallic specimens.

Of the 800 references pertaining to the measurement of the thermal conductivity solids this century, 600 employ linear heat flow methods. These methods can be divided into four categories, namely electrical methods, direct methods, lateral heat flow methods and comparative methods. Laubitz[36], in his analysis of measuring techniques used to measure thermal conductivity, concludes that the Forbes bar method (lateral heat flow) is a better technique for measuring thermal conductivity than the guarded linear heat flow technique.

Comparative methods compare the conductivity of an unknown material with that of a known standard. The most common method is to place the unknown and standard sample in series with the same rate of heat flow through both. Comparative methods are less accurate than direct methods but their use can be justified in circumstances where it is difficult to form or machine specimens of a specific geometry. This is especially applicable to brittle specimens such as ceramics and intermetallic compounds. Generally comparative tests are a quick, cheap way of measuring thermal conductivity.

3. EXPERIMENTAL METHODS

3.1 Specimen preparation and history

In this project three RuAl samples and a TiAl sample were investigated. The three RuAl samples were prepared by Mintek using a reactive hot isostatic pressing (RHIP) method.

Ruthenium and aluminium powder were mixed in the correct proportions and then compacted in a die. The compacts were then heated in a graphite resistance furnace, using an argon atmosphere, until the exothermic reaction had taken place. The reacted compacts were then milled into fine RuAl powder and sieved. Pellets containing varying proportions of elemental powder were then produced again by compaction. The samples were wrapped in molybdenum foil, vacuum sealed in titanium capsules and RHIPped at 1400°C and 1.46×10^8 Pa for six hours in an argon atmosphere.

The samples were then subjected to cylindrical grinding, initially using a silicon carbide abrasive wheel, and then an alumina wheel. The first sample received, R94, was not annealed (homogenised) while samples R160 and R161 were annealed for 12 hours in a vacuum furnace at 1500°C. The RuAl specimens were received as cylindrical rods and were prepared for thermal conductivity and electrical resistivity measurements as well as for microstructural analysis.

The TiAl sample was wire cut from a cast ingot. A summary of the samples and their processing routes is given in table 3.1.

Sample	Composition	Processing	Treatment
R94	$Ru_{53}Al_{47}$	30% pr-reacted powder - RHIP	-
R160	$Ru_{50}Al_{50}$	30% pr-reacted powder - RHIP	Homogenised at 1500°C for 12hrs
R161	$Ru_{47}Al_{53}$	30% pr-reacted powder - RHIP	Homogenised at 1500°C for 12hrs
TiAl	$Ti_{48}Al_{52}$	Cast	-

Table 3.1: Intermetallic samples and their processing routes.

3.2 Specimen characterisation

As discussed in section 2.2.3, the thermal conductivity of metallic alloys is affected by many factors. A critical part of any thermal conductivity analysis is therefore the microstructural and chemical analysis of the alloyed sample.

Slices (1mm thick) were wire cut from the bulk specimens as shown in figure 3.1. These slices were mounted, ground and polished and then examined microscopically. No etchant was necessary for the RuAl specimens while Kellers reagent was used on the TiAl sample. The specimens were examined under a Reichert MeF3A light microscope and a Cambridge scanning electron microscope. The resulting micrographs are shown in section 5.1.

Compositional analysis is important in any thermal conductivity investigation. However, because of the excellent chemical resistance of ruthenium - aluminium alloys they have not been successfully tested by chemical means. Smith[19] has attempted to analyse ruthenium-aluminium alloys using inductively coupled plasma spectroscopy with limited success. There is as yet, no absolute method for determining the chemical composition of these alloys.

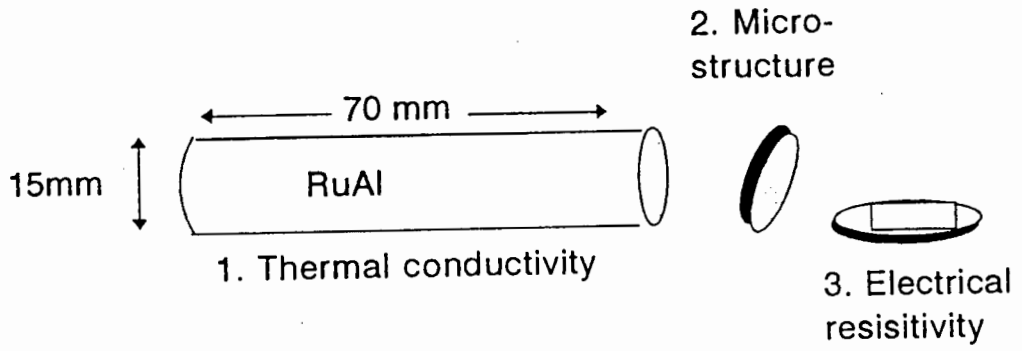

Figure 3.1: Preparation of RHIPped samples for analysis and measurement.

Non destructive methods for analysing metals also have shortcomings when it comes to evaluating ruthenium-aluminium alloys. X-ray microprobe techniques (XRM) can only examine a small area of a specimen at a time and require a standard. X-ray fluorescence techniques (XRF) have been attempted by Fleischer[53] with unsatisfactory results. This technique also requires a standard sample of which the composition is exactly known. Energy dispersive spectroscopy (EDS) cannot be considered an absolute method since it is a surface technique and the software relies on a standardless analysis. However, Smith[19] and Fleischer[15] found that EDS proved satisfactory in determining the relative compositions of ruthenium - aluminium alloys.

In this study EDS has been used to confirm the nominal compositions of the specimens. Since the samples were prepared in a closed environment (RHIP capsule), it is not unreasonable to assume that the nominal compositions are correct. However since many people and laboratories have handled the specimens and from past experience of labelling errors, it was decided to check the nominal compositions using EDS. These results are given in section 5.1.

3.3 Measurement of thermal conductivity

Since the thermal conductivity of the RuAl specimens was completely unknown, a simple comparative method was used initially to obtain an approximate value. The method described by Ingenhausz[31] uses two rods of the same dimensions, one of known conductivity and the other of unknown conductivity. The rods are coated with wax and then dipped in a bath whose temperature is higher than the melting point of the wax. If the wax melts to distances x_a and x_b along the rods the conductivities have the ratio:

$$\frac{k_a}{k_b} = (\frac{x_a}{x_b})^2 \qquad \text{Equation 3.1}$$

Comparisons were made between 3 rods having the same dimensions namely, 316 stainless steel, D65S aluminium and the ruthenium aluminide specimen. The rods were coated with paraffin wax (T_m of 65°C) and then dipped in a 70°C bath of water. After about 10 seconds the rods were removed and dipped into cold alcohol to freeze the melt interface. The distances x_a and x_b were then measured and recorded. These results are given in section 5.2.

From the above experiment it was determined that the RuAl specimens are good thermal conductors and so an appropriate thermal conductivity measuring technique had to be chosen.

The Forbes bar method has several advantages over other static heat flow methods as discussed in section 2.3.2. Apparatus based on that used by Hogan and Sawyer[44] was constructed with the intention of measuring the thermal conductivity of the intermetallic samples at room and elevated temperatures. The construction and testing of this apparatus is discussed in greater detail in section 4.1.

Unfortunately the dimensions of the RHIPped ruthenium aluminide samples did not satisfy the thin rod approximation used by Forbes (discussed in chapter 6) and an alternative test method had to be found.

Considering the dimensions of the brittle samples as well as time and cost implications a comparative method was chosen. Apparatus was built to accommodate the dimensions of the cylindrical intermetallic specimens without the need for any additional machining of the samples. This equipment was used to measure the thermal conductivity of the samples at room and elevated temperature, up to a maximum of 500°C. The construction and testing of this apparatus is described in detail in section 4.2. The results of the thermal conductivity measurements are given in section 5.2.

3.4 Measurement of electrical resistivity

Apparatus based on the Van der Pauw method[54] for measuring the resistivity of arbitrarily shaped discs was used to measure the resistivity of the intermetallic specimens. The specimen configuration and probe placement is shown in figure 3.2. The shaded areas indicate where contacts may be placed to satisfy the requirements of the Van Der Pauw method[54]. The voltages obtained from the two probe configurations shown in figure 3.2 are used to calculate the resistivity (ρ) of the sample using the following equation:

$$\rho = \frac{\pi d}{2\ln 2}\left(\frac{V_1}{I_1} + \frac{V_2}{I_2}\right) = \frac{\pi d}{2\ln 2}\left(\frac{R1 + R2}{2}\right) \qquad \text{Equation 3.2}$$

where d is the thickness of the sample.

The test apparatus was calibrated up to 500°C using a platinum specimen.

Slices from the bulk RHIPped specimens were wire cut as shown in figure 3.1. These slices were then cut into a square configuration measuring 12mm X 12mm and ground down to a thickness of approximately 0.2mm. The thin sheets were then placed in the specimen stage and the electrical resistivity was measured at a range of temperatures.

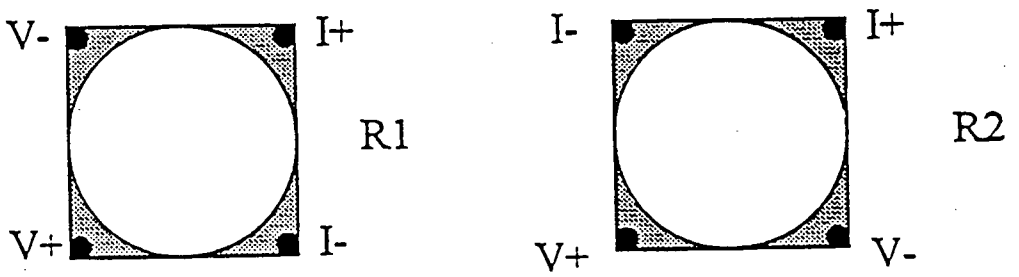

Figure 3.2: Probe placement to measure the two sheet resistances R1 and R2 for the Van der Pauw method (after Sun *et al*[55]).

The temperatures at which the electrical resistivity measurements were carried out matched the temperatures at which the thermal conductivity measurements had been made. A schematic diagram of the furnace configuration used to measure the electrical resistivity of the specimens is given in figure 3.3 and the measured results of the samples are given in section 5.3.

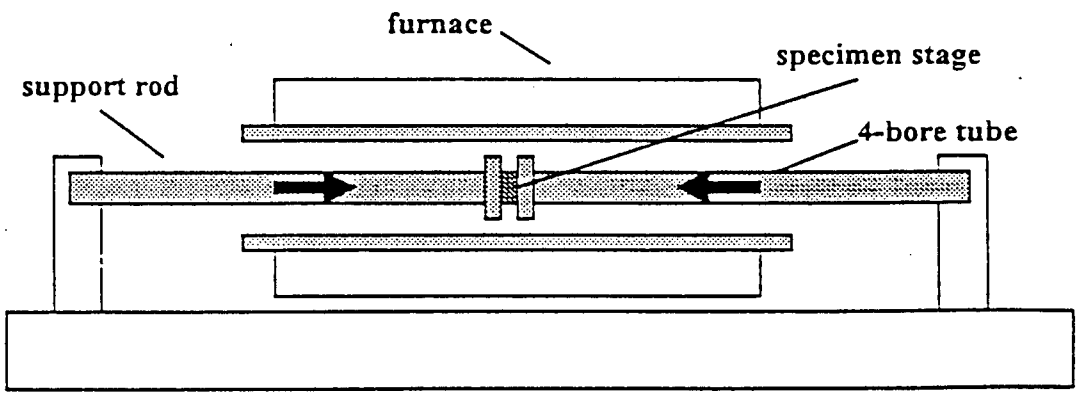

Figure 3.3: Furnace configuration of the apparatus used for measuring electrical resistivity based on the Van der Pauw method (after Smith[19]).

3.5 Measurement of specific heat

Specific heat is an important thermal property and when used in conjunction with the thermal diffusivity can be used to calculate the thermal conductivity of a material. With the future aim of obtaining thermal diffusivity results it was decided to measure the specific heat of the intermetallic specimens using a simple technique.

When heat is added to a system its temperature rises such that dT is proportional to dq. It is more convenient to write this relation as dq = CdT where the constant C is called the heat capacity of the system. The magnitude of C depends on the size and nature of the system and so it is appropriate to talk about the heat capacity of a given mass of material, i.e. the specific heat. Specific heat (c) is therefore defined as the amount of heat required to raise the temperature of a unit mass of material by one degree (either at constant volume or pressure).

The specific heat of a metal can be simply measured using the method of mixtures. A certain mass of metal is heated in a furnace and then placed in a water calorimeter. Heat is transferred from the metal to the water. It follows that:

Heat transferred from metal = Heat transferred to water

$$Q_m = Q_w \qquad \text{Equation 3.3}$$

$$c_m . m_m . \Delta T_m = c_w . m_w . \Delta T_w \qquad \text{Equation 3.4}$$

$$\text{Specific heat of metal } (c_m) = \frac{c_w . m_w . \Delta T_w}{m_m . \Delta T_m} \qquad \text{Equation 3.5}$$

Rods (stainless steel, aluminium, ruthenium aluminide) having the same dimensions were placed in a furnace set at 100°C. Each rod had a type - K sheathed thermocouple attached to it to monitor the temperature.

The rods were then removed separately from the furnace and placed in a calorimeter containing water of known temperature and mass. The temperature of the rod and water were monitored using thermocouples. Since the specific heat of the water is known the specific heat of the metal could be calculated from equation 3.5. The measured specific heats of the aluminium and stainless steel were then compared with known published values to gauge the accuracy of the technique. These results are recorded in section 5.4.

4. CONSTRUCTION OF MEASUREMENT APPARATUS

Crucial to the success of this project was the design and construction of equipment that could measure the thermal conductivity of the intermetallic specimens at room and elevated temperature. The apparatus was required to be simple, robust and inexpensive. Generally the measurement of thermal conductivity is awkward and cumbersome and the apparatus used can be impractical and difficult to work with. This is usually through no fault of the designer but rather due to the numerous physical problems associated with measuring thermal conductivity. These problems are discussed in greater detail below.

During this century researchers have attempted to design practical, simple pieces of equipment for measuring thermal conductivity. Many designs are novel and elegant but many of the problems of measuring thermal conductivity remain.

Tests done on the RuAl, as described in section 3.3, indicated that the material is a good thermal conductor and so an axial heat flow method was considered. The RuAl could be supplied in rod form and so it was decided to measure the thermal conductivity using the modified Forbes bar method based on the apparatus used by Hogan and Sawyer[44]. This apparatus was used successfully to measure the thermal conductivity of stainless steel rod and its construction is detailed below.

4.1 Construction of apparatus based on the Forbes bar method

The original specimen to be measured was a rod of 316 stainless steel with the dimensions, length 200mm and ØD 3.6mm. Copper rod (L=50mm, ØD 3.6mm) was brazed onto each end of the stainless steel rod to act as a heat sink and source. A Nichrome coil was placed around the copper rod acting as the source and insulated from the metal using ceramic cement. A schematic diagram of the test apparatus is shown in figure 4.1

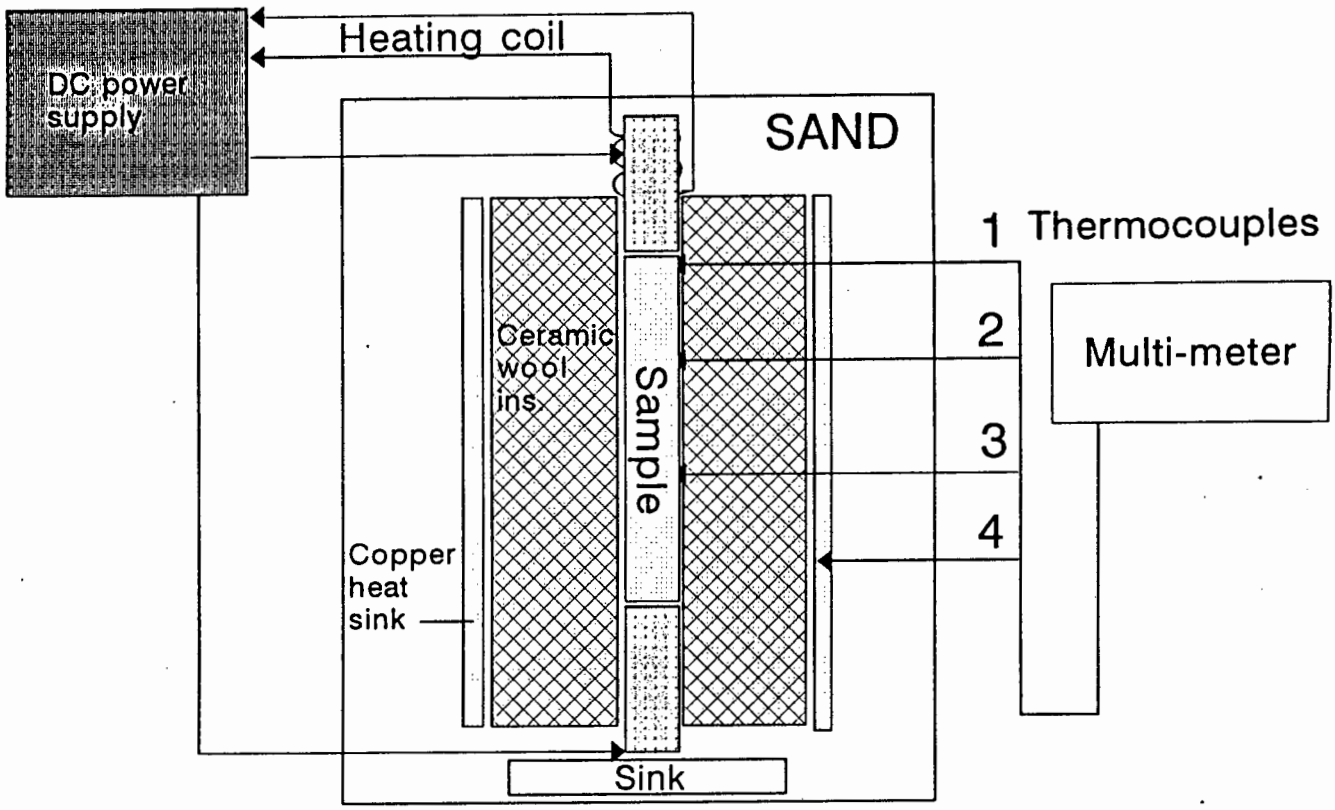

Figure 4.1: Schematic diagram showing test apparatus based on the Forbes Bar method.

Three type-K thermocouples were soldered onto the steel specimen at distances 17mm, 32mm, 80mm from the top of the rod (x=0). The entire specimen was then insulated using a ceramic furnace wool. This insulation was in turn surrounded by a thick copper tube (∅D 75mm) which acted as a heat sink to the lateral heat flow. A fourth thermocouple was attached to the copper tube. The entire apparatus was then insulated in river sand to prevent temperature fluctuations and convection from affecting steady state conditions.

As explained in section 2.3.2 the test method involves two separate experiments. Before each experiment the temperature of all the thermocouples was measured to ensure that the apparatus is in thermal equilibrium In experiment (a), the rod was heated at x=0 using the Nichrome wire coiled around the copper rod (source). The heat input was just sufficient to raise the furthest thermocouple by approximately 1°C above ambient temperature. The temperature gradient along the specimen and the lateral heat flow was then measured by attaching the thermocouples to a Philips PM2535 multimeter. Temperatures could be read to the nearest 0.025°C. A value was then calculated using the equation described in section 2.3.2, namely:

$$a = \left(\frac{x^2}{[\ln(\frac{\Delta t_0}{\Delta t_x})]^2}\right) \qquad \text{Equation 4.1}$$

The heat transfer coefficient (γ) was determined in a separate experiment (experiment b) by heating the rod using an axial current (I). The copper rods at each end of the specimen were attached to a DC power source and a current was allowed to flow through the specimen until a constant temperature was recorded along the sample length. This temperature, as well as the temperature of the copper tube was then recorded. Because of its large heat capacity the copper tube only changed its temperature slightly during the experiment. The current and axial potential gradient were also measured. A value was calculated using the following equation;

$$b = \frac{I}{A}\frac{dV}{dx}\frac{1}{(t_2 - t_1)} \qquad \text{Equation 4.2}$$

The thermal conductivity (k) was then calculated, where;

$$k = (a) \,.\, (b) \qquad \text{Equation 4.3}$$

This apparatus and test method was used successfully to measure the thermal conductivity of the thin rod of 316 stainless steel, giving a value close to that of the published value for the thermal conductivity of 316 stainless steel. Subsequent measurements were performed on a stainless steel rod having the same dimensions as the ruthenium aluminide specimens, namely length 70mm and ØD 15mm. The apparatus was changed slightly so as to accommodate the shorter, thicker specimens. Early experiments gave a value for the thermal conductivity approximately 50 times less than the published value for the thermal conductivity of stainless steel. Numerous changes were made to the measuring apparatus to improve the heat flow through the sample: the insulating material was changed, the heat sink made larger and the outer guard size increased; the attachment of the thermocouples to the specimen was also investigated. Thermocouples were peened into slots and placed into small holes on the surface of the specimen. All these changes did not significantly affect the results and the measured thermal conductivity of the sample remained 50 times less the published value.

After exhaustive experiments it became clear that the specimen dimensions did not conform to the boundary conditions needed to satisfy the thin rod approximation[36] as used by Hogan and Sawyer[44]. This is explained in more detail in chapter 6.

An alternative method had to be found such that the sample dimensions and brittleness would not complicate the experimental technique. A comparative method was chosen and the construction of the apparatus is detailed below.

4.2 Construction of apparatus based on comparative methods

The principle of the comparative method is simple. A uniform heat flow is established through two samples. If the conductivity (k) of one sample (reference) is known and its thermal gradient (ΔT) is determined, the rate of heat flow (q) can be calculated. If the unknown sample is placed in series with the reference material the unknown conductivity can be determined by measuring the thermal gradient in the sample. Lateral heat flow can be reduced by suitable insulation and guard methods.

A well characterised standard reference material of austenitic standard steel (SRM 1461) was purchased from the National Institute of Standards and Technology, U.S.A. This reference material had an outer diameter slightly less than the intermetallic specimens so that the rate of heat flow out of the reference could be assumed to be the same as the rate of heat flow into the sample. The reference material had a length of 50mm and an outer diameter of 12.7mm.

The temperature gradients in the reference and sample were measured using type-K sheathed thermocouples. Sheathed thermocouples gave good contact and were also easier to work with than insulated wires.

The thermocouples were inserted into small holes drilled into the material surface, these holes measured 1.6mm in diameter and were 2mm deep. The cross sectional area of the reference and sample were corrected for this small change. Mirkovich[50] used a heat stabiliser to eliminate heat channelling, however this adds an extra component to the apparatus and adds to the interfacial resistance. In this apparatus a heat stabilising region was left at the top of the reference material . The layout of the thermocouples on the reference and sample is shown in figure 4.2.

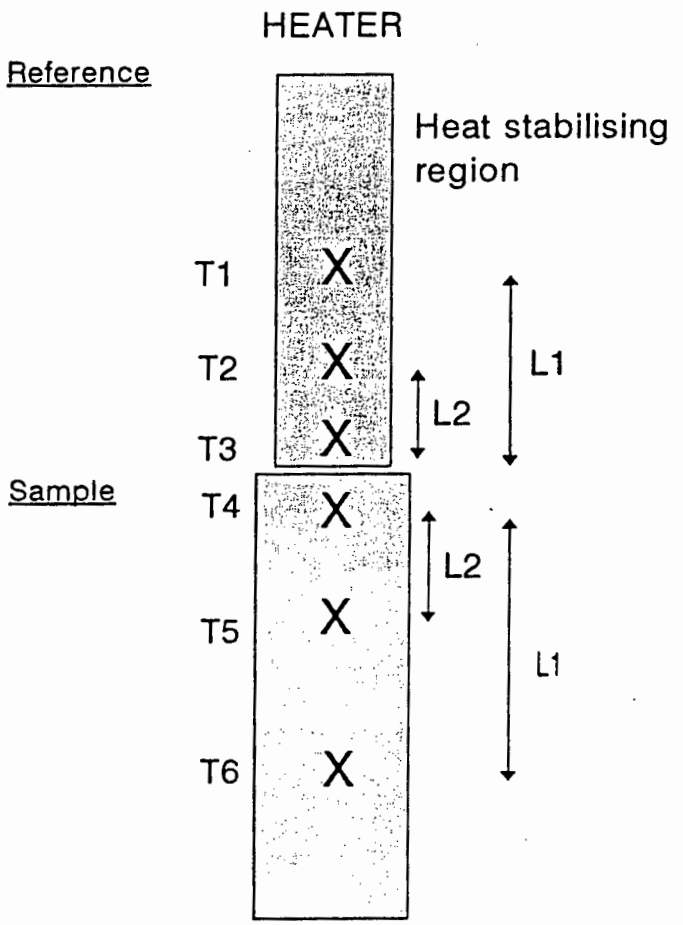

Figure 4.2: Schematic diagram of the thermocouple placement on the reference and sample.

A Nichrome wire heating coil was wound around a stainless steel mandrill and electrically insulated with ceramic cement. The central core of the apparatus consisted of the heating coil, the reference rod aligned in series with the sample to be tested and a copper heat sink. This central core was then clamped together using two ceramic plates and two long rods. All interfaces in the central core were polished to a three micron finish. The interfacial resistance was thus reduced by smooth surfaces and mechanical loading.

An alumina guard with an outer diameter of 75mm and a length of 200mm was placed around the central core. The space between the guard and core was insulated using silica and ceramic wool. Both ends were closed off by ceramic plates which were then bolted together. The thermocouple wires extended out of a hole in the top plate.

Heat guarding, achieved by matching the temperature of the heat guard to that of the reference and sample on the same level, was controlled by two heaters. These heaters were wound around the outside of the alumina guard tube. For elevated temperature measurements the entire apparatus was placed in a Naber furnace. All exposed wiring was insulated using ceramic beads. The complete apparatus is shown in figure 4.3.

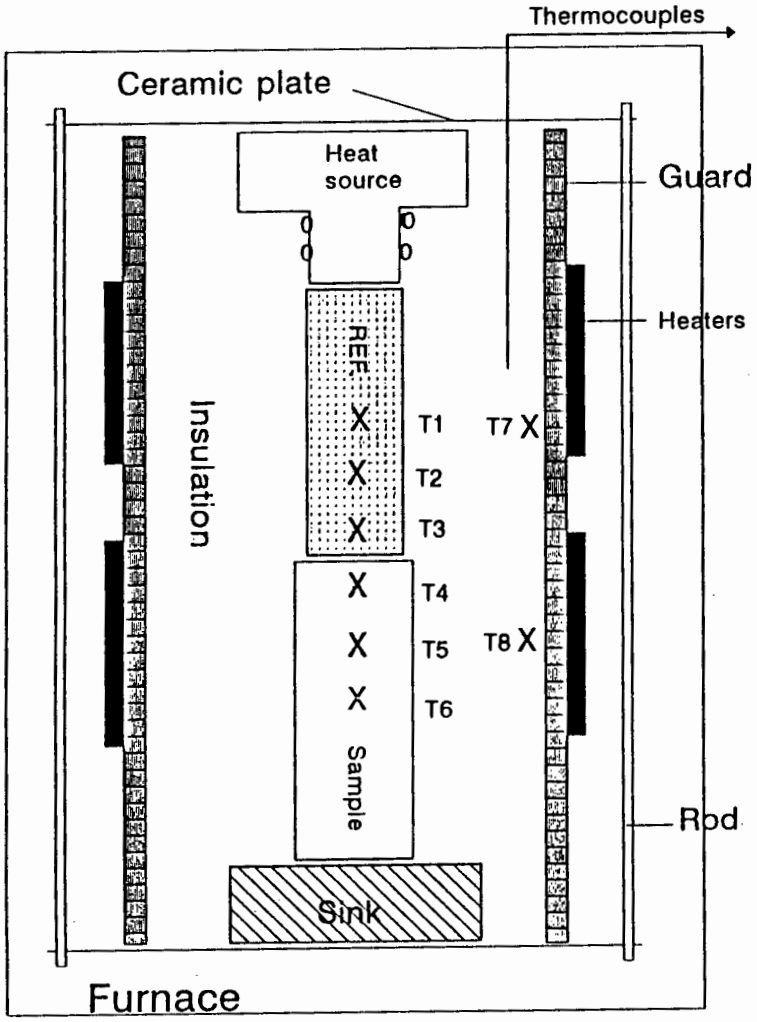

Figure 4.3: Schematic diagram of the test apparatus based on a comparative method.

Before testing began all thermocouples were checked to ensure that the apparatus was in thermal equilibrium. For room temperature measurements, a current of approximately 1A was put through the heating coil. This raised the last thermocouple a few degrees above ambient temperature. The guard heaters were adjusted until the thermocouples on the guard tube matched the temperatures on the corresponding points on the reference and sample (±1°C). After about four hours all thermocouples were in equilibrium and measurements were taken.

For the elevated temperature measurements the apparatus was placed in a furnace which was then set at the desired temperature. The equipment was left at the desired temperature for at least twelve hours so that good thermal equilibrium could be obtained. After this the heating coil was switched on and the test method repeated. At increasing temperatures it became more and more difficult to match the guard temperatures with that of the sample and reference. It was often found that the guard was at a higher temperature than the sample itself even when the guard heating coils were off. Temperature fluctuations in the furnace itself further frustrated the elevated temperature measurements. With care however, good results were obtained for the apparatus in the temperature range 25 - 500°C. These results are given in section 5.2. Photographs of the actual test apparatus are shown in figures 4.4, 4.5 and 4.6.

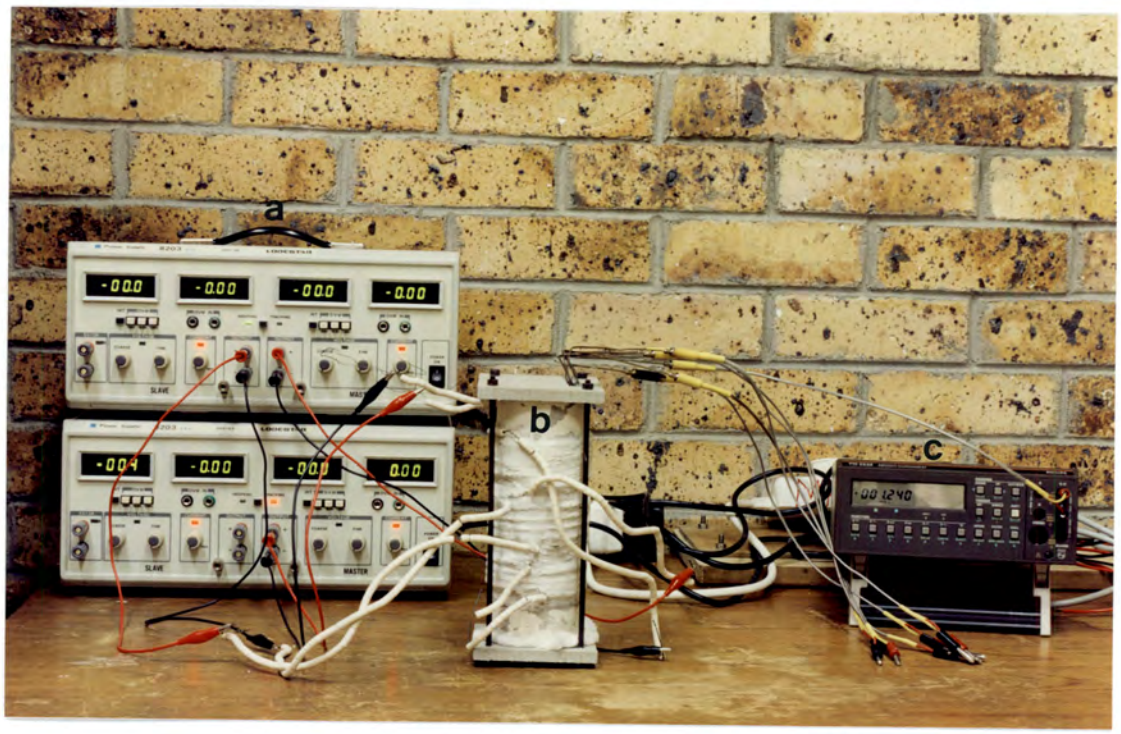

Figure 4.4: Photograph of complete test set-up for the measurement of the thermal conductivity of intermetallic compounds. DC power supply (a), test apparatus (b), multi-meter (c).

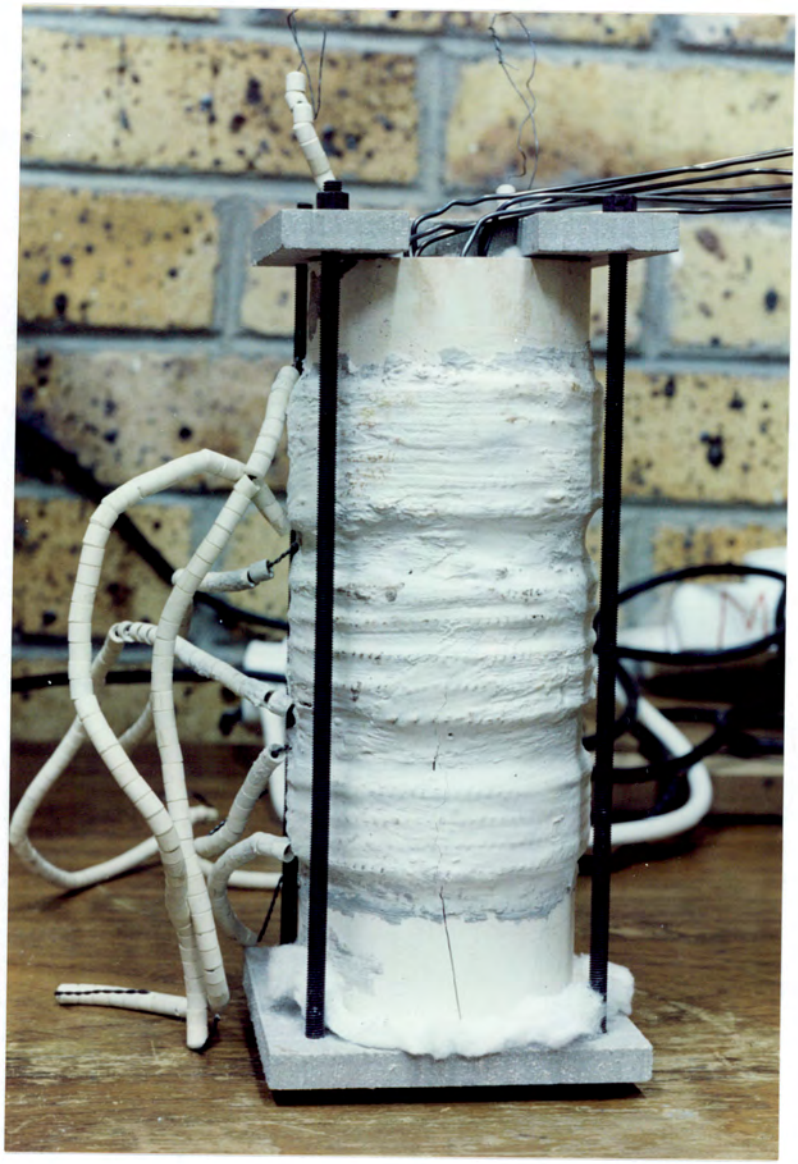

Figure 4.5: Photograph of alumina guard containing heating coils.

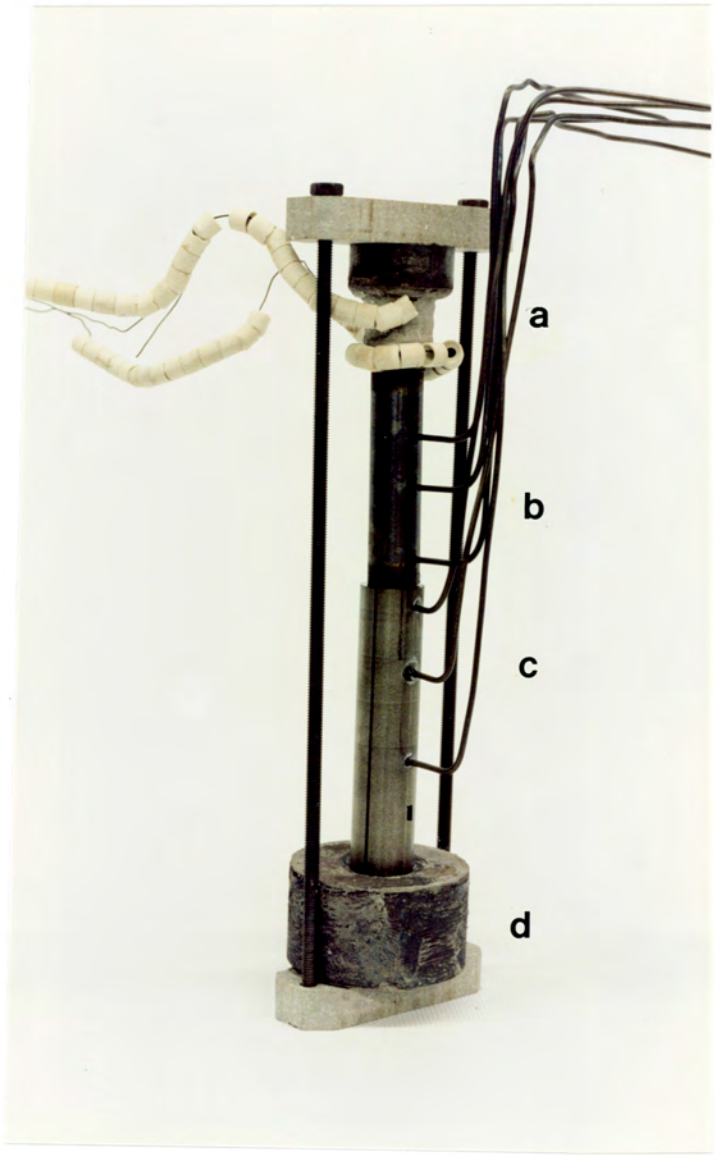

Figure 4.6: Photograph of the central core of the test apparatus showing heater (a), reference (b), sample (c) and heat sink (d).

5. RESULTS

Results presented in this section include specimen characterisation, thermal conductivity measurements, electrical conductivity measurements and specific heat measurements. The test methods employed have been described in chapter 3 and the results are discussed in greater detail in chapter 6.

5.1 Specimen characterisation

The results of the microstructural and energy dispersive spectrometry (EDS) examination of the specimens are presented in this section and provide the background to the thermal and electrical results which are presented later in the chapter. The thermal conductivity and electrical conductivity of materials is not only dependent on the chemical composition of the materials involved but also on the phases present, the distribution of phases and manufacturing defects such as porosity. Light microscopy and scanning electron microscopy was used to investigate and characterise the microstructure of each sample. EDS was used to identify the phases present in the materials as well as to confirm the nominal compositions of the test specimens. A summary of the test specimens is given in table 5.1 below.

Sample	Composition	Processing	Treatment
R94	$Ru_{53}Al_{47}$	30% pr-reacted powder - RHIP	-
R160	$Ru_{50}Al_{50}$	30% pr-reacted powder - RHIP	Homogenised at 1500°C for 12hrs
R161	$Ru_{47}Al_{53}$	30% pr-reacted powder - RHIP	Homogenised at 1500°C for 12hrs
TiAl	$Ti_{48}Al_{52}$	Cast	-

Table 5.1: Summary of test samples and their processing routes.

$Ru_{53}Al_{47}$

The microstructure of the $Ru_{53}Al_{47}$ specimen, shown in figures 5.1 and 5.2, shows the presence of two phases, the majority dark phase being ruthenium aluminide and the secondary light phase, hexagonal closed packed α-ruthenium. Fleischer[15] noted similar microstructures in ruthenium rich arc melted specimens with the α-ruthenium phase as an intergranular eutectic. The dark spots on the micrographs are an indication of the porosity in the specimens.

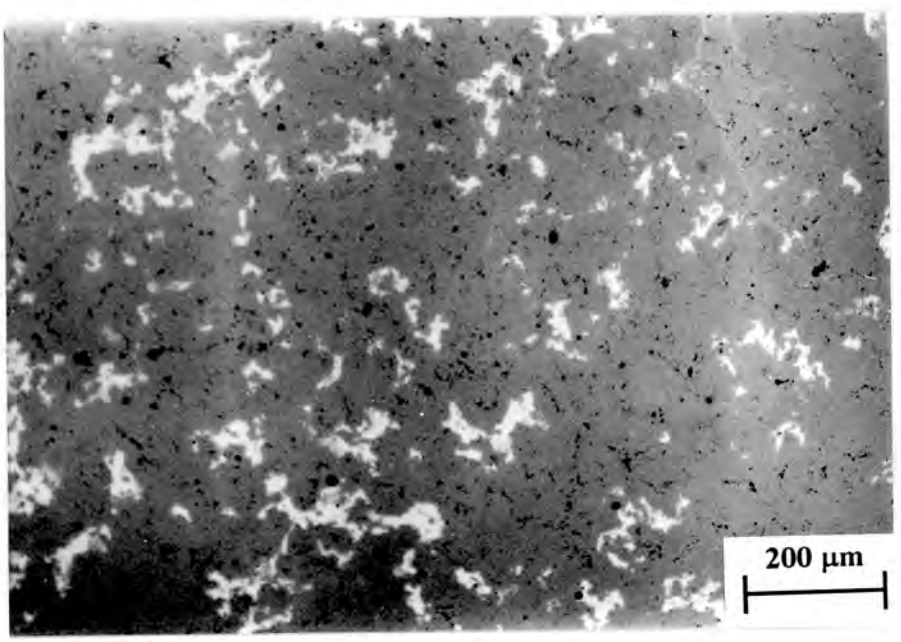

Figure 5.1 Light micrograph of $Ru_{53}Al_{47}$ specimen showing the presence of two phases. The dark majority phase is ruthenium aluminide and the light minority phase α-ruthenium. Dark spots represent porosity.

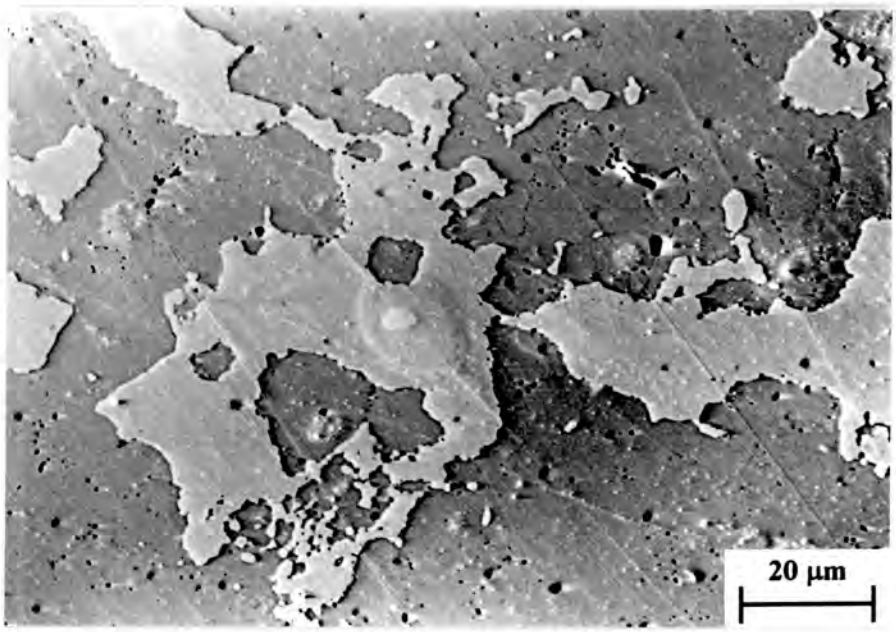

Figure 5.2: Scanning electron micrograph of $Ru_{53}Al_{47}$ showing the presence of two phases and the degree of porosity in the specimen.

Figures 5.3 and 5.4 show the energy dispersive spectroscopy (EDS) analysis of the two phases present in the $Ru_{53}Al_{47}$ specimen. The light phase consists of ruthenium and aluminum while the dark phase is almost entirely ruthenium.

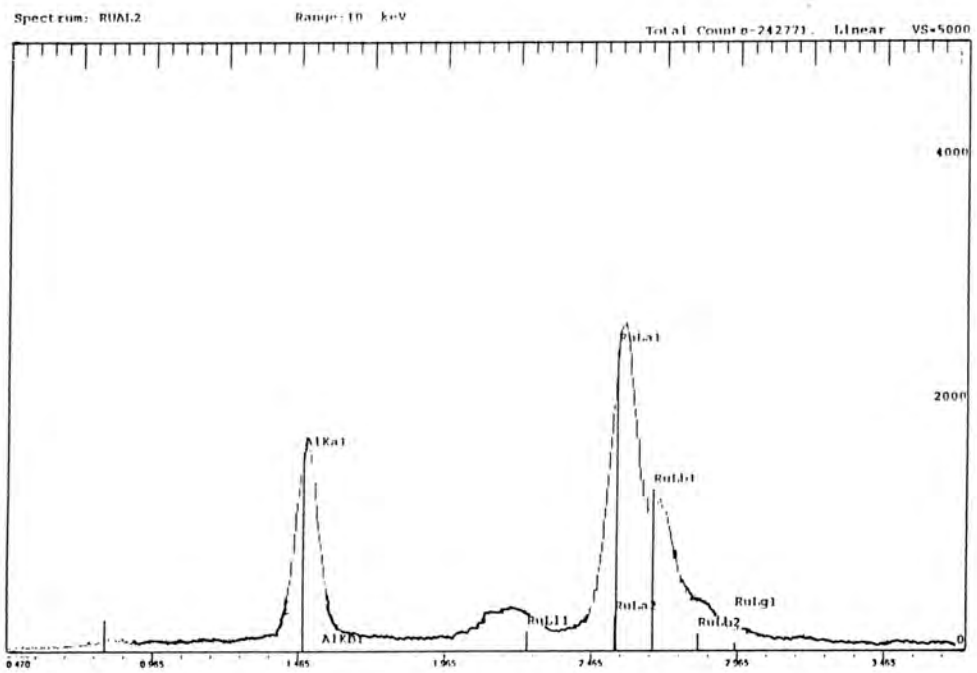

Figure 5.3: EDS scan of dark phase present in $Ru_{53}Al_{47}$ specimen confirming the presence of RuAl.

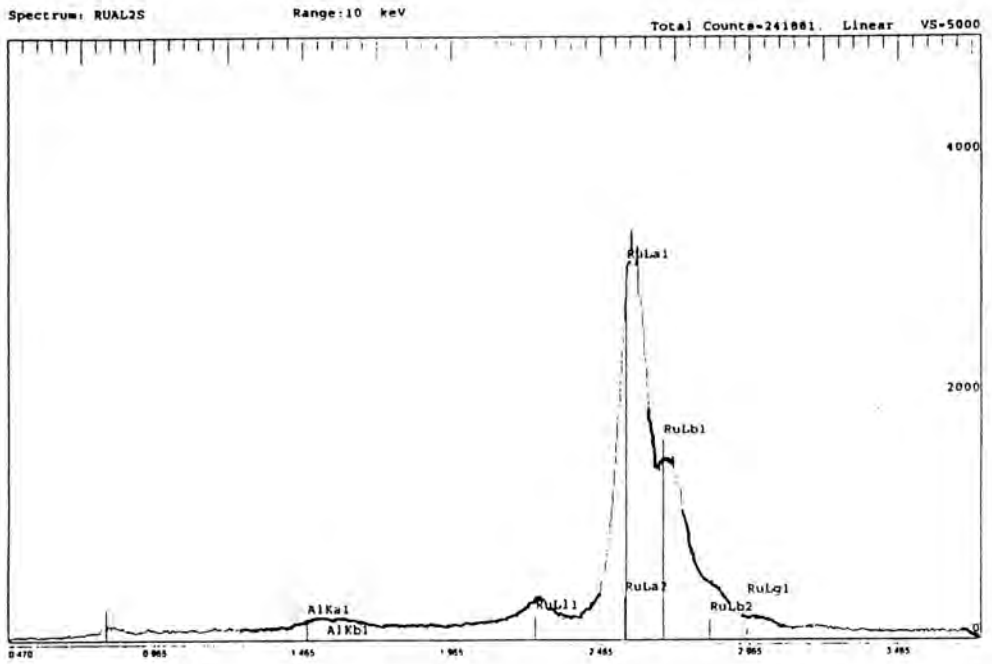

Figure 5.4: EDS scan of light phase present in $Ru_{53}Al_{47}$ specimen confirming the presence of α-ruthenium.

$Ru_{50}Al_{50}$

The microstructure of the $Ru_{50}Al_{50}$ specimen, shown in figures 5.5 and 5.6, again shows the presence of two phases. The light α-ruthenium phase is less than that recorded in the $Ru_{53}Al_{47}$ specimen which is consistent with the reduced amount of ruthenium in the specimen. EDS confirmed the identity of the two phases and the scans were similar to those recorded for the $Ru_{53}Al_{47}$ specimen.

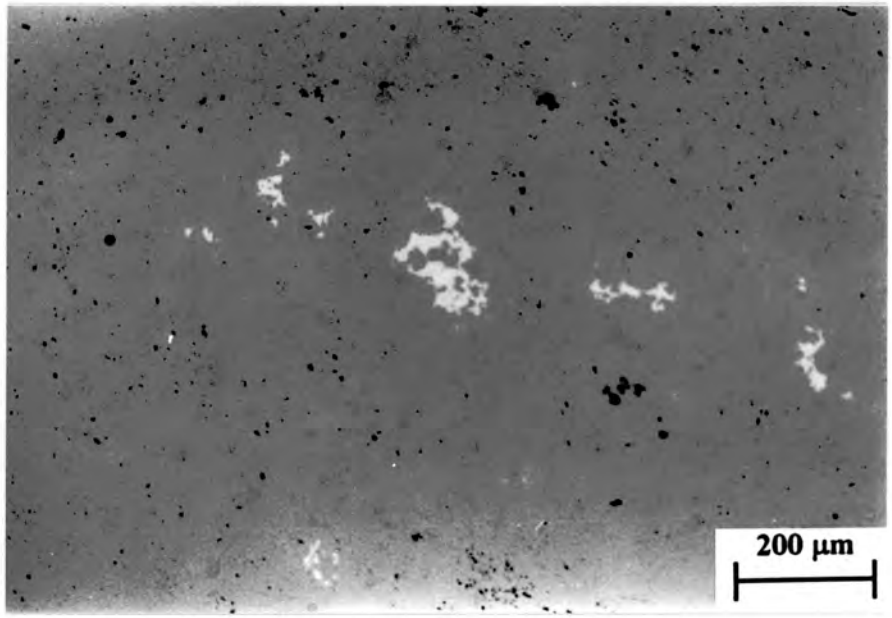

Figure 5.4 Light micrograph of $Ru_{50}Al_{50}$ specimen showing the presence of two phases. The dark majority phase is ruthenium aluminide and the light minority phase α-ruthenium. Dark spots represent porosity.

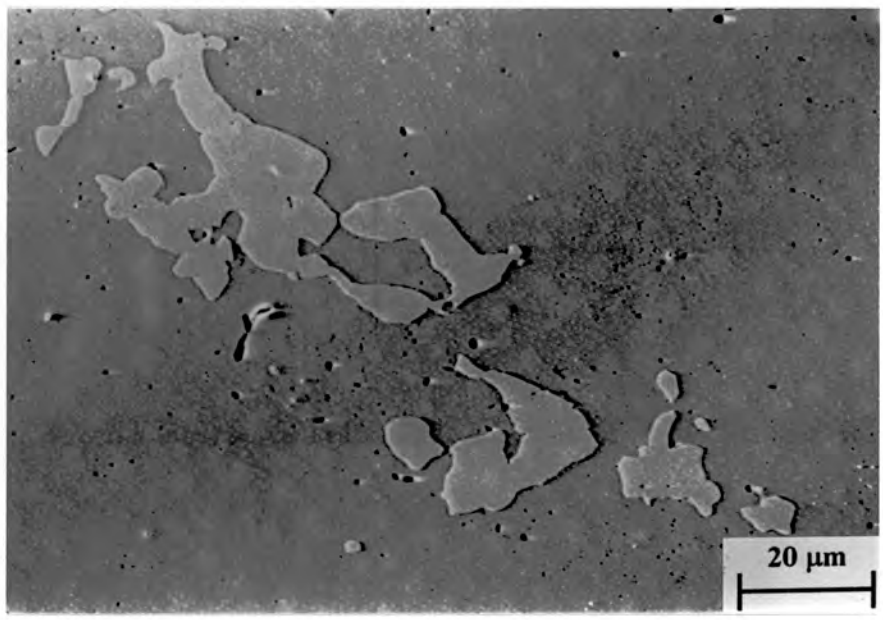

Figure 5.6: Scanning electron micrograph of $Ru_{50}Al_{50}$ showing the presence of the two phases and degree of porosity in the specimen.

$Ru_{47}Al_{53}$

The micrographs of the $Ru_{47}Al_{53}$ specimen, shown in figures 5.7, 5.8, and 5.9, show the presence of only one phase. No α-ruthenium phase is present and this is consistent with the reduced amount of ruthenium in this specimen.

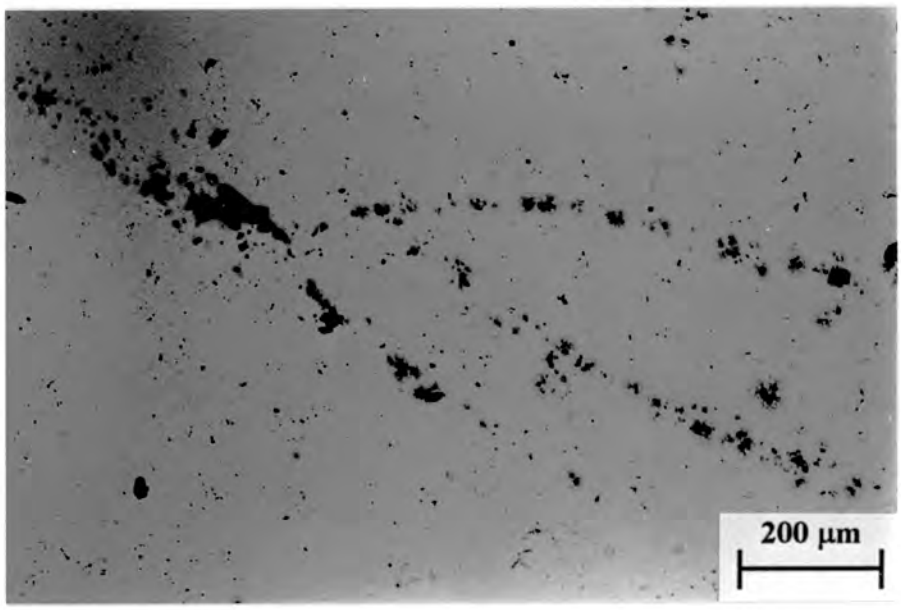

Figure 5.7: Light micrograph of $Ru_{47}Al_{53}$ showing the presence of single phase ruthenium aluminide and an increase in porosity.

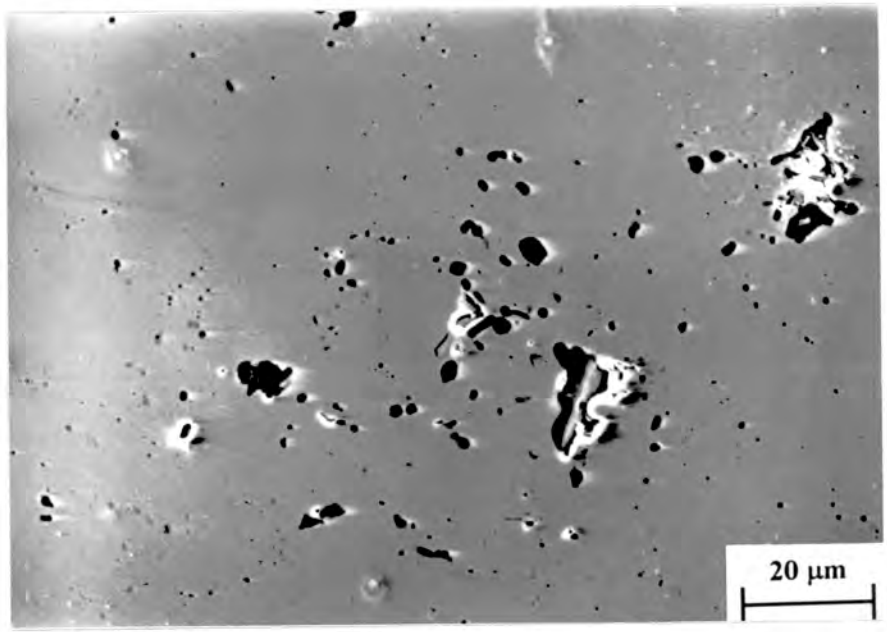

Figure 5.8 : Scanning electron micrograph of $Ru_{47}Al_{53}$ showing the presence of a single phase and the increased amount of porosity in the specimen.

The increased amount of aluminium in this compound has a deleterious effect on the sample. Porosity has increased dramatically and grain boundary cracking is evident, as shown in figure 5.9. This confirms Fleischers[15] observation that aluminium-rich compositions are intergranularly brittle and have low toughness. The brittleness of this compound made sample preparation extremely difficult.

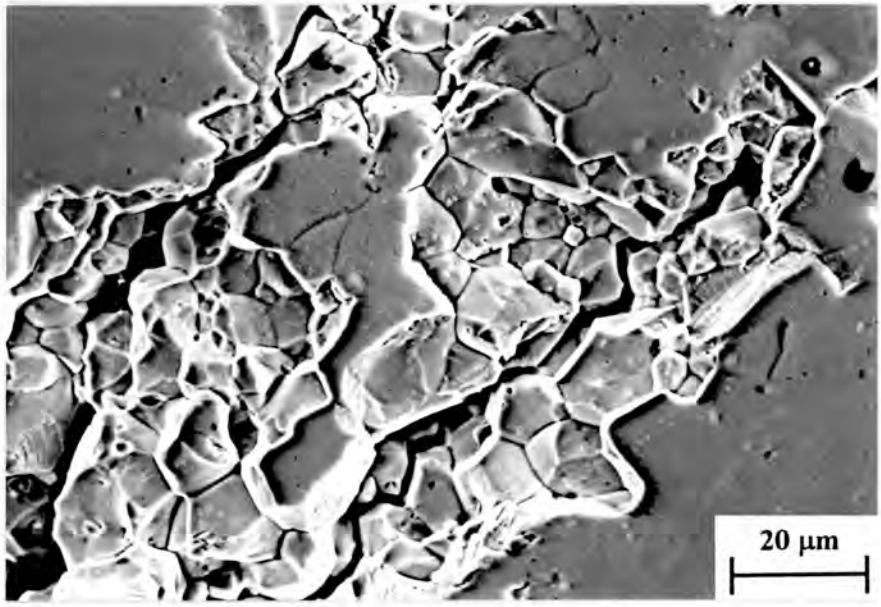

Figure 5.9: Scanning electron micrograph of $Ru_{47}Al_{53}$ showing grain boundary cracking.

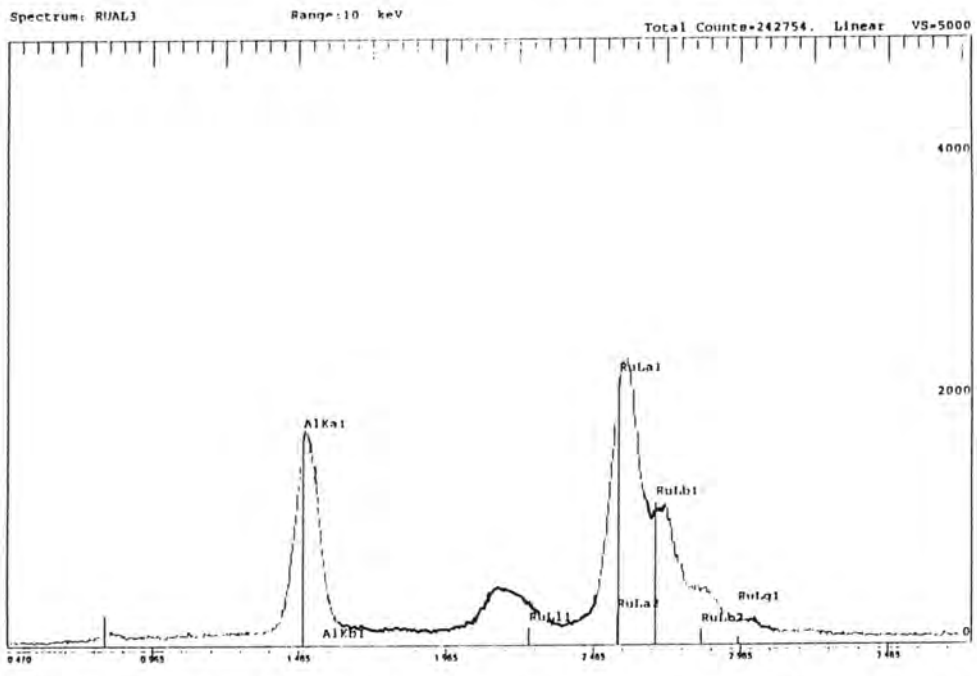

Figure 5.10: EDS scan of the single phase present in the $Ru_{47}Al_{53}$ specimen confirming the presence of ruthenium aluminide.

$Ti_{48}Al_{52}$

The macrostructure of the cast titanium aluminide ingot consisted of a rim of columnar grains and a central region of equiaxed grains. The test specimen was wire cut from the equiaxed region of the ingot. The microstructure of the sample consists mainly of equiaxed γ grains as shown in figures 5.11.

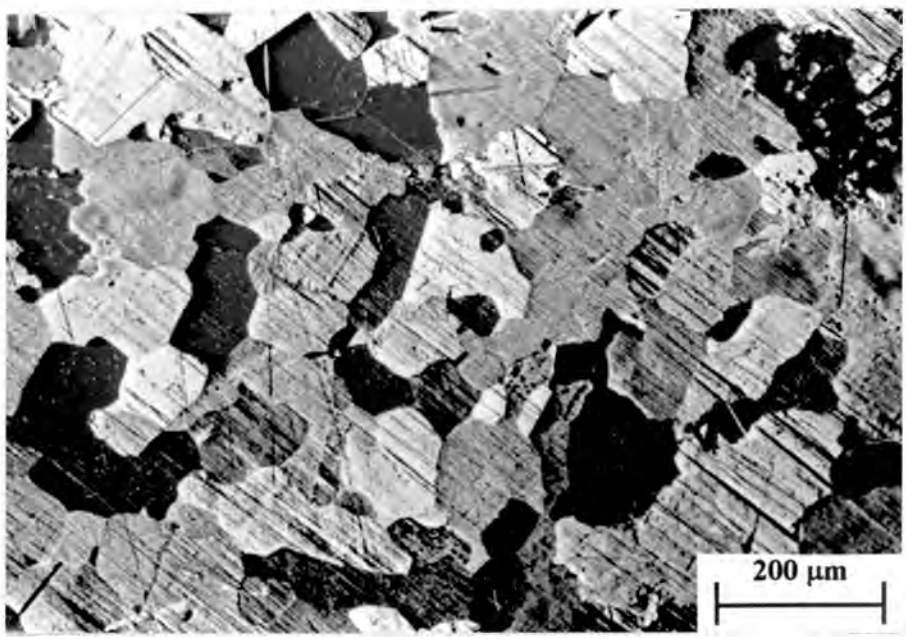

Figure 5.11: Scanning electron micrograph of $Ti_{48}Al_{52}$ showing equiaxed γ grains.

The EDS scan of the $Ti_{48}Al_{52}$ specimen, shown in figure 5.12, shows the presence of titanium and aluminium. Trace amounts of niobium, an alloying element, are also present. Each grain visible in the micrographs shows the same composition and the different contrast of each grain is therefore due to the crystalographic orientation of the grains.

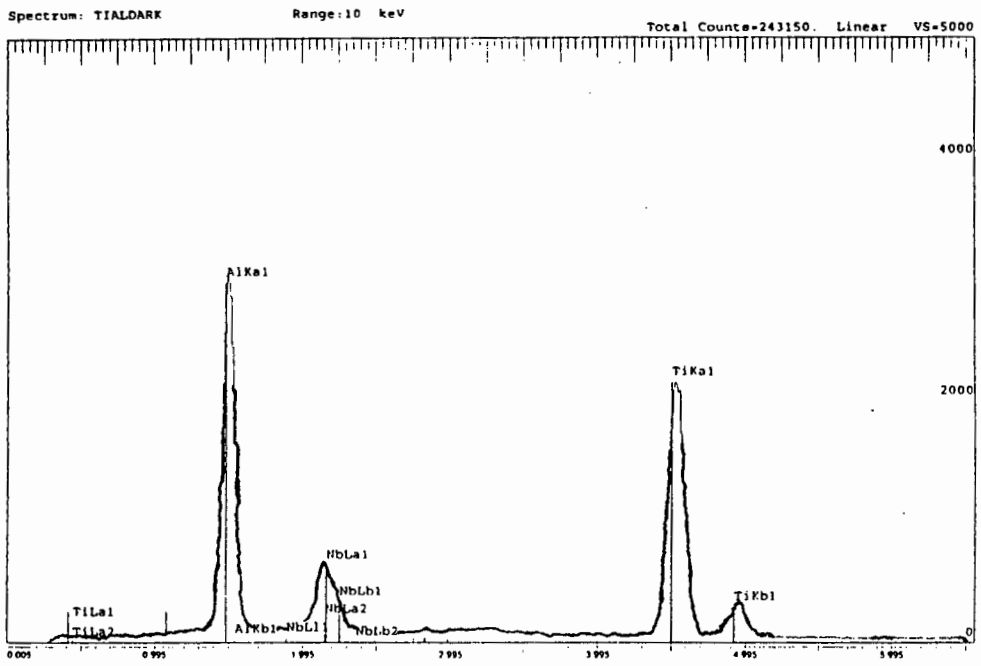

Figure 5.12: EDS scan of $Ti_{48}Al_{52}$ specimen confirming the presence of titanium aluminide.

To summarise, the ruthenium aluminide specimens contain different amounts of ruthenium and aluminium. The microstructures of the samples contain different amounts of α-ruthenium. The ruthenium rich specimen, $Ru_{53}Al_{47}$, contains the most α-ruthenium while the aluminum rich sample, $Ru_{47}Al_{53}$, contains no α-ruthenium. The stiochiometric combination of ruthenium and aluminum contains some α-ruthenium. The identity of the light α-ruthenium phase was confirmed by EDS analysis while the dark matrix was confirmed to be ruthenium aluminide. The microstructure of the aluminum rich sample was mechanically deleterious in terms of porosity and grain boundary cracking. The titanium aluminide specimen, $Ti_{48}Al_{52}$, consisted of equiaxed γ grains.

5.2 Thermal conductivity

The thermal conductivity results are divided into three sections. The first section consists of the early experiments based on Ingenhausz's wax experiment[31]. These tests were carried out so as to gain an approximate value for the thermal conductivity of the ruthenium aluminide specimen. The next section deals with the results of the experiments based on the Forbes method used by Hogan and Sawyer[44]. In these tests the thermal conductivity of stainless steel rod of varying dimensions was compared to the published values for stainless steel rod. The final section contains the results of the thermal conductivity of the intermetallic specimens using a comparative method.

5.2.1 Ingenhausz's wax experiment

The test method is described in more detail in section 3.3. In Ingenhausz's original experiment[31] the following equation is valid:

$$\frac{k_a}{k_b} = \left(\frac{x_a}{x_b}\right)^2$$

where x is the distance to which the wax melts in the two specimens. The thermal conductivity of the unknown specimen is therefore:

$$k_a = \left(\frac{x_a}{x_b}\right)^2 k_b$$

Two samples, namely 316 stainless steel and D65S aluminium, having the same dimensions as the ruthenium aluminide rod (∅D 16mm and length 70mm) were used to obtain a comparative value for the thermal conductivity of the ruthenium aluminide.

The measured values obtained for the thermal conductivity of the stainless steel and aluminium rod were similar to the published values for the thermal conductivity of these materials. It is therefore reasonable to assume that the value obtained for the thermal conductivity of the ruthenium aluminide specimen is correct within the experimental error of the experiment.

The measured thermal conductivity of the ruthenium aluminide rod was found to be **70±10 $W.m^{-1}.K^{-1}$.** This means that ruthenium aluminide is a good thermal conductor and so an appropriate measuring technique must be employed.

5.2.2 Forbes bar method.

The test method adopted here was based on the experimental work of Hogan and Sawyer[44] and is described in more detail in section 4.1. In experiment (a), the rod is heated at x=0 using Nichrome wire coiled around the copper rod (source). The temperature gradient along the specimen is then measured and a value calculated using the equation described in section 2.3.2, namely:

$$a = \left(\frac{x^2}{\left[\ln\frac{\Delta t_0}{\Delta t_x}\right]^2}\right)$$

The heat transfer coefficient (γ) is determined by heating the rod using an axial current (I), experiment (b). The source and sink at either end of the specimen are attached to a DC power source and a constant temperature recorded along the sample length. This temperature, as well as the temperature of the copper tube is then recorded. The current and axial potential gradient are also measured. A value is then calculated using the following equation:

$$b = \frac{I}{A}\frac{dV}{dx}\frac{1}{\left(t_2 - t_1\right)}$$

The thermal conductivity (k) was then calculated, where:

$$k=(a).(b)$$

The initial tests were carried out on stainless steel rod having similar dimensions as that used by Hogan and Sawyer[44], namely, ØD 1.8mm and length 200mm. The measured results of **15-20 $W.m^{-1}.K^{-1}$** agree with the published value of 14-16$W.m^{-1}.K^{-1}$ for 316 stainless steel[56].

The apparatus was then adapted to accomodate specimens having the same dimensions as the ruthenium aluminide samples. Tests were conducted on stainless steel rod measuring ØD 16mm and length 70mm. The measured results of approximately **0.3 $W.m^{-1}.K^{-1}$** clearly do not reflect the published values for 316 stainless steel. Numerous changes were made to the apparatus and exhaustive tests were conducted but the results remained the same, approximately 50 times smaller than the published values. Obviously the sample dimensions of the larger sample were having a deleterious effect on the measured results. This is discussed in detail in chapter 6. Since the dimensions of the intermetallic specimens could not be changed and the Forbes bar method seemed inappropriate, a comparative method was adopted to measure the thermal conductivity of the intermetallic specimens.

5.2.3 Comparative results

As described in section 2.3.2, comparative measurements compare the conductivity of an unknown material with that of a known standard. The most common method is to place the unknown and standard samples in series, with the same rate of heat flow through both[48]. The test method and apparatus is described in detail in section 4.2.
From equation 2.6 it follows that:

$$k_{sample} = k_{ref} \frac{A_r\left(\frac{\Delta T}{\Delta x}\right)_r}{A_s\left(\frac{\Delta T}{\Delta x}\right)_s}$$

The thermal conductivity of the reference material, austenitic stainless steel, is given in figure 5.13. The data used to construct the graph in figure 5.13 was supplied by the National Institute of Standards Technology, USA and was used to determine the unknown thermal conductivity of the intermetallic specimens. The supplied data is shown in the appendix.

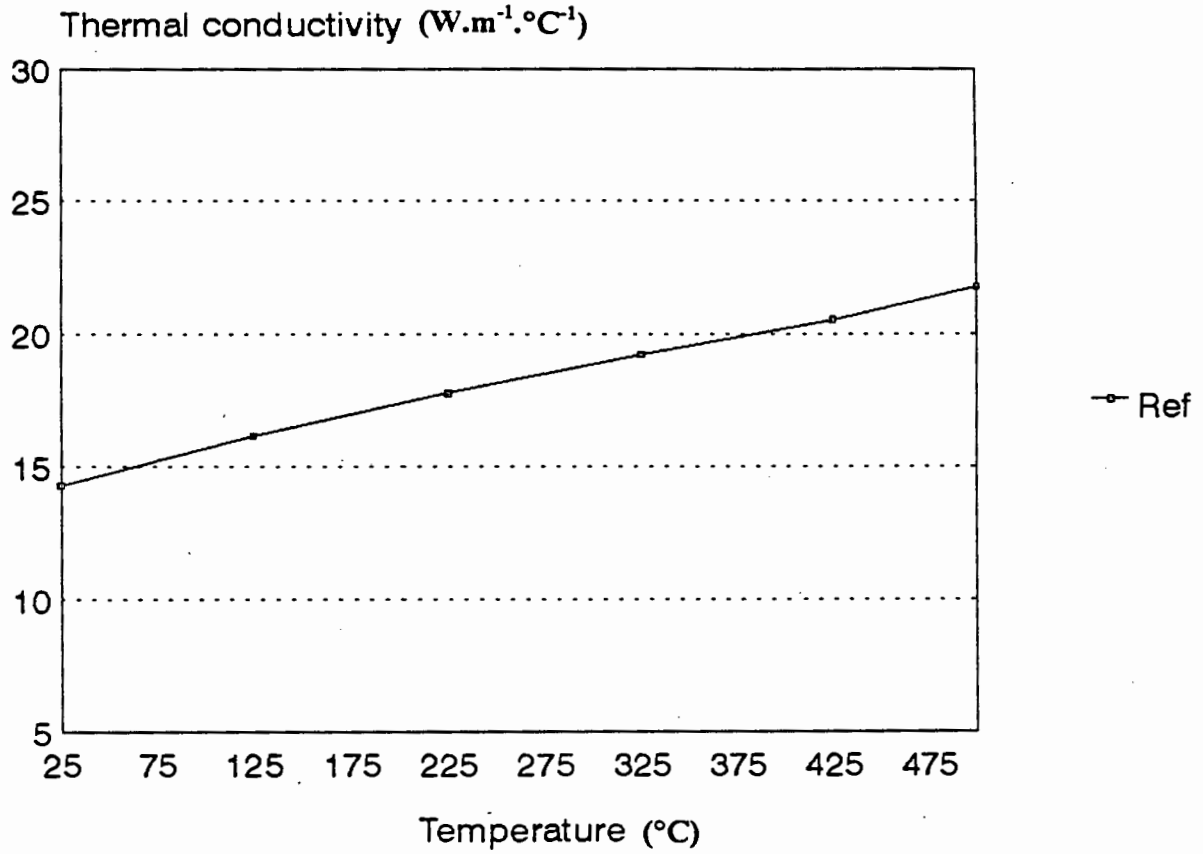

Figure 5.13: Thermal conductivity of reference austenitic stainless steel vs temperature. Data supplied by the National Institute of Standards and Technology, USA.

As before, tests were conducted on 316 stainless steel having the same dimensions as the intermetallic specimens, so as to determine the accuracy of the apparatus. These results are presented in figures 5.14 and 5.15.

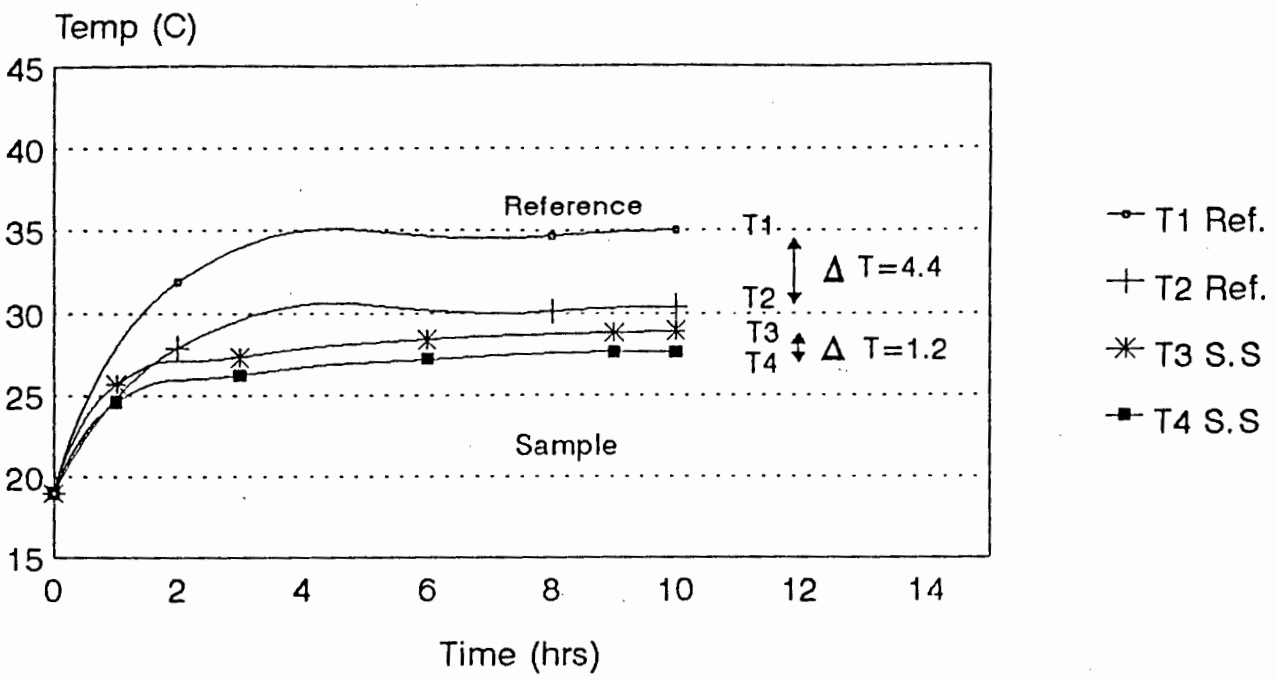

Figure 5.14: Temperature in reference and 316 stainless steel sample vs time, illustrating the establishment of a thermal gradient.

Figure 5.14 shows the temperature in the reference material and the stainless steel sample vs time. Before the heating coil is turned on all the thermocouples are at the same temperature, ie the apparatus is in thermal equilibrium. After about three hours the thermocouples reach a new equilibrium showing a thermal gradient in the reference and sample. By using this thermal gradient the thermal conductivity of the stainless steel specimen was calculated. The measured value agrees with the published value for the room temperature thermal conductivity of 316 stainless steel, as shown in figure 5.15.

Figure 5.15 shows the measured thermal conductivity of the stainless steel vs temperature. These results are compared with the values supplied for the austenitic stainless steel reference material. The measured results are in within 5% of the reference values and it is reasonable to assume that the apparatus is measuring consistently and accurately.

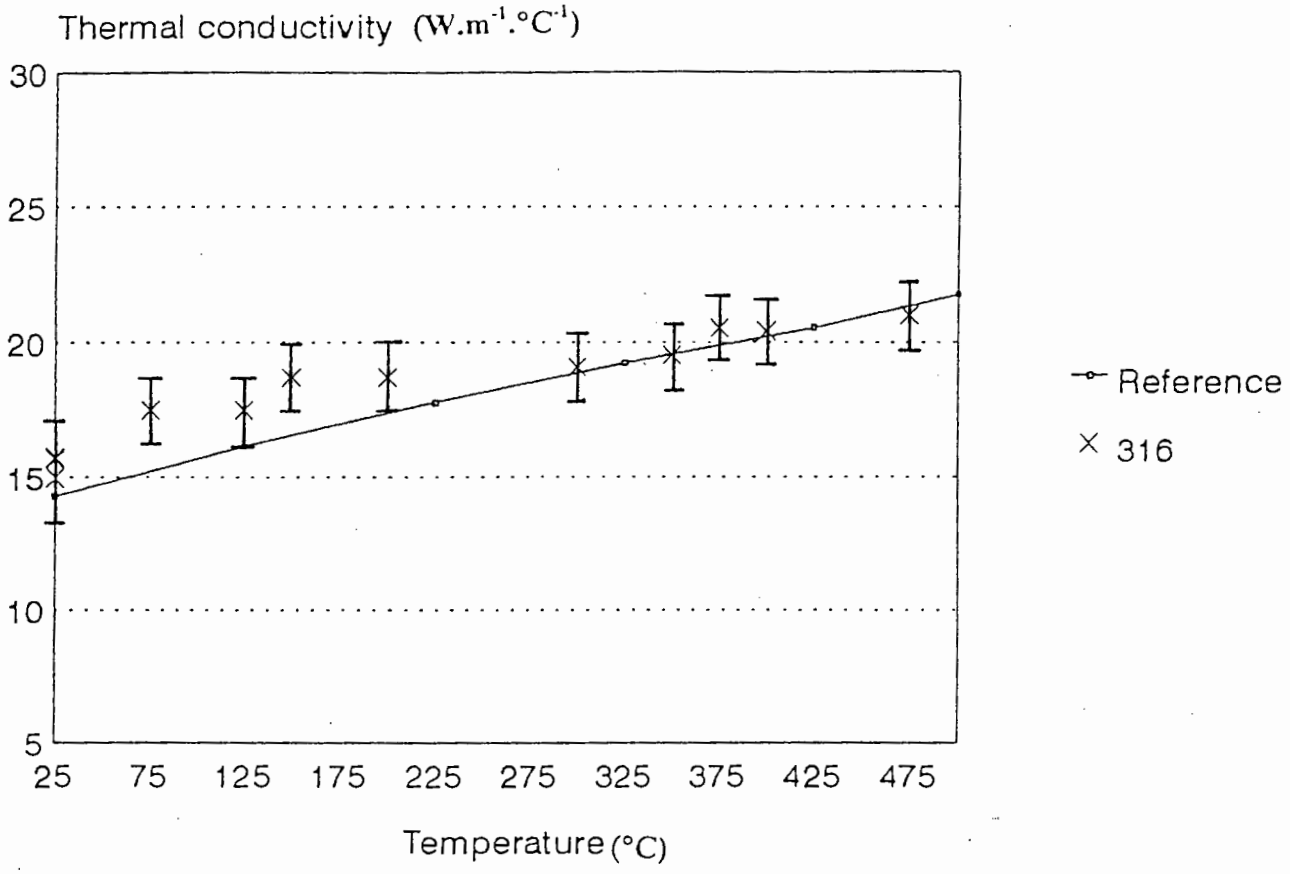

Figure 5.15: Measured thermal conductivity of 316 stainless steel vs temperature as compared with reference stainless steel.

The thermal gradients in the reference and ruthenium aluminide sample show a similar trend to that observed in the stainless steel sample, as shown in figure 5.16. Before the heating coil is turned on all the thermocouples are at the same temperature. Once the heating coil is turned on the thermocouples reach a new equilibrium after about three hours. The thermal gradient between the thermocouples in the ruthenium aluminide sample is smaller than the thermal gradient in the stainless steel sample. This is to be expected since the thermal conductivity of the ruthenium aluminide sample is greater than the stainless steel sample, as measured in section 5.2.1.

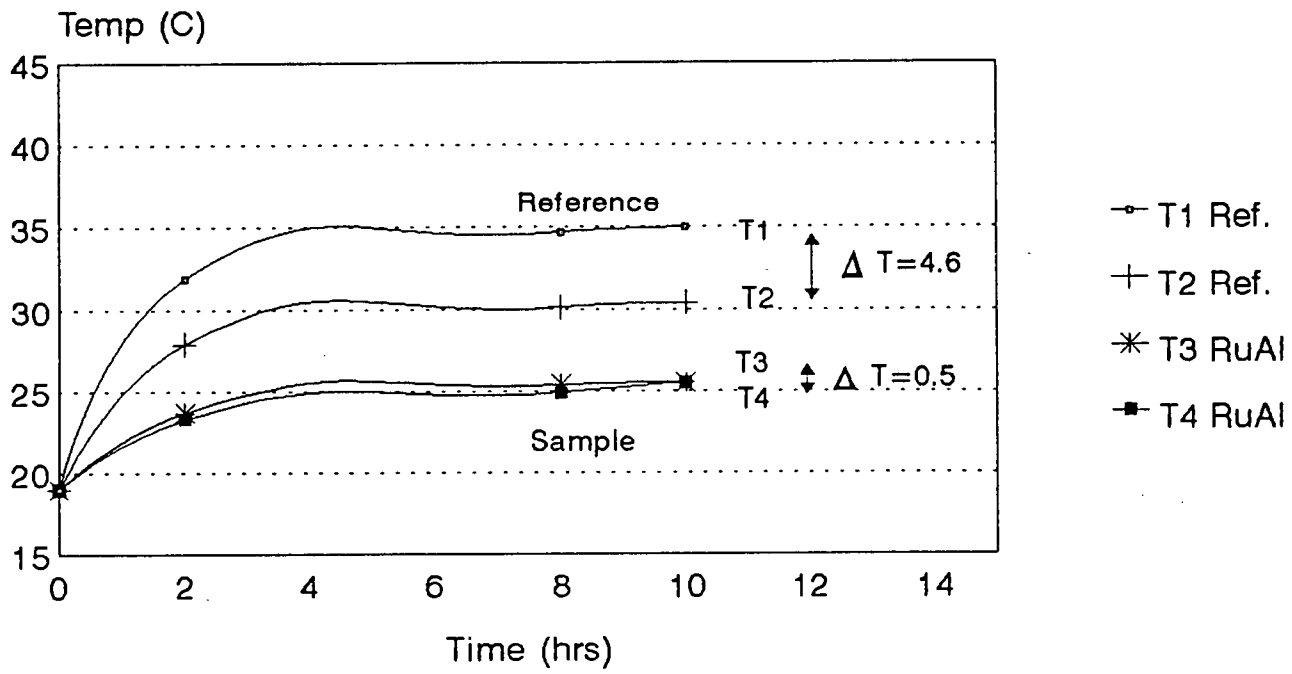

Figure 5.16: Temperature in reference and ruthenium aluminide sample vs time, illustrating the etablishment of a thermal gradient.

The following pages contain the measured thermal conductivities of the four intermetallic specimens from room temperature up to 500°C. The test procedure and apparatus is described in detail in section 4.2. In each test the measuring apparatus and sample were left in a furnace for twelve hours to reach thermal equilibrium. After this the heating coil was turned on. After 4 hours the thermal gradients in the reference and sample were measured and the unknown thermal conductivities calculated.

$Ru_{53}Al_{47}$

The thermal conductivity of the $Ru_{53}Al_{47}$ specimen vs temperature is shown in figure 5.17. There is an increase in the thermal conductivity of the specimen with increasing temperature.

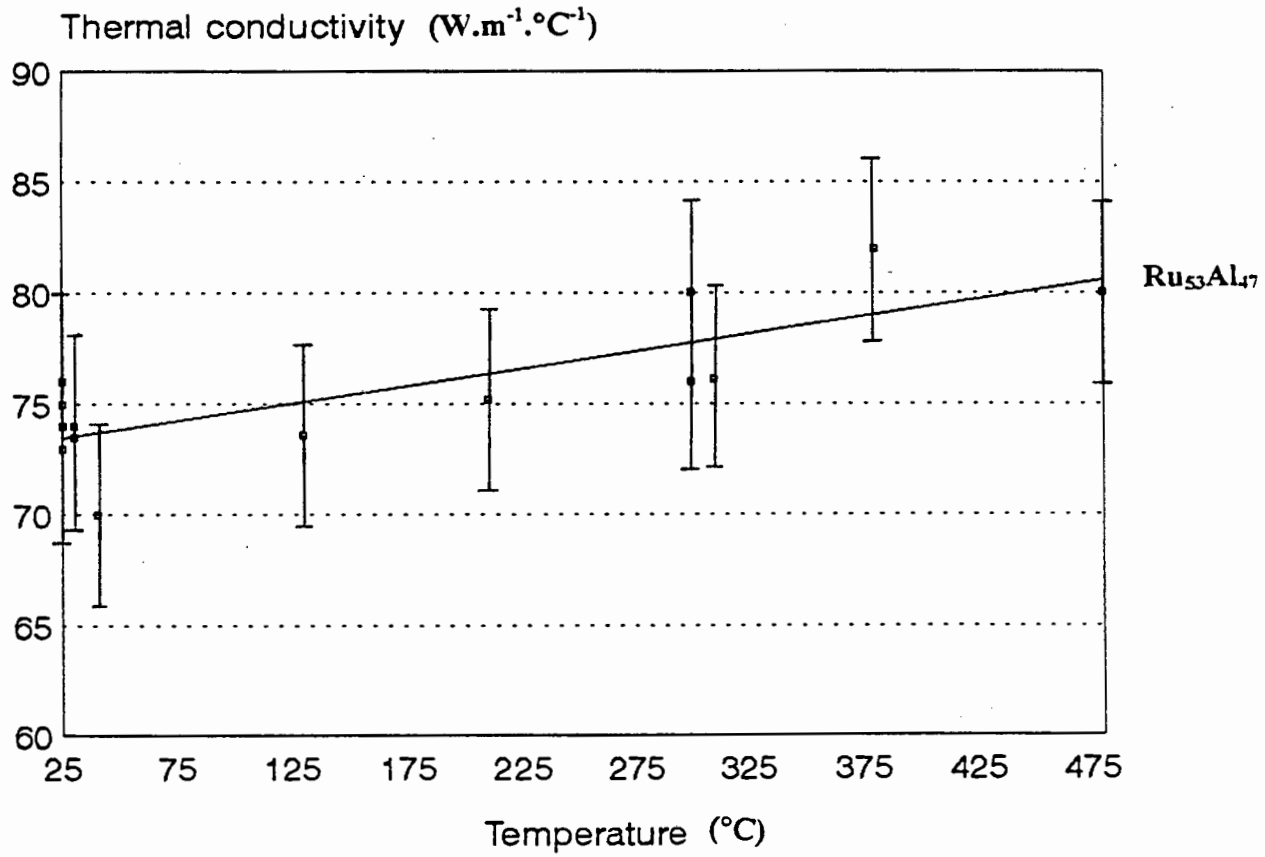

Figure 5.17: Thermal conductivity of $Ru_{53}Al_{47}$ specimen vs temperature.

$Ru_{50}Al_{50}$

The measured thermal conductivity of $Ru_{50}Al_{50}$ vs temperature is shown in figure 5.18. Again the thermal conductivity of the specimen increases with increasing temperature. The measured results are similar to those recorded for the $Ru_{53}Al_{47}$ specimen.

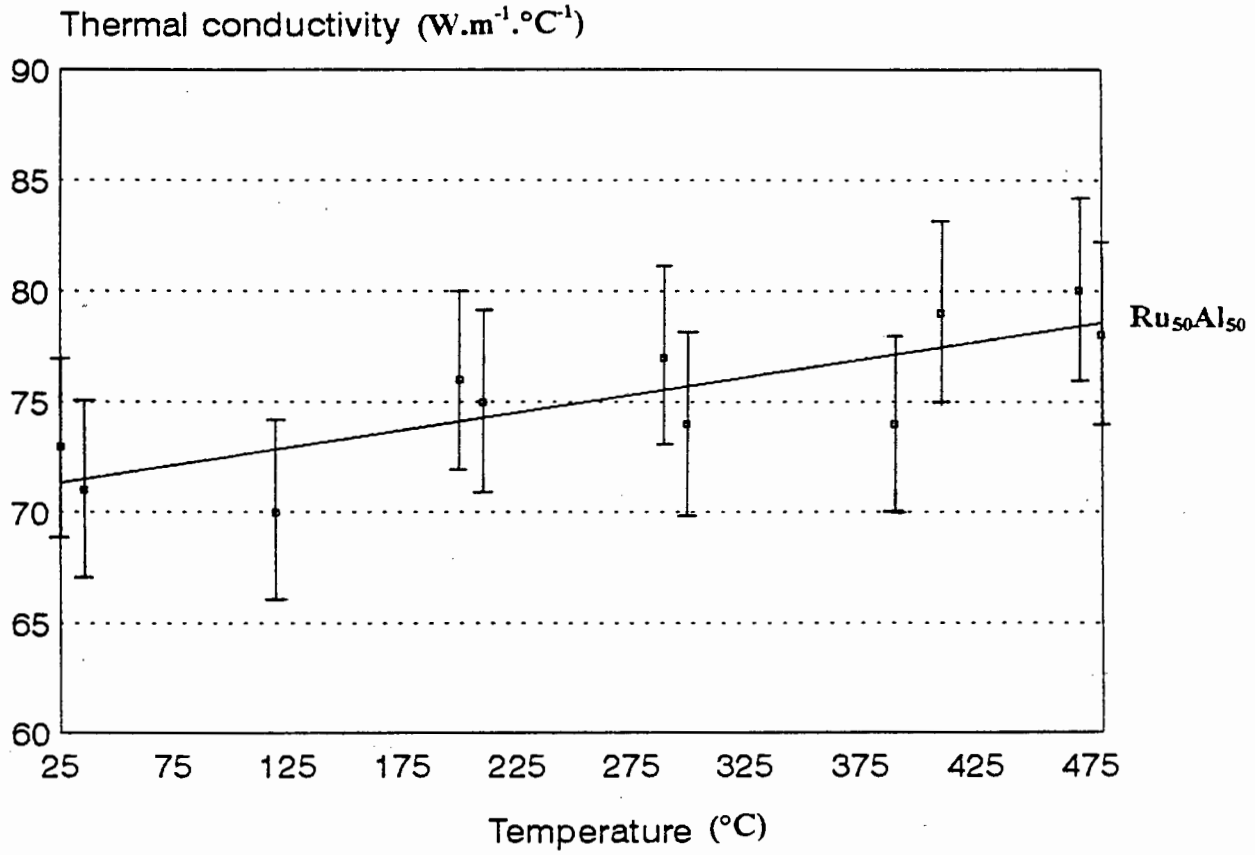

Figure 5.18: Thermal conductivity of $Ru_{50}Al_{50}$ specimen vs temperature.

$Ru_{47}Al_{53}$

The measured thermal conductivity of the $Ru_{47}Al_{53}$ specimen vs temperature is shown in figure 5.19. The thermal conductivity of this specimen is lower than the conductivity of the other two ruthenium aluminide specimens. This may be due to the increased porosity and grain boundary cracking in this sample.

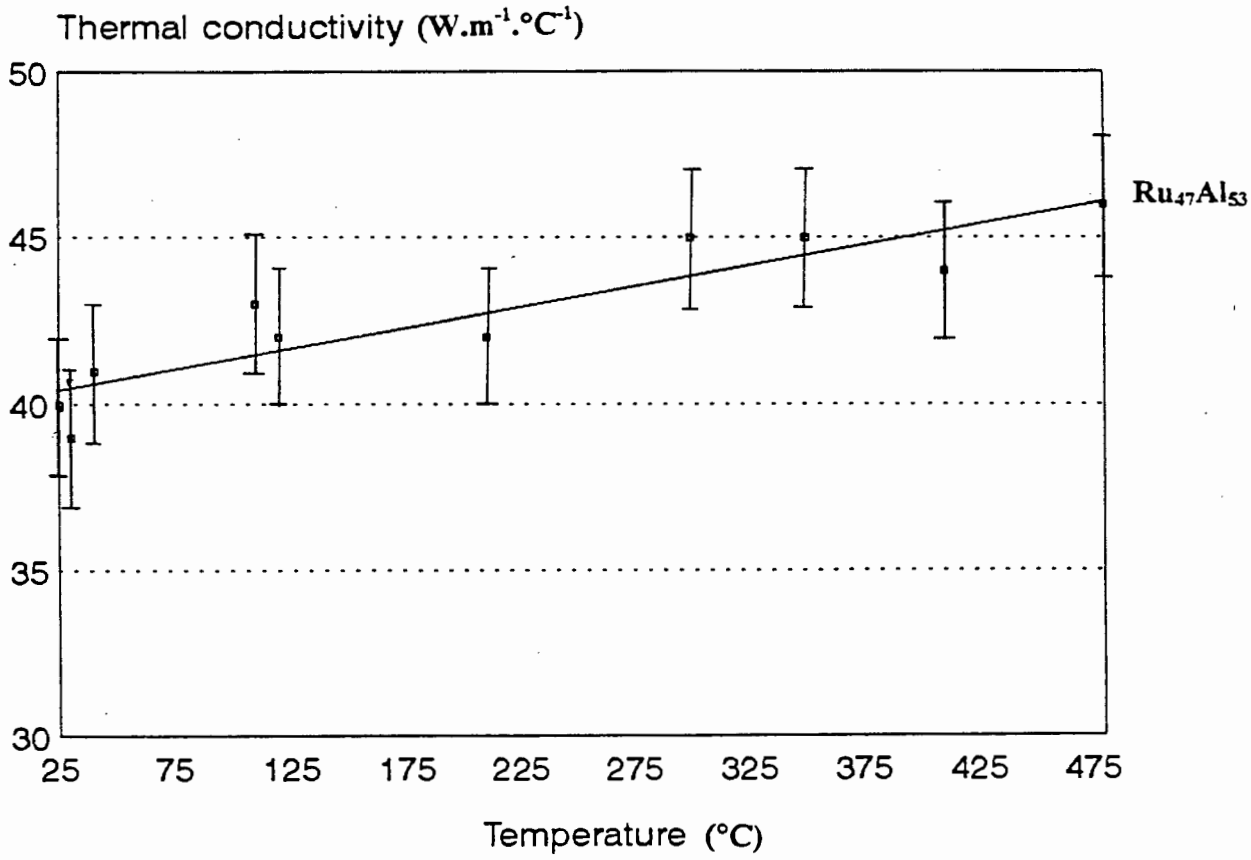

Figure 5.19: Thermal conductivity of $Ru_{47}Al_{53}$ specimen vs temperature.

$Ti_{48}Al_{52}$

The measured thermal conductivity of the $Ti_{48}Al_{52}$ specimen vs temperature is shown in figure 5.20. The thermal conductivity of the titanium aluminide specimen is lower than that of the ruthenium aluminide samples and also shows an increase in thermal conductivity with increasing temperature.

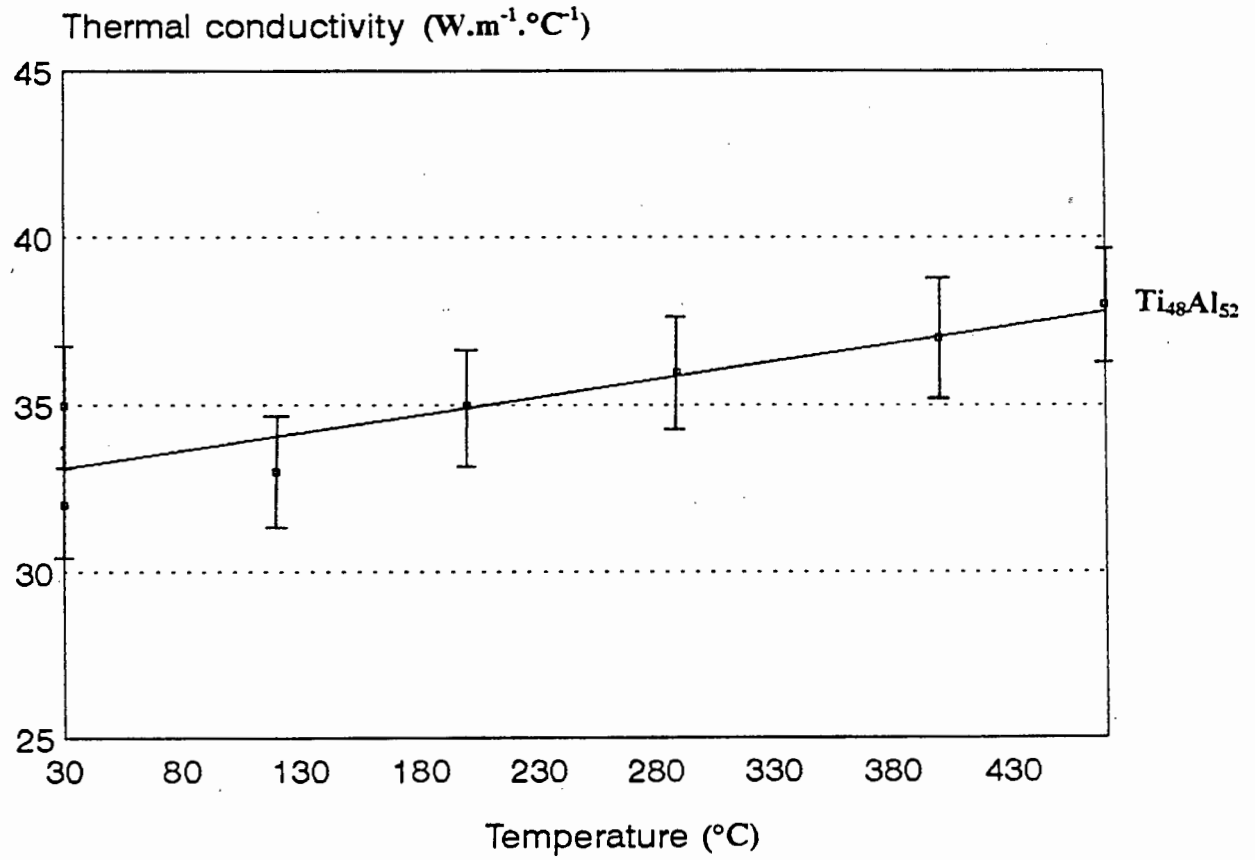

Figure 5.20: Thermal conductivity of $Ti_{48}Al_{52}$ specimen vs temperature.

Table 5.2 shows a summary of the measured thermal conductivity results for the four intermetallic specimens. Of the three ruthenium aluminide specimens, $Ru_{50}Al_{50}$ and $Ru_{53}Al_{47}$ had the highest thermal conductivity while $Ru_{47}Al_{53}$ had the lowest. There is an increase in the thermal conductivity of the specimens with increasing temperature.

	Thermal Conductivity ($W.m^{-1}.°C^{-1}$)			
Temperature (°C)	**$Ru_{53}Al_{47}$**	**$Ru_{50}Al_{50}$**	**$Ru_{47}Al_{53}$**	**$Ti_{48}Al_{52}$**
25	74±4	72±4	40±2	33±2
100	75±4	73±4	41±2	34±2
250	77±4	75±4	43±2	35±2
450	80±4	78±4	46±2	38±2

Table 5.2: Summary of the measured thermal conductivity data for the four intermetallic specimens.

5.3 Electrical resistivity

Apparatus based on the Van der Pauw method[54] for measuring the resistivity of arbitrarily shaped discs was used to measure the resistivity of the intermetallic specimens. The apparatus was first calibrated up to 500°C using a platinum specimen. The test method is explained in detail in section 3.4. The resistivity (ρ) of the samples was calculated using the following equation:

$$\rho = \frac{\pi d}{2\ln 2}\left(\frac{V_1}{I_1} + \frac{V_2}{I_2}\right) = \frac{\pi d}{2\ln 2}\left(\frac{R1 + R2}{2}\right)$$

where d is the thickness of the sample.

Each sample, measuring 12mm by 12mm, was ground down to a thickness of between 0.4mm and 0.3mm. The samples could not be made thinner due to the brittleness of the specimens. The following pages contain the measured electrical resistivity of the four intermetallic specimens, from 25°C up to 500°C.

$Ru_{53}Al_{47}$

Figure 5.21 shows the variation of electrical resistivity of $Ru_{53}Al_{47}$ with temperature. There is a linear increase of resistivity with increasing temperature.

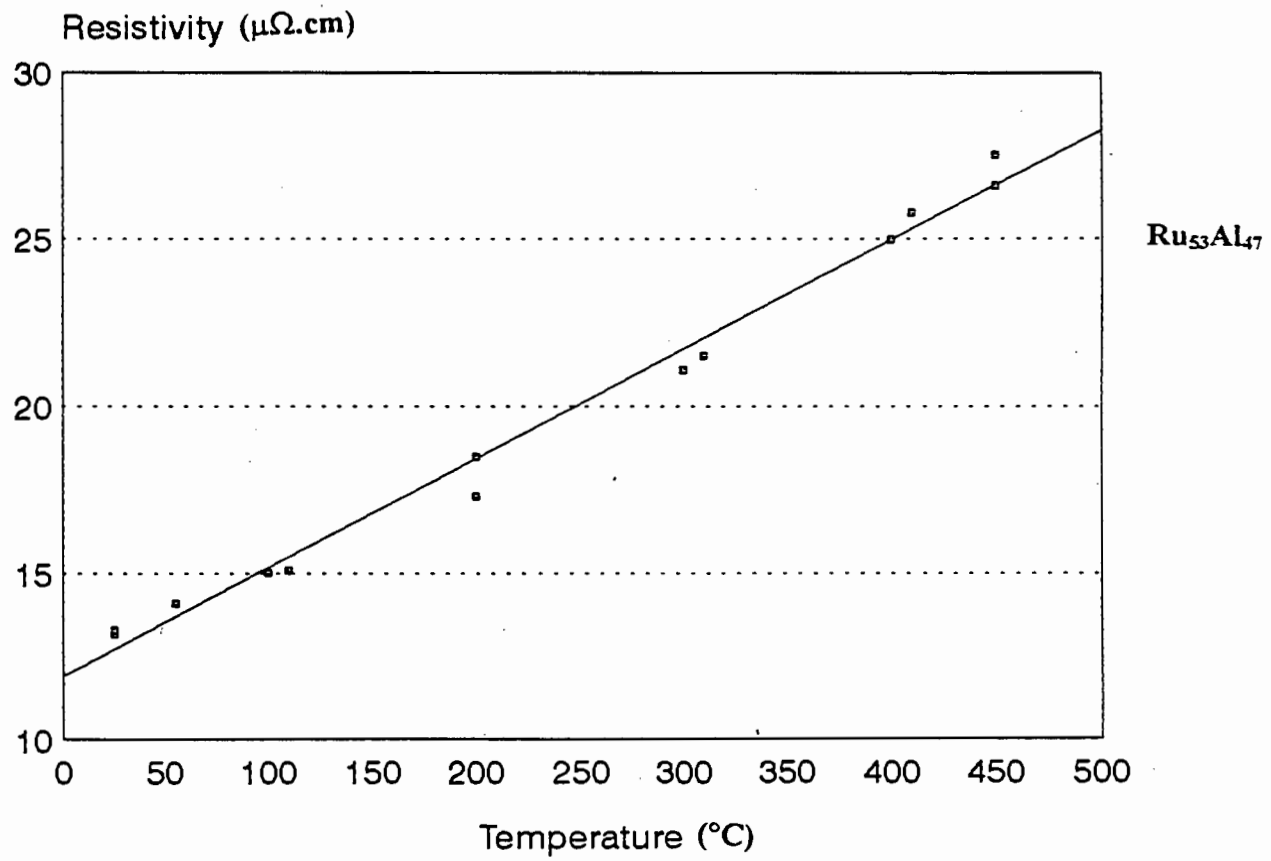

Figure 5.21: Measured electrical resistivity of $Ru_{53}Al_{47}$ vs temperature.

$Ru_{50}Al_{50}$

Figure 5.22 shows the variation of electrical resistivity of $Ru_{50}Al_{50}$ with temperature. The results are similar to those obtained for $Ru_{53}Al_{47}$ and as before there is a linear increase of resistivity with increasing temperature.

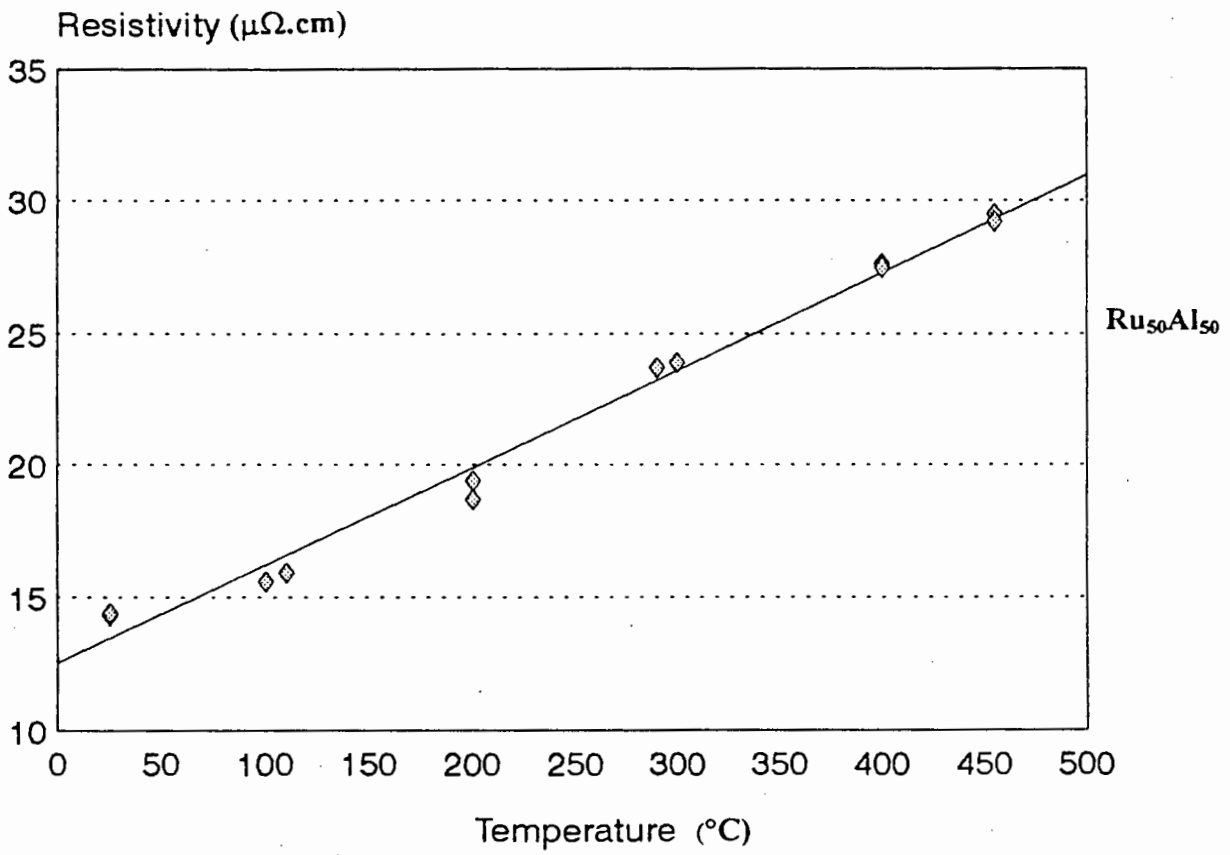

Figure 5.22: Measured electrical resistivity of $Ru_{50}Al_{50}$ vs temperature.

$Ru_{47}Al_{53}$

Figure 5.23 shows the variation of electrical resistivity of $Ru_{47}Al_{53}$ with temperature. This specimen shows a much higher electrical resistivity than the other two ruthenium aluminide specimens. This is probably due to the porosity and microcracking in the sample.

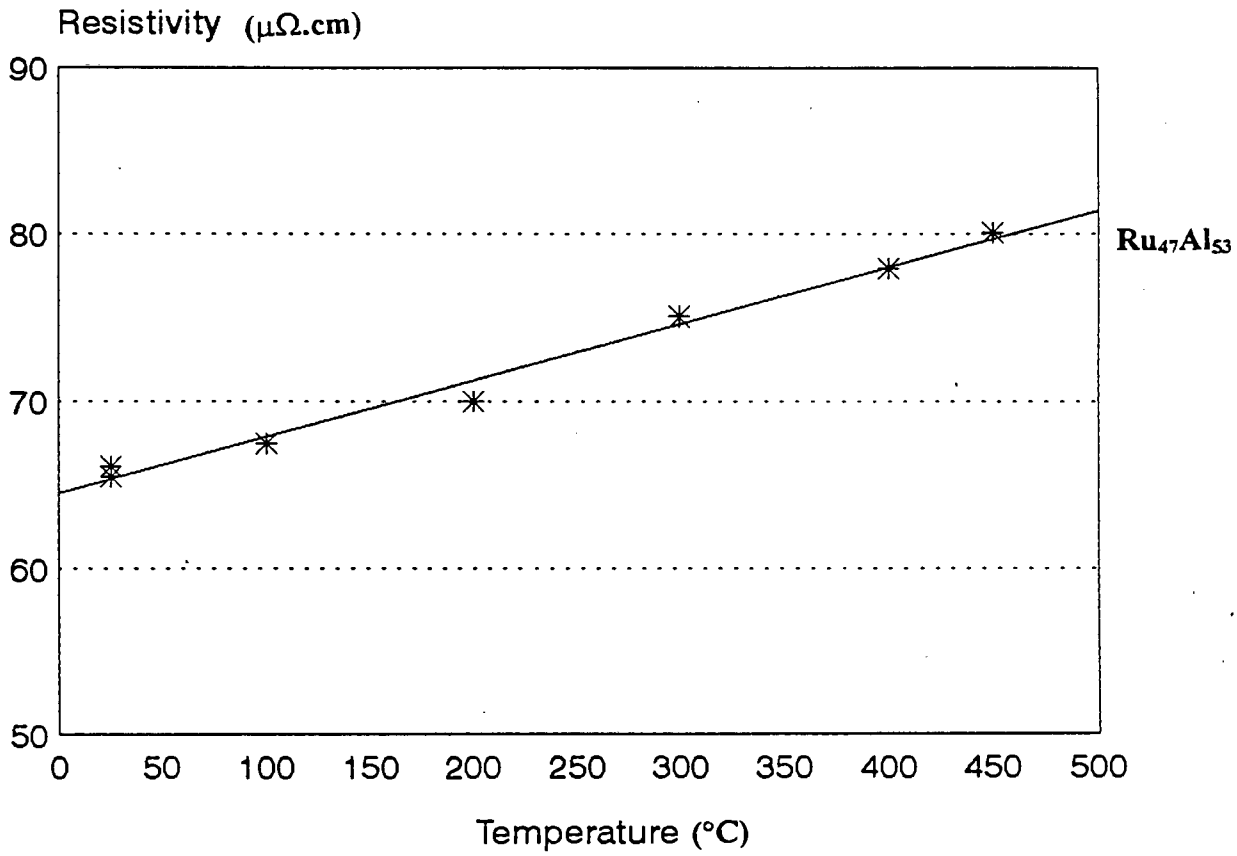

Figure 5.23: Measured electrical resistivity of $Ru_{47}Al_{53}$ vs temperature.

$Ti_{48}Al_{52}$

Figure 5.24 shows the variation of electrical resistivity of $Ti_{48}Al_{52}$ with temperature. Again there is a linear increase of resistivity with increasing temperature. The resistivity of this specimen is generally higher than that of the ruthenium aluminide samples.

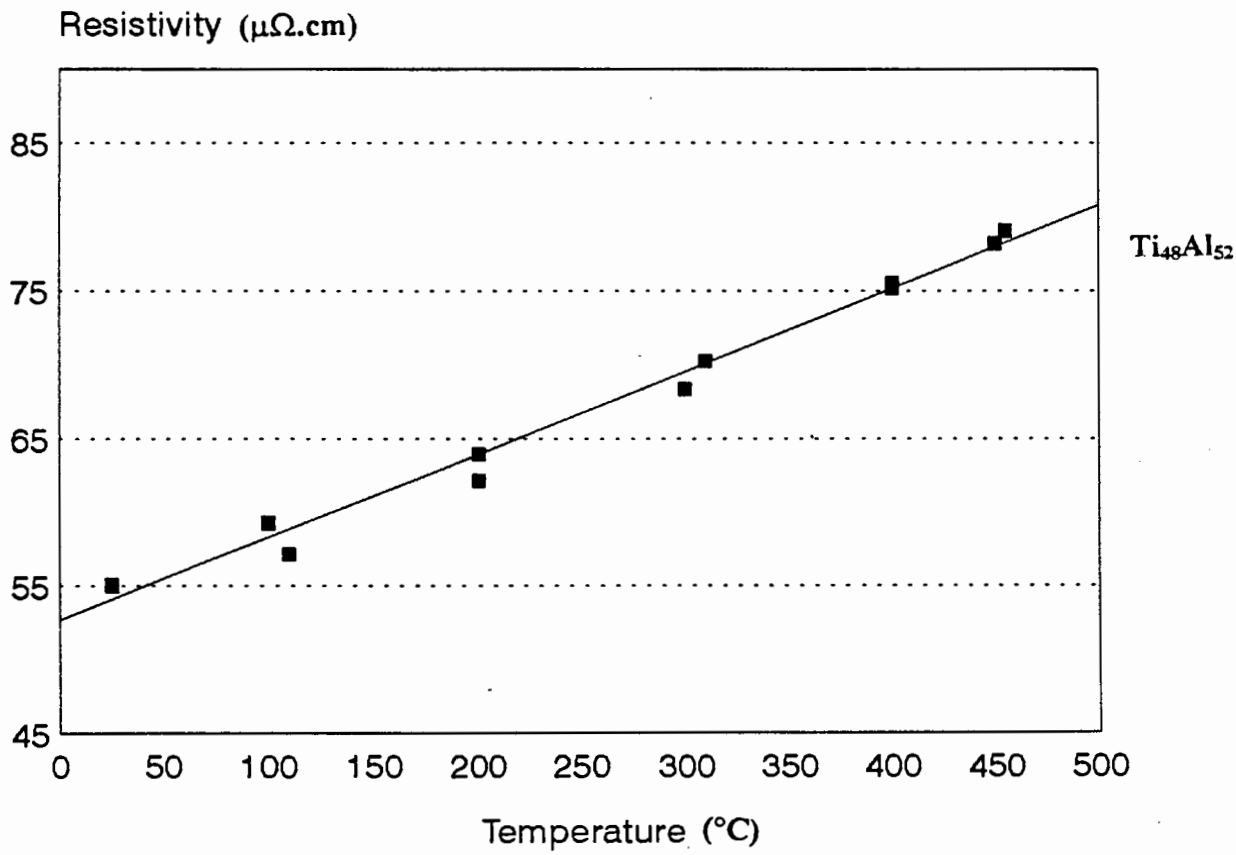

Figure 5.24: Measured electrical resistivity of $Ti_{48}Al_{52}$ vs temperature.

Figure 5.25 provides a summary of the measured electrical resistivity data for the four intermetallic specimens investigated. Generally the resistivity data follows the same trend as that observed in the thermal conductivity results. Of the three ruthenium aluminide specimens, $Ru_{50}Al_{50}$ and $Ru_{53}Al_{47}$ had the lowest resistivity results while $Ru_{47}Al_{53}$ had the highest. The $Ru_{47}Al_{53}$ specimen seems to be affected by the poor integrity of its microstructure. There is a linear increase in resistivity with increasing temperature for all the specimens specimens.

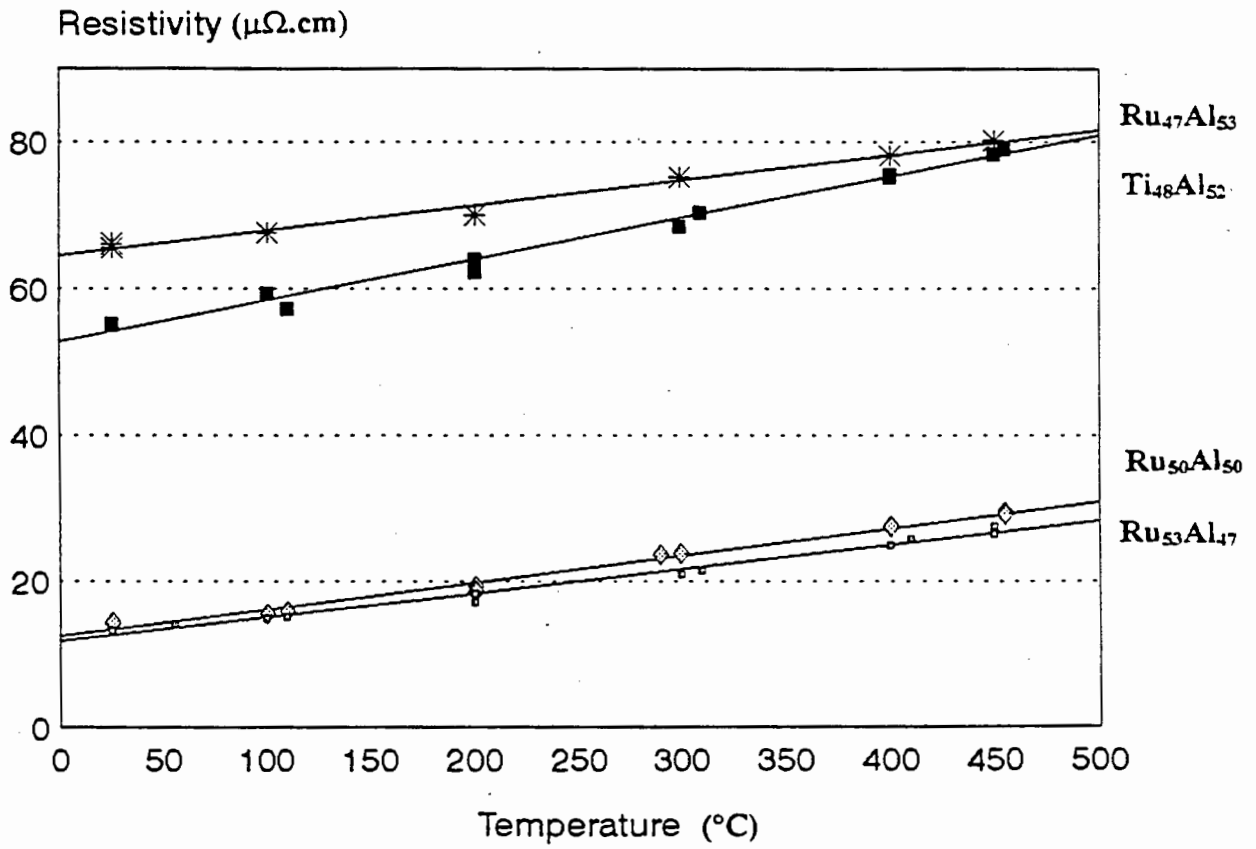

Figure 5.25: Summary of the measured electrical resistivity data for the intermetallic specimens.

5.4 Specific heat

The determination of the specific heat of the specimens was conducted using the method of mixtures. The test procedure is explained in detail in section 3.4. From the method of mixtures:

$$\text{Specific heat of the metal } (c_m) = \frac{c_w m_w \Delta T_w}{m_m \Delta T_m}$$

where c_w (22°C) = 4180.8 $J.kg^{-1}.°C^{-1}$.

All samples tested had similar dimensions, namely, ∅D 16mm and length 70mm. Stainless steel and aluminum rods were used to test the accuracy of the measurements. The results are presented in table 5.3.

Sample	Measured specific heat ($J.kg^{-1}.°C^{-1}$)	Published specific heat ($J.kg^{-1}.°C^{-1}$)
316 stainless steel	480±12	480-500[56]
D65S Aluminium	910±23	900-920[56]
$Ru_{53}Al_{47}$	490±12	-
$Ru_{50}Al_{50}$	500±13	-
$Ru_{47}Al_{53}$	450±11	-
$Ti_{48}Al_{52}$	650±16	-

Table 5.3: Measured and published results for the specific heats of the intermetallic specimens.

The results for the stainless steel and aluminum samples are in agreement with the published values and so it is reasonable to assume that the results are accurate within the experimental error of the experiment, which is estimated to be about 5%.

5.5 Summary

The microstructural investigation of the ruthenium aluminide alloys showed the presence of two phases in the $Ru_{53}Al_{47}$ and $Ru_{50}Al_{50}$ specimens. These phases were identified using energy dispersive spectroscopy. The majority phase was found to be RuAl while the minority phase was α-ruthenium. The aluminum rich specimen, $Ru_{47}Al_{53}$, consisted of single phase RuAl. This specimen was inherently brittle, was susceptible to grain boundary cracking and contained many pores. The cast $Ti_{48}Al_{52}$ specimen consisted of equiaxed γ grains and had no porosity.

316 Stainless steel is resistant to oxidation in the temperature range of interest, namely 25-450°C, so oxidation was not considered a factor in the calibration of the test equipment. Since ruthenium aluminide is extremely resistant to oxidation even at elevated temperatures (>1000°C) it was considered to have no effect on the measured thermal conductivity results.

The $Ru_{53}Al_{47}$ and $Ru_{50}Al_{50}$ specimens had the highest thermal conductivities and lowest electrical resistivities of all the specimens measured. The results were similar for each specimen and showed a linear increase in both thermal conductivity and resistivity with increasing temperature. The thermal conductivity of the $Ru_{47}Al_{53}$ specimen was almost half that of the other two ruthenium aluminide samples and this was probably due to the poor microstructural properties of this sample.

6. DISCUSSION

This chapter is divided into two sections. Firstly a discussion is presented on the methods of measuring thermal conductivity and the problems encountered in the measurement of the thermal conductivity of intermetallics. Finally a discussion of the measured results, and an attempt to relate the thermal and electrical properties of intermetallics to composition and atomic structure, is presented. Specific emphasis is placed on ruthenium aluminide alloys in an attempt to understand the transport mechanisms that operate in these alloys.

6.1 The measurement of thermal conductivity

Initial tests on the ruthenium aluminide alloys, using Ingenhausz's[31] wax experiment, indicated that the materials were good thermal conductors and so a suitable measuring technique had to be adopted. The different techniques for measuring the thermal conductivity of metallic solids are discussed in detail in Chapter Two. Following from the analysis of different methods and the conclusions reached by Laubitz[36], it was decided to use a modified Forbes bar method for the measurement of the thermal conductivity of the intermetallic specimens. The method adopted was that based on the work of Hogan and Sawyer[44] but as can be seen in the results recorded for stainless steel this method was unsuitable because of the sample dimensions.

The basic relation for heat transfer by conduction was proposed by Fourier (1822)[31].

$$\text{Rate of heat flow} = -kA\frac{dT}{dx} \qquad \text{Equation 6.1}$$

The rate of change of temperature of a volume element in terms of C, the heat capacity is[31];

$$CT = -\nabla\bullet q = \nabla\bullet(k\nabla T) \qquad \text{Equation 6.2}$$

Measurements can be described in terms of the heat transfer coefficient γ, which is the rate at which heat flows from the surface per unit area and per unit temperature difference between surface and surroundings. For a **long thin rod** of radius r, with its axis in the x direction the equation becomes[31];

$$CT = \left(\frac{d^2T}{dx^2}\right) - \left(\frac{2\gamma}{r}\right)\Delta T = 0 \qquad \text{Equation 6.3}$$

For a **semi-infinite rod** with the end (x=0) maintained at a constant temperature T_o the solution of the equation of steady heat flow is[31]:

$$T_x = T_o \exp\left[-\left(\frac{2\gamma}{rk}\right)^{\frac{1}{2}} x\right] \qquad \text{Equation 6.4}$$

The emphasis here is long thin rod or semi-infinite rod. Hogan and Sawyer[44] note that from their experimental results that a 30cm rod is essentially semi-infinite provided that the conductivity does not exceed 100 $W.m^{-1}.°C^{-1}$. They conclude that the temperature function in their experiments can be written (in my symbols) as;

$$T(0.3175,x) = T_o \exp\left[-x\left(\frac{Z}{k}\right)^{\frac{1}{2}}\right] \qquad \text{where } Z = \frac{2\gamma}{r} \qquad \text{Equation 6.5}$$

which is the exact solution for the problem of a thin wire losing heat to its surroundings with one end maintained at a temperature T_o. It represents the temperature distribution for a rod 0.3175cm in radius and 30cm long (aspect ratio of 80) whose thermal conductivity lies between 10 - 100 $W.m^{-1}.°C^{-1}$.

Carslaw and Jaeger[57] state that the solution to the equation of steady heat flow in a semi-infinite rod may be used for a bar of finite length (x) **provided** the value of $x\left(\frac{2\gamma}{rk}\right)^{\frac{1}{2}}$ is large. Essentially this means one needs a long thin test specimen and the thermal conductivity range of the experiment depends on how long and how thin your material is. This was verified by the measurement of stainless steel rod (r= 1.8mm, x=20cm) having a measured thermal conductivity of 16 $W.m^{-1}.°C^{-1}$, consistent with published results. Aluminium rod (r=2mm, x=20cm) did not appear to satisfy this condition, perhaps due to its high conductivity of 175 $W.m^{-1}.°C^{-1}$.

Laubitz[36] states that the thin rod approximation used by Forbes is no limitation since it readily allows for the treatment of a wide variety of boundary conditions and temperature variations of conductivity. Even in parametrically unsuitable systems, where the approximation may yield errors, Laubitz claims that it is easier to use the thin rod approximation and correct for the errors on the basis of simple boundary conditions, than to attempt a more rigorous calculation for complex conditions.

The large ratio of the length of the specimen to the diameter, which Hogan and Sawyer[44] used to satisfy the requirements of the semi-infinite rod, is perhaps convenient but certainly not necessary. In an experiment designed to determine the Lorenz number of the noble metals at high temperature, Laubitz[45] employed a finite-rod technique with a fair measure of success although the experimental set-up and computations are relatively complex. The specimen was 2cm in diameter and 20cm long.

Researchers who have used generalised Forbes Bar methods to measure thermal conductivity do not state (with the exception of Laubitz[45] perhaps) what their experimental boundary conditions are, but rather conclude after their experimental work that their test material satisfied the conditions explained above.

Although a method has been developed and apparatus is available to measure the thermal conductivity of thin metallic rod specimens having a thermal conductivity range of approx. 10-100 W/m°K, this apparatus is not suitable for the measurement of the thermal conductivity of specimens with a low aspect ratio, such as the intermetallic specimens studied here.

From exhaustive experiments on stainless steel and ruthenium aluminide rods having an aspect ratio of 5, it became obvious that the specimens did not conform to the boundary conditions needed to satisfy the thin rod approximation[44]. Since it was beyond the scope of this project to investigate and compute the boundary conditions and experimental set-up needed to apply the generalised Forbes Bar method to the specimen parameters required for this study, a comparative method was adopted.

A major obstacle that had to be overcome in both experiments was the attachment of thermocouples to the specimen surface. Films of glue and poor contact adversely affect results and so different methods of attachment where investigated. When thermocouple beads were placed into small holes drilled into the sample, spurious results were obtained. The thermocouples were then peened into thin slots cut on the surface of the specimen. This was an improved method but there was no certainty that the thermocouple bead was making good contact with the metal. This was tested by drilling holes next to the peened slots and placing other thermocouples in the holes. These thermocouples were held in place by narrow alumina tubes. The temperature at each point was then determined by the two sets of thermocouples. This experiment highlighted the importance of the thermocouple attachment since some readings differed by as much as 1.5 °C.

For the thin specimens used in the modified Forbes bar method thermocouples were best attached to the rod by either soldering or butt welding. For the thicker specimens (∅D=16mm), used in the comparative tests, a small hole was drilled into the sample surface (∅D=1.6mm, L=3mm) and a Type K, sheathed thermocouple was then fitted into the hole. The sheath ensured that good thermal contact was maintained.

This method appeared to work well and was used to measure the thermal conductivity of the intermetallic specimens. It was found that the smaller the temperature gradient in the sample the more accurate the results and so the current through the heating coil was adjusted so that the thermocouple furthest from the heating source was raised only a few degrees above ambient temperature. The spacing between the thermocouples was chosen so that each thermocouple was a few degrees higher or lower than the thermocouple next to it. These distances are explained in figure 4.2.

A final problem encountered was that of temperature fluctuations within the furnace. As explained in chapter four, the whole measuring apparatus was placed in a furnace and allowed to stand overnight so that a uniform temperature could be achieved before testing began. In reality a completely uniform temperature was not achievable and before the heating coil was switched on the six thermocouples attached to the reference and sample always differed by small amounts. These differences increased at higher temperatures. The assumption was made that once the heating coil was switched on the reference and sample reached a new thermal equilibrium which reflected the true temperature gradient in the two. Ideally a cylindrical furnace should be constructed around the alumina guard so as to give uniform heating of the apparatus.

There are many sources of error in thermal conductivity measurements; some are quantifiable while others need to be estimated. Contributions to error in the comparative apparatus include, (1) errors in the measurement of the temperature gradients and absolute temperature, (2) errors in the measurement of dimensions, (3) errors in the temperature mismatch between the specimen, guard and furnace, and (4) errors in the thermal conductivity of the reference material.

Other sources of error that are more difficult to quantify include, heat losses from the surface of the reference and sample by radiation, contact resistance between the reference and sample and heat loss via the thermocouple sheaths.

Type-K thermocouples were used to measure the temperature gradients and absolute temperatures. The thermocouples measured to an accuracy of 0.025°C although measurements were usually made to the nearest 0.05°C. The combined errors in the temperature measurements was estimated to be 1%. The measurement of dimensions was performed using Vernier calipers with an error of approximately 1%. Temperature mismatches between a specimen, guard and furnace were analysed by Laubitz[36] and were found to be between 1-3% for equipment using the guarded linear heat flow technique. Errors in the thermal conductivity of the reference specimen are estimated to be 1-2%. Heat losses from the test specimen are estimated to be 1-2% due to the careful design and insulation of the apparatus. The combined errors for the test apparatus is therefore considered to be **5-10%.**

6.2 Thermal conductivity results

The measured thermal conductivities of the intermetallic specimens highlight a few important points about the thermal conductivity of intermetallics. The conductivities measured are fairly high for alloys and exhibit properties similar to those of pure metals. The thermal conductivities of the ruthenium aluminide alloys are similar to those observed in nickel aluminide and the pure metal platinum. Finally there seems to be only a slight increase in thermal conductivity with increasing temperature. This section will attempt to explain these observations.

6.2.1 Microstructure and processing

It is interesting to relate the measured thermal conductivities of the ruthenium aluminide specimens to their composition and microstructure. The ruthenium rich ($Ru_{53}Al_{47}$) and stoichiometric ($Ru_{50}Al_{50}$) samples have similar thermal conductivities. The results cannot be differentiated since they lie within the experimental error of the experiment (5-10%). There is however a large difference between the thermal conductivities of these two samples and the aluminium rich ($Ru_{47}Al_{53}$) specimen. The thermal conductivity of $Ru_{47}Al_{53}$ is almost half that of the other two specimens.

This large difference can be explained by the structural differences between the specimens which are in turn related to the compositional variations of the specimens. The aluminium rich sample contains a large number of pores, intergranular cracks and is inherently brittle. These defects in the structure impede the heat flow through the sample and so reduce the thermal conductivity of the specimen. Terada[30] noted similar behaviour in CoAl where aluminium rich samples could not be prepared, because brittleness prevented the forming of precisely shaped specimens.

The cause of these defects is related to the microstructure of the aluminum rich specimen. While the microstructure of the ruthenium rich ($Ru_{53}Al_{47}$) and stoichiometric ($Ru_{50}Al_{50}$) specimens contained α-ruthenium at the grain boundaries, α-ruthenium was absent in the aluminum rich specimen. α-Ruthenium appears to impart structural integrity to the ruthenium aluminide specimens and must therefore be present in the microstructure, as an intergranular phase, to aid in the processing of these alloys and in so doing prevent grain boundary cracking and to impart a degree of ductility to the specimen. Fleischer[15] found that aluminum rich compositions are intergranularly brittle while ruthenium rich and stoichiometric compositions, which contain α-ruthenium at the grain boundaries, have substantial toughness. The presence of α-ruthenium in the microstructure of these alloys aids in the processing of specimens by imparting structural integrity and reducing processing flaws such as micro-cracks that can reduce the thermal conductivity of the specimen.

6.2.2 Atomic order

Thermal conductivity is influenced by the amount of order in a solid. Disorder impedes the flow of heat carriers and so a well ordered system is expected to have a higher thermal conductivity than its disordered counterpart. This is reflected in the measured results for the thermal conductivity of nickel aluminide as given by Darolia[29]. The room temperature thermal conductivity of nickel aluminide is given as 74 $W.m^{-1}.°C^{-1}$ which is 4-8 times greater than the thermal conductivity of nickel based superalloys. Nartova[58] measured the thermal conductivity of Ti_3Al and found that it increased with increasing temperature from 10-18 $W.m^{-1}.°C^{-1}$ over the temperature range 50-700°C. This is 20% higher than the thermal conductivity of other titanium alloys[58]. The measured results of 35-40 $W.m^{-1}.°C^{-1}$ for the thermal conductivity of the ordered intermetallic $Ti_{48}Al_{52}$ in this study is therefore 3-4 times higher than the thermal conductivity of conventional titanium alloys.

Order and the degree of ordering in intermetallic systems therefore has a profound effect on the thermal conductivity of intermetallic compounds. Since maximum order should improve the thermal conductivity of compounds, the thermal conductivity of intermetallics should reach a maximum at stoichiometry and decrease with deviations from stoichiometry.

This has been observed by Terada[30] for nickel aluminide and cobalt aluminide and is shown in figure 6.1.

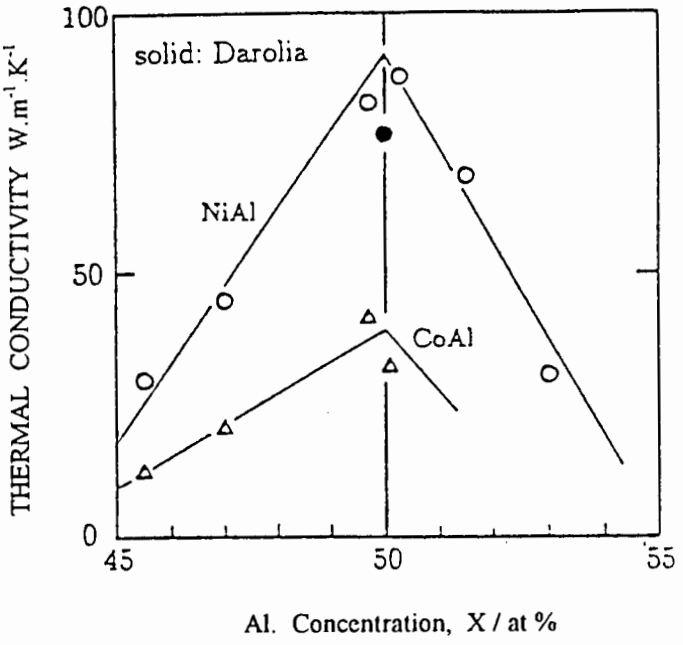

Figure 6.1: Thermal conductivity of NiAl and CoAl as a function of aluminium concentration at room temperature (after Terada[30]). NiAl result by Darolia[29] also shown.

This effect was not observed in the ruthenium aluminide alloys for a number of reasons:

(1) Fairly large samples were measured. The structural integrity and microstructure of the three samples was not the same, as explained above.

(2) Only three samples were available for studies, each with a different processing route.

(3) The measuring apparatus was not sensitive enough to differentiate between small differences in thermal conductivity.

(4) Ruthenium aluminide has a narrow phase field (compared with nickel aluminide) which means that differences occur over a small compositional range.

Generally electrical measurements are used to determine these variations, since electrical measurements are usually more accurate than thermal measurements. This is discussed in more detail in section 6.3.

It is useful to compare the room temperature thermal conductivity of stoichiometric ruthenium aluminide with that of other B2-type aluminides and platinum. Table 6.1 compares the measured thermal conductivity of $Ru_{50}Al_{50}$ with that of FeAl, CoAl and NiAl as reported by Darolia[29] and Terada[30] and platinum as reported by Laubitz[33].

Material	Thermal conductivity ($W.m^{-1}.°C^{-1}$)
$Ru_{50}Al_{50}$	75±4
NiAl	74[29]
NiAl	92[30]
CoAl	37[30]
FeAl	12[30]
Pt	72[33]

Table 6.1: Thermal conductivity of various aluminides at stoichiometry and platinum.

It can be seen from table 6.1 that ruthenium aluminide has a similar thermal conductivity to that of nickel aluminide and platinum. Terada[30] has shown that the thermal conductivity of the B2-type aluminides of the first transition series (FeAl, CoAl, NiAl) increases with atomic number. This is shown in figure 6.2.

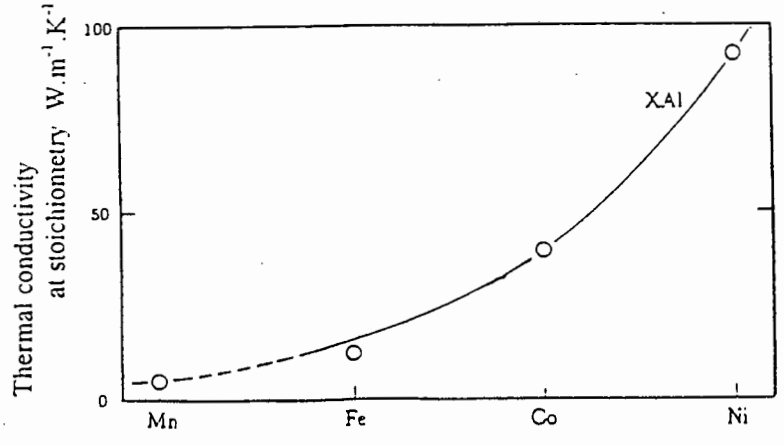

Figure 6.2: Thermal conductivity at stoichiometry of aluminides from 1st transition series (after Terada[30]).

Terada[30] applies Norbury's rule[59] to explain this trend. The rule states that the electrical resistivity of binary alloys at room temperature is further increased as the position of the solute element becomes distant from that of the host component on the periodic table. So it is expected that the thermal conductivity of NiAl is largest and that of FeAl is the smallest among the aluminides. This however does not explain the similarity between the thermal conductivity of nickel aluminide and ruthenium aluminide. This is discussed in more detail in section 6.4.

The thermal conductivity of ruthenium aluminide is also similar to that of the pure platinum. This indicates that electrons are the primary source of heat conduction through the compound and this is discussed in detail in section 6.4.

6.2.3 Temperature

Finally, there seems to be a trend of increasing thermal conductivity with increasing temperature in all the ruthenium aluminide alloys. Darolia[29] has show that the thermal conductivity of nickel aluminide decreases slowly over the temperature range 25-1200°C. The ruthenium aluminide alloys however exhibit a trend observed in platinum as recorded by Laubitz[33]. This trend of increasing thermal conductivity with increasing temperature is difficult to explain. Generally, the thermal conductivity of a pure metal decreases with increasing temperature as the electrons experience more thermal scattering. It has been shown that platinum is not the only element to exhibit this behaviour of a thermal conductivity that increases with increasing temperature. Vanadium and palladium show similar trends[60]. This abnormal behaviour posses an interesting theoretical problem and is not fully understood. Possible explanations include electron-electron scattering and the movement of the Fermi surface (Fermi smearing)[60].

6.3 Electrical resistivity results

The electrical resistivity results of the intermetallic specimens follow the same pattern observed for the thermal conductivity measurements. The sample with the highest thermal conductivity has the lowest electrical resistivity and vice versa. The temperature dependence of the resistivity of the ruthenium aluminide alloys is similar to that of platinum. The resistivity results are also consistent with the results obtained by Smith[19] for the electrical resistivity of ruthenium aluminum alloys.

Ruthenium aluminide alloys are more resistive than platinum partly because of the higher resistance associated with alloying additions. This contribution should be highest near equiatomic compositions where there is maximum disruption of the host lattice[61]. As in thermal conductivity, disorder in the lattice means that electrons are more likely to be scattered resulting in an increase in resistivity. Ordering at equiatomic compositions causes a drop in resistivity and this offsets the increase due to alloying additions. However, the degree of disorder in the compound is not the only contribution to resistivity.

NiAl, CoAl and FeAl are discussed by Sellmyer[62] in terms of the two band s-d model of transition metal electronic structure of Mott[63]. This model proposes a low density of mobile s electrons which are primarily responsible for conductivity and a high density of relatively immobile electrons in d-states at the Fermi energy into which the s electrons are scattered causing the major contribution to resistivity in transition metals. The resistivity of NiAl is low because there is a small s-d contribution to resistivity while CoAl and FeAl are subject to s-d scattering and therefore have a higher resistivity. Table 6.2 shows the electron configuration of some transition elements and their compounds.

Material	Electronic Configuration
Aluminium	$(3s)^2(3p)^1$
Cobalt	$(4s)^2(3d)^7$
Nickel	$(4s)^2(3d)^8$
Iron	$(4s)^2(3d)^6$
Nickel aluminide	$(3d)^{10}(s,p)^{1.5}$
Cobalt aluminide	$(3d)^{9.2}(s,p)^{1.4}$
Iron aluminide	$(3d)^{8.6}(s,p)^{1.2}$

Table 6.2: Electronic configuration of some aluminides and their constituents (after Sellmeyer[62]).

It can be seen from table 6.2 that the d band in NiAl can be regarded as completely filled while states in the d band of CoAl are left vacant. These vacant states increase the possibility of s electrons being scattered into d-states because of the higher density of states.

Since ruthenium is a transition metal, ruthenium aluminide alloys considered here are expected to have s-d scattering contributions to their resistivity. The variation of the density of states with energy of ruthenium aluminide shows potential for s-d scattering in that the d band overlaps the s band at the Fermi energy, as shown in figure 6.3. However, this contribution to resistivity must be relatively small in that the conductivity of RuAl is similar to that of NiAl.

Transition metal aluminide systems all show ordering dependent resistivity phenomena near 50 at.% aluminium. The concentrations at which this occurs in NiAl and CoAl depends on the size (width) of the aluminide phase field. This behaviour is similar to the thermal conductivity results for these aluminides as reported by Terada[30].

It is useful to compare the electrical resistivity behaviour of nickel aluminide with that of ruthenium aluminide. As has been discussed above the electrical resistivity of nickel aluminide shows a minimum at approximately 50 at%. This behaviour has also been observed in ruthenium aluminide alloys as reported by Smith[19]. The depth of the minimum is dependent on the degree of order at the stoichiometric composition and the electronic structure at that composition. Nickel aluminide has a high degree of order and has a wide phase field. The contribution to s-d scattering in NiAl is expected to be small in view of the low density of d states at the Fermi energy. The resistivity of NiAl should therefore have a deep wide minimum at the equiatomic composition. To illustrate this the phase diagram and resistivity of nickel aluminide are reproduced in figure 6.3 and figure 6.4.

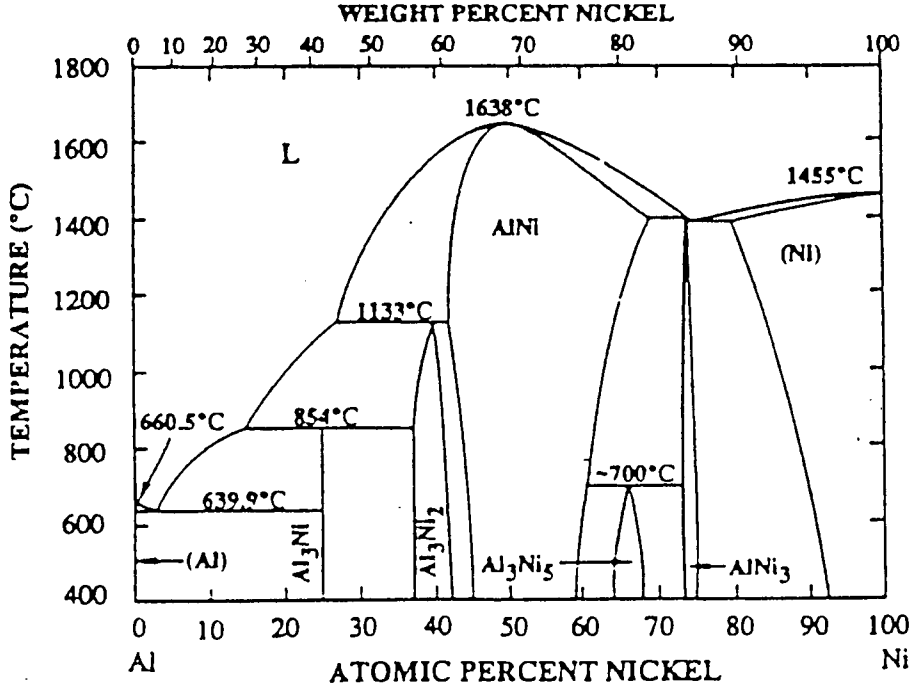

Figure 6.3: Equilibrium phase diagram of the nickel aluminium system (after Miracle[64]).

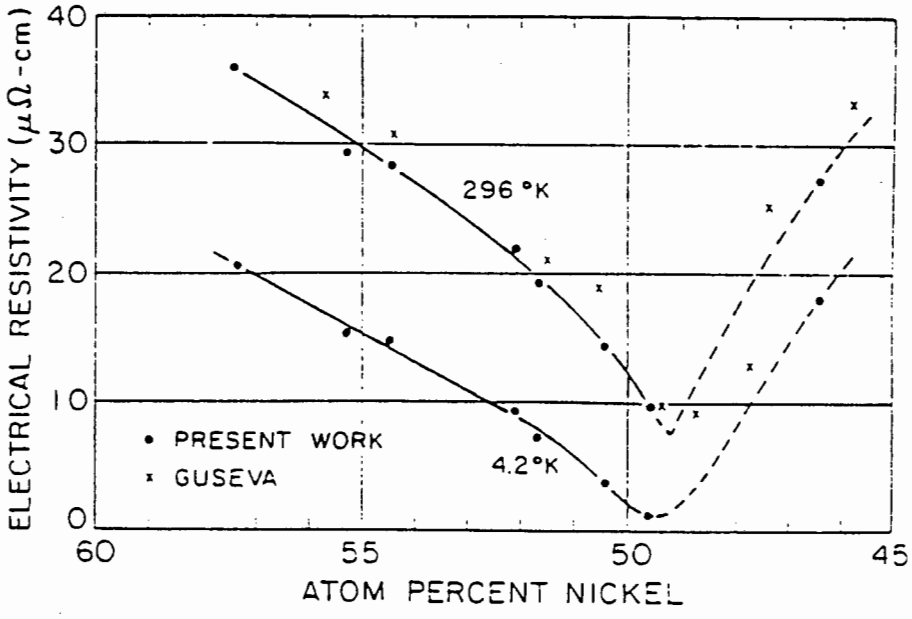

Figure 6.4: The dependence of resistivity on composition in the nickel aluminium system near 50 at% aluminium (after Sellmyer[62]).

Ruthenium aluminide has a narrow phase field (5 at%), at 500°C, and therefore a narrow resistivity minimum. This means that optimisation of compositions requires carefully controlled processing. This point was also made in the previous section on the thermal conductivity of these alloys. The resistivity of equiatomic nickel aluminide as reported by Sellmyer[64] is similar to that of equiatomic ruthenium aluminide as measured in this work.

Transition elements in group VIII of the periodic table are assumed to have zero valency according to the bonding theory of Hume-Rothery[7]. Therefore no conduction electrons from the transition element need be considered in the electronic band structure.

CoAl, and NiAl are considered as electron compounds[62] having a Hume-Rothery ratio of $\frac{3}{2}$. A change in composition, by substituting one atom for another can change the electron to atom ratio and therefore alter the free energy of the system. In NiAl an increase in aluminium concentration results in the formation of vacancies at the nickel sites in order to maintain the number of electrons per unit cell. Thus a defect lattice is formed in order to maintain the electron concentration. Fleischer[15] notes that RuAl has both aluminium and vacancies occuring at ruthenium sites. These defects in the lattice will have the effect of increasing the resistivity of the compound on either side of the stoichiometry minimum. Since the defects are different in each compound the effect on the resistivities will also be different, ie. the slopes on either side of the minimum will not be the same.

Finally there is a strong similarity of temperature dependence of resistivity of ruthenium aluminide compared to that of platinum. This is shown in figure 6.5. This was also noted in the previous section on the thermal conductivity of these two materials. The stability of the atomic structure and its lack of susceptibility to heat treatment is evident from the linearity of the resistivity vs temperature curve. This is an important feature required for high temperature electrical applications. Ruthenium aluminide therefore compares well with platinum, a commonly used material in high temperature electrical applications.

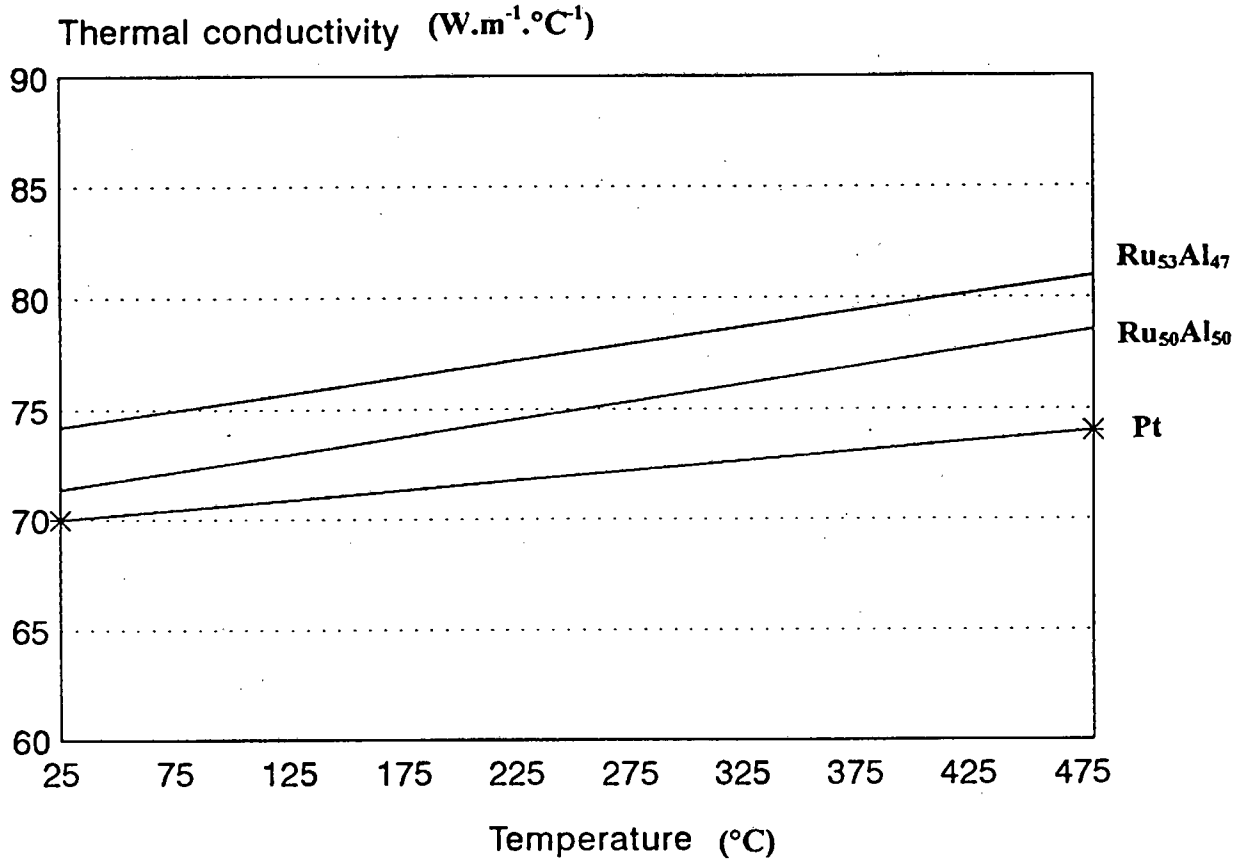

Figure 6.5: Dependence of resistivity on temperature for platinum and selected compositions of ruthenium aluminide.

6.4 Heat transport mechanisms

As has been observed in the previous sections, ruthenium aluminide is a good thermal conductor and has low electrical resistivity. Its behaviour over the temperature range 25-500°C is similar to that of platinum and to another electron compound, nickel aluminide. Since ruthenium aluminide is an intermetallic compound but acts like a metal it would be useful to determine the transport mechanisms that operate in the compound.

As has been discussed in chapter two, the thermal conductivity (k) of a material is the sum of the lattice and electronic component:

$$k = k_g + k_e$$

It is useful to be able to relate k_e to the electrical resistivity of a metal. From the pioneer experiments of Weidemann and Franz and later the theoretical work of Lorenz, at room or higher temperatures the ratio of $\frac{k\rho}{T}$ is roughly constant for most metals with a value approximating to the theoretical Sommerfeld value of:

$$L_0 = (\frac{\pi^2}{3})\frac{K^2}{e^2} = 2.445 \text{ x } 10^{-8} \text{ J.}\Omega\text{.s}^{-1}\text{.K}^{-2}$$

A simple test to determine the charge carriers in a material is to compute the Weidemann-Franz ratio and compare it to L_0. Since phonon transport increases without affecting ρ, the Weidemann-Franz ratio will exceed L_0 when k_g becomes important. The Weidemann-Franz values and the reduced Weidemann-Franz values were computed from the measured data for the $Ru_{53}Al_{47}$ and $Ru_{50}Al_{50}$ alloys and the results shown in table 6.3 and 6.4.

Sample	Temp (K)	k ($W.cm^{-1}.K^{-1}$)	ρ (Ω.cm)	$\frac{k\rho}{T}$ ($W.\Omega.K^{-2}$)	$\frac{k\rho}{TL_0}$
$Ru_{53}Al_{47}$	300	0.75	$13.3x10^{-6}$	$3.3x10^{-8}$	1.35
	473	0.76	$18.5x10^{-6}$	$2.9x10^{-8}$	1.2
	573	0.78	$21.1x10^{-6}$	$2.8x10^{-8}$	1.1
	653	0.82	$25.0x10^{-6}$	$3.1x10^{-8}$	1.3
	753	0.80	$28.0x10^{-6}$	$2.9x10^{-8}$	1.2

Table 6.3: Weidemann-Franz ratio and reduced ratio at various temperatures for $Ru_{53}Al_{47}$

Sample	Temp (K)	k ($W.cm^{-1}.K^{-1}$)	ρ (Ω.cm)	$\frac{k\rho}{T}$ ($W.\Omega.K^{-2}$)	$\frac{k\rho}{TL_0}$
$Ru_{50}Al_{50}$	300	0.73	$14.3x10^{-6}$	$3.5x10^{-8}$	1.42
	473	0.76	$19.0x10^{-6}$	$3.0x10^{-8}$	1.25
	573	0.76	$23.5x10^{-6}$	$3.1x10^{-8}$	1.25
	673	0.77	$27.6x10^{-6}$	$3.2x10^{-8}$	1.3
	753	0.78	$29.5x10^{-6}$	$3.0x10^{-8}$	1.25

Table 6.4: Weidemann-Franz ratio and reduced ratio at various temperatures for $Ru_{50}Al_{50}$.

The reduced Weidemann-Franz ratios are tabulated in tables 6.3 and 6.4 and plotted against temperature in figure 6.6. The reduced ratio for platinum, after Laubitz[33], is shown in figure 6.7.

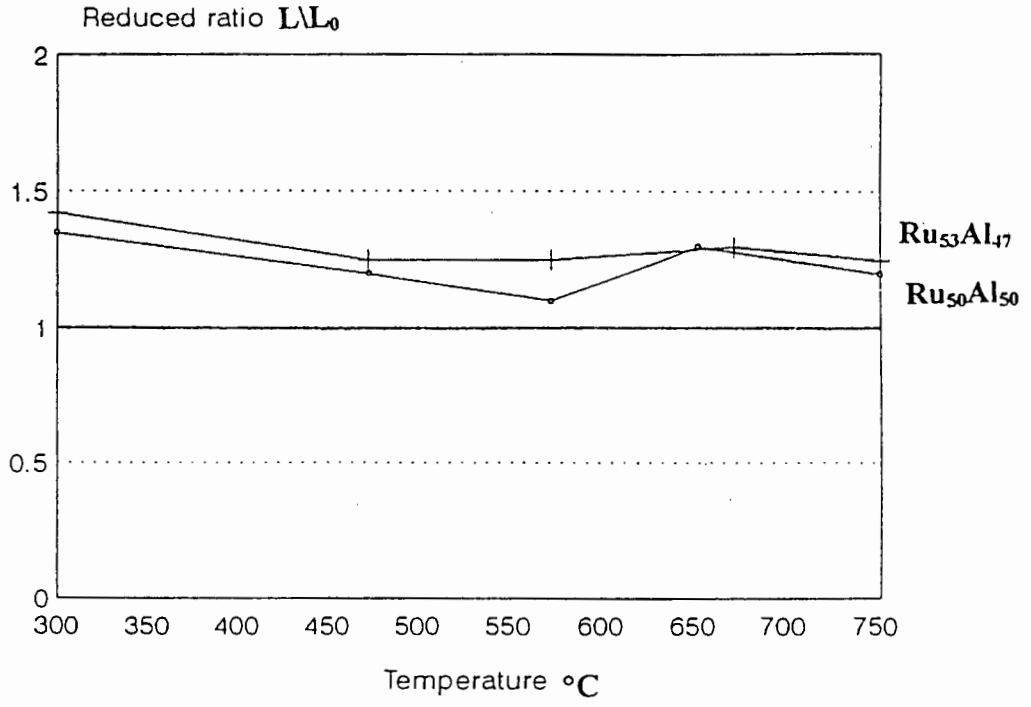

Figure 6.6: Reduced ratio for $Ru_{53}Al_{47}$ and $Ru_{50}Al_{50}$ plotted vs temperature.

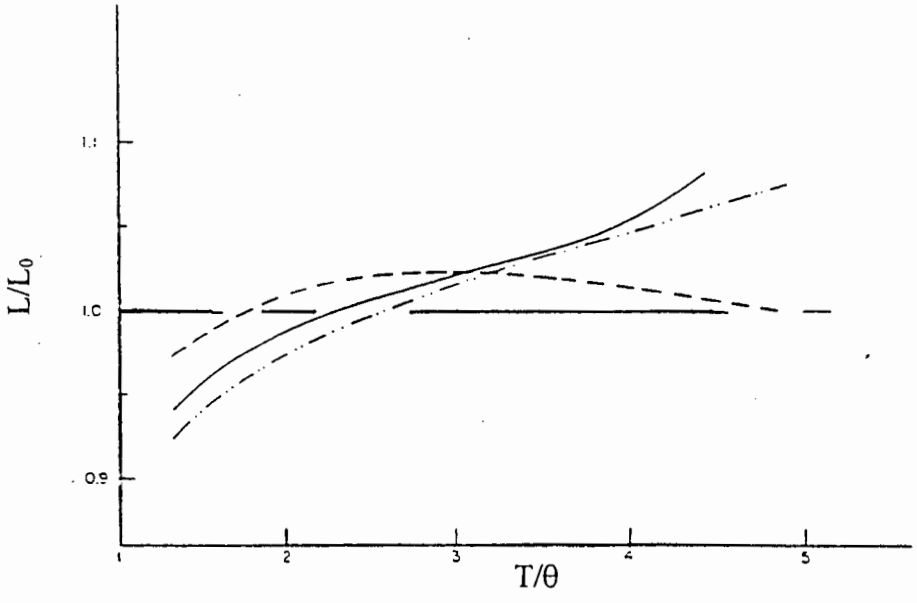

Figure 6.7: Reduced ratio of platinum vs temperature (after Laubitz[32]).

The reduced ratio of the ruthenium aluminide alloys is slightly higher than that of platinum and does not show an increase with increasing temperature. The Weidemann-Franz ratio of the ruthenium aluminide alloys is approximately 20% larger than the Sommerfeld value. These results suggest that the primary source of heat conduction in these alloys is by electronic movement and the contribution by the lattice is relatively small. This is consistent with the conclusions reached by Terada[30] that the Weidemann-Franz law is applicable to B2-type intermetallics and that the heat carriers are electrons rather than phonons. The results presented above for ruthenium aluminide are superimposed on the results presented by Terada[30] in figure 6.8.

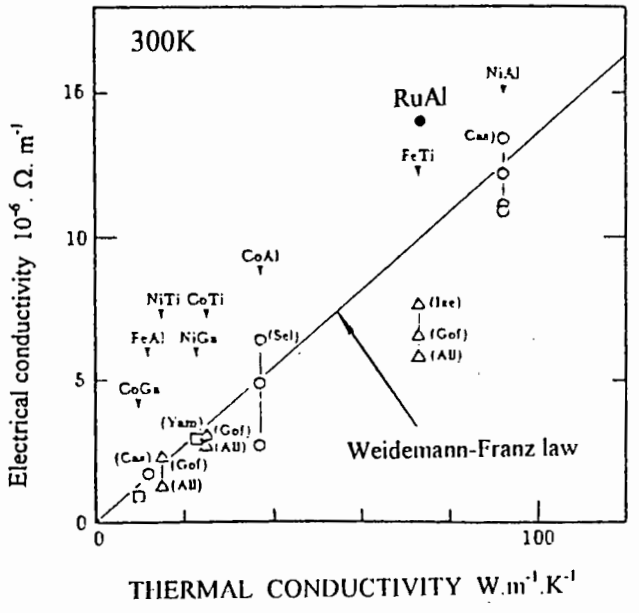

Figure 6.8: Deviations from the Weidemann-Franz ratio for B2-type intermetallics at stoichiometry (after Terada[30]). Closed circle represents ruthenium aluminide from this study.

It can be seen from figure 6.8 that the result obtained for ruthenium aluminide lies close to the Weidemann-Franz line. Terada[30] concludes that it is reasonable to say that all plots fall on the Weidemann-Franz ratio line. This indicates that the B2-type intermetallics satisfy the Weidemann-Franz ratio at room temperature, as do pure metals. Therefore, electrons rather than phonons are the dominant carriers of heat, which is typical of metallic behaviour.

The experimental results cited for NiAl and presented for RuAl provide ample evidence that intermetallics behave like metals. They have high thermal and electrical conductivity and their charge carriers are primarily electrons. This would indicate that they are bonded by free electrons as in metals. However, intermetallics are also inherently brittle and are said to have a degree of covalency in their bonding which challenges the metallic model and creates a dilemma when trying to understand the transport mechanisms in these compounds.

The intermetallic aluminides discussed above all contain a transition metal element which affects the electronic structure and bonding characteristics of the compounds involved. In transition metals there is an expansion of the group 8 (s^2p^6) electrons into the 18 ($s^2p^6d^{10}$) group and so consideration of the transition elements requires a knowledge of the way in which the d electrons contribute to bonding in contrast to s and p electrons. Any transport property involving transition elements is therefore complicated because the electronic states are multiband and hybridization of the orbitals occurs[65].

Current data in the literature[66] indicate that the ductilities exhibited by transition-metal intermetallics can be associated with ordering energy, differences in electronegativity, valence electron states, atomic size differences and deviations from stoichiometry. The presence of anti-phase boundaries affects both the mechanical and electronic properties of ordered compounds. Since RuAl and NiAl are similar in terms of their thermal and electrical conductivities, as determined in this study, it is useful to compare their electronic structure, bonding characteristics and ductility. The band structure and density of states show that the d and Al-p hybridization plays an important role in the formation of these compounds[17].

Lin[17] has shown that there is a similarity in bonding character between NiAl and RuAl. Bonding in NiAl along <111> directions arises from the strong Ni-d and Al-p hybridization and by contrast the predominant d-d bonding between Ru and Ru atoms in RuAl lies along the <100> directions[17].

The increase in electron density between nearest neighbour Ni-Al atom pairs, along the <111> direction results in a strong covalent bond between nearest Ni and Al atoms and a weak ionic repulsion between second nearest neighbour atoms along <100> direction. These directional bonds are superimposed over a metallic bond[64]. In other words the cohesion of NiAl is dominated by p-d covalent bonding combined with some metallic bonding contribution[17]. For RuAl, a Ru-d electron charge distribution shows only d-d bonding along the <100> direction between Ru atoms. The 4d electrons in RuAl also show greater metallic character than the Ni 3d electrons in NiAl[17].

Both compounds show strong directional bonding (covalent bonding) in certain directions, and metallic bonding characteristics in other directions. The covalent type bonding in certain directions would impart the elevated temperature strength that is characteristic of these compounds. NiAl has a lower room temperature ductility than RuAl and this is due to insufficient slip systems avaliable, a higher anti-phase boundary energy and stronger covalent features than RuAl[17]. Ogwu[66] suggests that the introduction of electrons into a supperlattice by selective alloying will create a region of disorder and so reduce the directionality of the covalent bond and in so doing improve the ductility of the compound.

Free electrons originate from areas in the unit cell that have a predominately metallic character and give these compounds their high thermal and electrical conductivities. Lin[17] notes that the overall charge distribution for ruthenium aluminide and nickel aluminide is similar and this is possibly why they both have such similar conductivities. The presence of covalent as well as metallic bonds in these compounds, due mainly to the transition metals involved, are the reason why these compounds exhibit metallic characteristics and at the same time are inherently brittle.

7. SUMMARY and CONCLUSIONS

1. Apparatus for the measurement of the thermal conductivity of intermetallics at elevated temperatures has been designed and constructed.

2. The thermal conductivity and electrical resistivity of ruthenium aluminium alloys have been measured in the temperature range 25°-500°C.

3. The Weidemann-Franz ratio of these alloys indicates that the primary source of heat conduction in these alloys is by electronic movement and the contribution by the lattice is relatively small.

4. The thermal and electrical properties of ruthenium aluminide are similar to those of pure platinum. This has important industrial implications for the possible use of ruthenium aluminide in certain high temperature applications.

5. The properties of ruthenium aluminide are also similar to that of another B2-type intermetallic, namely nickel aluminide. The dual nature of the bonding in these compounds, due mainly to the transition metals involved, are the reason why these compounds exhibit metallic characteristics and at the same time are inherently brittle.

6. Optimizing ruthenium aluminide alloys for high thermal and electrical conductivity requires careful compositional control and good processing techniques.

8. REFERENCES

[1] R.W. Cahn. "Physical Metallurgy." *North Holland, London,* 1970, p.229.

[2] R.W. Cahn. *MRS Bulletin* ***16, No.5,*** 1991, p.18.

[3] C.H. Desch. "Intermetallic compounds." *Longmans Green, London,* 1914, p.6.

[4] D. Porter and K. Easterling. "Phase Transformations in Metals and Alloys." *Chapman and Hall, London,* 1991, p.27.

[5] C. Johansson and J. Linde. *Ann. Physik* ***78,*** 1925, p.439.

[6] C. Sykes and H. Evans. *J. Inst. Metals* ***58,*** 1936, p.255.

[7] W. Hume-Rothery. "Structure of Metals and Alloys." *Institute of Metals, report series No.1,* 1936, p.88.

[8] J.H. Westbrook. "Mechanical Properties of Intermetallic Compounds." *Wiley, New York,* 1969.

[9] R.W. Cahn. *Metals Materials and Processes* ***1,*** 1989, p.2.

[10] C.T. Liu. *Internat. Metals Reviews* ***29,*** 1984, p.168.

[11] K. Aoki and O. Izumi. *J. Jpn. Inst. Met.* ***43,*** 1979, p.1190.

[12] M. Cortie, I. Wolff and L.A. Cornish. *South African Journal of Science* ***88,*** 1992, p.142.

[13] G.K. White in "Intermetallics - Principles and Practice" ed. J. Westbrook and R. Fleischer. *Wiley, London, Vol. 1,* 1995, p.1017.

[14] T.D. Boniface and L.A. Cornish. *Proc. Sino-South African Symposium on Materials Processing,* Tainan, Taiwan, 1994, p.173.

[15] R. Fleischer, R. Field and C. Briant. *Metallurgical Transactions* ***22A,*** 1991, p.403.

[16] R. Fleischer. "Intermetallics-Principles and Practice" ed. J. Westbrook and R. Fleischer. *Wiley, London, Vol. 1,* 1995, p.250.

[17] W. Lin, Jian-hau Xu and A.J. Freeman. *J. Mater. Res.* ***7,*** 1992, p.592.

[18] R. Fleischer and D.W. Mckee. *Metallurgical Transactions* ***24A,*** 1993, p.759.

[19] E.G. Smith and C.I. Lang. *Scripta. Met. 33, No. 8,* 1995, p.1225.

[20] W. Kingery. "Property measurements at high temperature." *Wiley, New York,* 1959, p.88.

[21] C. Kittel. "Introduction to Solid State Physics." *Wiley, New York,* 1953.

[22] P.G. Klemens and R.K. Williams. *Internat. Metals Reviews 31,* 1986, p. 198.

[23] M.J. Laubitz. *Can. J. Phys. 45,* 1967, p.3677.

[24] P. Klemens in "Thermal Conductivity" ed. R.P. Tye. *Academic Press, London,* 1969, p.45.

[25] J.P. Moore, R.K. Williams and R.S. Graves. *J. Appl. Phys. 48,* 1977, p.610.

[26] M.J. Laubitz and T. Matsumura. *Can. J. Phys. 51,* 1973, p.1247.

[27] M.J. Laubitz and T. Matsumura. *Can. J. Phys. 50,* 1972, p.196.

[28] E. Collings, J. Enderby and J. Ho. "Electron density of states." *NBS Spec. Publ. No.323,* 1971, p.483.

[29] R. Darolia. *J. Metals 43,* 1991, p.44.

[30] Y. Terada, K. Ohkubo, K. Nakagawa, T. Mohri and T. Suzuki. *Intermetallics 3,* 1995, p.347.

[31] N. Pearlman in "Methods of experimental physics." *Vol 6A, Academic Press, New York,* 1959, p.385.

[32] E. Griffiths and G. Kaye. *Proc. Phys. Soc. 1,* 1924, p.71.

[33] M. J. Laubitz and M. P. van der Meer. *Can. J. Phys. 44,* 1966, p.3173.

[34] K. Kobayasi. *JSME International Journal 31, No. 1,* 1988, p.1.

[35] American Soc. Testing Materials. ASTM Standards 1955. Test-C177.

[36] M. J. Laubitz in "Thermal Conductivity" ed. R.P Tye. *Academic Press, London* 1969, p.110.

[37] A. Worthing and D. Halliday. "Heat." *Wiley, New York,* 1959, p.161.

[38] L. Armstrong and T. Dauphinee. *Can. J. Res. 25A,* 1947, p357.

[39] R. Powell. *Proc. Phys. Soc. 46,* 1934, p.659.

[40] R. Powell. *Proc. Phys. Soc. 51,* 1939, p.409.

[41] M. Moss. *Rev. Sci. Instr. 26, No.3,* 1955, p.276.

[42] R. Powell and R. Tye. *Engineer 209,* 1960, p.729.

[43] T. Watson and H. Robinson. *Trans. Am. Soc. Mech. Engrs. 83C,* 1961, p.403.

[44] C.L. Hogan and R.B. Sawyer. *J. Appl. Phys. 23, No.2,* 1952, p.177.

[45] M.J. Laubitz. *Can. J. Phys. 41,* 1963, p.1663.

[46] M.J. Laubitz. *Can. J. Phys. 43,* 1965, p.227.

[47] D. Ditmars and D. Ginnings. *J. Res. Natn. Bur. Stand. 59,* 1957, p.93.

[48] J. Francl and W. Kingery. *J. Am. Ceram. Soc. 37,* 1954, p.80.

[49] M. Van Dusen and S. Shelton. *J. Res. Natn. Bur. Stand. 12,* 1934, p.48.

[50] T. Vasilos and W. Kingery. *J. Am. Ceram. Soc. 37,* 1954, p.409.

[51] V. Mirkovich. *J. Am. Ceram. Soc. 48,* 1965, p.387.

[52] J.M. Corsan. *J. Phys. E 17,* 1984, p.800.

[53] R. L. Fleischer. *Acta Metall. Mater. 41,* 1993, p.863.

[54] L. J. van der Pauw. *Philips. Res. Repts. 13,* 1958, p.1.

[55] Y. Sun, O. Ehrmann, J. Wolf and H. Reichl. *Rev. Sci. Instr. 63,* 1992, p.3752.

[56] K. Raznjevic. "Handbook of Thermodynamic Tables and Charts." *Hemisphere, Washington,* 1976.

[57] H. Carslaw and J. Jaeger. "Conduction of Heat in Solids." *Clarendon Press, Oxford,* 1947.

[58] T.T. Nartova. *Soviet Powder Metallurgy and Metal Ceramics 5,* 1966, p. 630.

[59] A.L. Norbury. *Trans. Faraday Soc. 16,* 1921, p.570.

[60] S. L'vov, P. Mal'ko, V. Nemchenko. *Fiz. Metal. Metalloved 31, No.1,* 1971, p.108.

[61] P.L. Rossiter. "The Electrical Resistivity of Metals and Alloys." *Cambridge Univ. Press,* 1987.

[62] D.J. Sellmyer, G.R. Caskey and J.M. Franz. *J. Phys. Chem. Solids* ***34***, 1973, p.1179.

[63] N.F. Mott and H. Jones. "The Theory of the Properties of Metals and Alloys." *Clarendon, Oxford*, 1936.

[64] D.B. Miracle. *Acta Metall. Mater.* ***41***, 1993, p.649.

[65] W. Hume-Rothery in "Electron Structure and Alloy Chemistry of Transition Elements." ed. P. Beck, *Wiley. New York*, 1963, p.83.

[66] A. Ogwu and T. Davies. *J. Mater. Sci.* ***28***, 1993, p.847.

APPENDIX

National Bureau of Standards

Certificate

Standard Reference Materials 1460, 1461, and 1462

Austenitic Stainless Steel Thermal Conductivity (λ) and Electrical Resistivity (ρ) as a Function of Temperature from 2 to 1200 K

J. G. Hust and A. B. Lankford

These Standard Reference Materials (SRM's) are to be used in calibrating methods for measuring thermal conductivity and electrical resistivity. They are available in rod form. SRM 1460 is 0.64 cm in diameter; SRM 1461 is 1.27 cm in diameter; and 1462 is 3.4 cm in diameter. All rods are 5.0 cm in length.

T(K)	λ ($W \cdot m^{-1} \cdot K^{-1}$)	ρ ($n\Omega \cdot m$)	T (K)	λ ($W \cdot m^{-1} \cdot K^{-1}$)	ρ ($n\Omega \cdot m$)
			50	6.08	599
2	0.152	593	60	6.98	606
3	.249	593	70	7.72	613
4	.352	593	80	8.34	622
5	.462	594	90	8.85	630
6	.575	594	100	9.30	639
7	.693	594	150	10.94	683
8	.814	594	200	12.20	724
9	.938	594	250	13.31	767
10	1.064	594	300	14.32	810
12	1.323	594	400	16.16	885
14	1.588	594	500	17.78	944
16	1.858	593	600	19.23	997
18	2.132	593	700	20.54	1045
20	2.407	593	800	21.75	1088
25	3.092	592	900	22.86	1127
30	3.763	592	1000	23.90	1162
35	4.404	593	1100	24.86	1197
40	5.01	595	1200	25.77	1234
45	5.57	597			

The technical and support aspects involved in the preparation, certification, and issuance of this Standard Reference Material were coordinated through the Office of Standard Reference Materials by Lee J. Kieffer.

Washington, DC 20234
May 14, 1984
(Revision of Certificates dated 12-11-74, 3-5-75, and 1-17-79)

Stanley D. Rasberry, Chief
Office of Standard Reference Materials

(over)